

OCCLUSION DETECTION AND LOCALIZATION IN MULTI-INFUSION SYSTEMS WITH ALARIS GH SYRINGE PUMPS

MASTER THESIS

By

MAX WESSELS

25/6/2017

Submitted to Hanze University of Applied Science Groningen

In partial fulfilment of the requirements of fulltime Honours Master Sensor System Engineer

OCCLUSION DETECTION AND LOCALIZATION IN MULTI-INFUSION SYSTEMS WITH ALARIS GH SYRINGE PUMPS

By

MAX WESSELS

25/6/2017

ABSTRACT

In Intensive Care Units, drugs are administered to critically ill patients intravenously using infusion systems. Unfortunately, the occurrence of occlusions (blockades) in infusion systems are a relatively common phenomenon. Fluctuations in, or absence of, drug delivery can have serious and even fatal consequences for the patient. In addition, false occlusion alarms can lead to nurse alarm fatigue and patient distress. This thesis presents a new method for detecting and localizing occlusions in multi-infusion systems. The goal was to develop an algorithm capable of early occlusion detection and localization in multi-infusion systems. Data was obtained using a test setup comprising of Alaris GH syringe pumps and an IDA 4 infusion device analyser. A new algorithm for automatic occlusion detection was successfully implemented and benchmarked on 30 signals. The time to occlusion alarm was reduced by 86% on average, with only one occlusion being marked incorrectly. In conclusion, a new method was developed for rapid automatic occlusion detection and localization. Thus far the method yielded promising results and although it requires further testing, it is expected that optimization of the occlusion detection algorithm will significantly increase patient-safety.

DECLARATION

I hereby certify that this report constitutes my own product, that where the language of others is set forth, quotation marks so indicate, and that appropriate credit is given where I have used the language, ideas, expressions or writings of another.

I declare that the report describes original work that has not previously been presented for the award of any other degree of any institution.

Signed,

Max Wessels

A handwritten signature in blue ink that reads "Max Wessels". The signature is written in a cursive style with a large, looping initial 'M'.

ACKNOWLEDGEMENTS

First I would like to thank Maarten Nijsten for the opportunity to work on this project at the Adult Intensive Care Unit of the UMCG. Secondly, I would like to thank Frank Doesburg for supervising me and for the form of discussion and feedback during the entirety of the project.

Additionally, I would like to thank Ward van der Houwen for being my graduation supervisor and for the extensive feedback on the content of this thesis.

TABLE OF CONTENTS

TABLE OF CONTENTS.....	5
DEFINITIONS.....	6
1 RATIONALE.....	7
1.1 Research questions	8
1.2 Test setup.....	8
1.3 Related projects	8
2 SITUATIONAL & THEORETICAL ANALYSIS	9
2.1 Introduction	9
2.2 Ethical considerations and legislation	9
2.3 Multi-infusions and intravenous versus peripheral therapy	10
2.4 IV-line occlusions	10
2.5 Occlusion implications.....	12
2.6 In-line pressure monitoring	12
2.7 Automatic occlusion detection.....	13
2.8 Occlusion localization	14
2.9 Hypothesis.....	14
3 CONCEPTUAL MODEL.....	15
4 RESEARCH DESIGN	17
5 RESULTS	19
5.1 Multithreading and synchronised sampling	20
5.2 Time occlusion alarm and infusion rate	21
5.3 Resistance slope steepness and infusion rate	22
5.4 Test-dataset.....	23
5.5 Pressure and resistance slope coefficients.....	24
5.6 Occlusion detection using sliding slope coefficients	25
5.7 Dynamic window size	27
5.8 Sliding slope coefficient threshold.....	30
5.9 Sliding slope coefficient algorithm implementation	31
5.10 Sliding slope coefficient algorithm validation	34
5.11 Occlusion localization	37
6 DISCUSSION, CONCLUSION & RECOMMENDATIONS	38
6.1 Conclusion.....	38
6.2 Discussion	39
6.3 Recommendations	40
BIBLIOGRAPHY.....	41
APPENDIX A: PATENT RESEARCH ON IV-LINE OCCLUSION DETECTION SYSTEMS.....	46
APPENDIX B: INTERVIEWS ADULT INTENSIVE CARE NURSES	50
APPENDIX C: JAVA INTERFACE FOR COMMUNICATING AND CONTROLLING THE ALARIS GH AND THE IDA 4.....	54
APPENDIX D: BENCHMARK RESULTS OF THE SLIDING SLOPE COEFFICIENT ALGORITHM USING THE VALIDATION-DATASET	57

DEFINITIONS

Central venous catheter: single, double or triple lumen intravenous catheter that is surgically inserted to the superior vena cava, or other large veins under sterile conditions [1]. Depending on the type, central venous catheters can be used from several days up to 6 months [2].

Disposable: designed to be used once and discarded and not reused or recycled [3].

Extravasation: passage or escape from circulation into tissue of an agent that causes inflammation. [3]

Hard occlusion: complete blockage of flow through an IV-line or catheter.

Infiltration: the process whereby a non-vesicant fluid passes into the tissues [3].

Infusate: a parenteral fluid slowly introduced into a patient over a specific period [3].

Intravenous catheter: a catheter that is inserted into a vein for supplying medications or nutrients directly into the bloodstream or for diagnostic purposes such as measuring central venous blood pressure [3].

Intravenous (IV) therapy: the administration of fluids into a vein through a needle or small-calibre catheter [3].

Intravenous infusion: a solution administered into a vein through an infusion set that includes a plastic or glass vacuum bottle or bag containing the solution and tubing connecting the bottle to a catheter or a needle in the patient's vein. [3]

Intensive Care Unit (ICU): constant complex health care as provided in various acute life-threatening conditions such as multiple trauma, severe burns, or myocardial infarction or after certain kinds of surgery. Care is most frequently given by specially trained personnel in a unit equipped with various technologically sophisticated machines and devices for treating and monitoring the condition of the patient. [3]

Lumen: the cavity or channel within a catheter. [3]

Peripheral catheter: catheter inserted via venipuncture into a hand or arm vein [1]. Short peripheral catheters, less than 7.5 cm in length, are typically used days [4]. Midline peripheral catheters, between 7.5 and 20 cm long, can be used for longer periods [5].

Three-way stopcock: A valve or turning plug that controls the flow of fluid through a tube. A three-way stopcock is often used in IV therapy to turn off one solution and turn on another. [3]

Thrombophlebitis: inflammation of a vein accompanied by the formation of a clot. It occurs most commonly as the result of trauma to the vessel wall [3].

Tubing: the topology of an arrangement of various bedside disposables between a set of infusion pumps and the patient. This includes (but is not limited to) IV-lines, valves and their interconnections.

Vesicant: a drug capable of causing inflammation when tissue is exposed to it. [3]

1

RATIONALE

The hospital's Intensive Care Unit (ICU) treats critically ill patients. These patients require a continuous and simultaneous flow of electrolyte solutions or pharmaceutical compounds. The infusion of liquid substances directly into a vein is called intravenous (IV) therapy. The substances are infused into a vein via IV catheters, which can infuse up to three different solutions in case of a triple-lumen catheter. These solutions are infused into the veins of the patient with the use of infusion pumps. Infusion pumps can be classified as syringe and volumetric pumps. Volumetric pumps are mostly used to hydrate the patient, whereas syringe pumps are often used to administrate drugs [6]. The fluid pathway, starting at the pump, flowing through an IV-line, enters the patient via a catheter. The infusion of multiple drugs through one infusion set and catheter is called multi-infusion [7].

Patients in the ICU often receive fast acting and short lasting, blood pressure altering drugs [8, 9]. Fluctuations in, or absence of, drug delivery in these situations can have fatal consequences. Early detection of blockage (called occlusions) in infusion systems can help increase patient safety, through optimal medication delivery [10]. Moreover, reducing the number of false alarms will reduce nurse alarm fatigue [11] and patient distress [12].

The goal of this thesis is to develop an algorithm, capable of early occlusion detection in multi-infusion systems. Moreover, the possibility of occlusion localisation was explored. In this project, the Alaris GH syringe pump was used, due to its availability and serial connection capabilities. The pressure signals generated by syringe pumps were integrated into a centralized system.

My task at the UMCG ICU research department was to create a theoretical framework for, and perform applied research into, the concept of multi-infusion occlusion detection and localisation. The research is ultimately aimed at developing and validating an occlusion detection and localisation system. In this system, the occlusion detection and localization algorithm will be implemented as a software module, in a central monitoring system.

1.1 Research questions

The central research question in this project is defined as the following:

How can the pressure signals from multiple Alaris GH syringe pumps be combined in a centralized system to detect and localize hard occlusions in a multi-infusion setup?

The sub-questions, defined to aid in answering the central research question, are the following:

1. What are the major causes for hard occlusions in infusion systems?
2. How can the signals from multiple syringe pumps be integrated into a central processing unit?
3. How can the signals from multiple syringe pumps be combined, to reduce the time to occlusion alarm, in multi-infusion systems?
4. What information on occlusion location can be obtained by combining the pressure sensor information from multiple syringe pumps?

1.2 Test setup

After literature research was completed, a test setup was created in which common multi-infusion scenarios were simulated. The occlusion detection and localisation algorithm were developed in a simulated environment, in which real-world data obtained from the test setup was utilized. To validate the pressure data from the syringe pumps, the IDA 4 Plus Infusion Device Analyser [13] by Fluke was made available by the UMCG.

The communication with the syringe pumps was realised with a JAVA interface, developed by Frank Doesburg. This interface was extended upon by implementing data logging functionality. Moreover, a communication protocol compatible with the IDA 4 was reverse engineered from software included by Fluke [14]. This allowed the logging of data with multiple infusion pumps and pressure monitoring channels from the IDA 4, on a synchronised time scale.

1.3 Related projects

This project was used as an addition to the PhD research by Frank Doesburg. Frank Doesburg is performing research on the possibility of multiplexing infusion fluids in a single IV-line, to reduce the number of required catheters [15]. This project complements the Multiplex infusion project, as both projects take advantage of new possibilities when multiple infusion pumps are monitored and controlled by a central system.

2

SITUATIONAL & THEORETICAL ANALYSIS

In this chapter, the concepts of infusion therapy and multi-infusion are introduced. Moreover, occlusions in infusion therapy and measurement techniques are reviewed. The theoretical framework presented here is concluded with a hypothesis.

2.1 Introduction

This project will utilize a new concept of integrating information from multiple pumps into a centralized system. This concept enables the development of new methods of occlusion detection and localization. Having an interdisciplinary background in hardware and software development, will aid me in investigating the possibilities, within the set timeframe of 5 months.

Stakeholders of this thesis include nurses and doctors, as end users of the systems. Patients are indirect users, as they will be influenced by its performance but not operate the system. Pump manufacturers will be influenced by the successful creation of the system, as new systems can create competition.

2.2 Ethical considerations and legislation

At the intensive care, patients are heavily dependent on a constant, and known flow of medication for their health. Therefore, systems that provide information and/or advice on the usage of infusion lines, must be extremely reliable and unmistakably clear in presenting its findings. Especially the ‘clearness’ of the presented data raises an ethical issue: who is to blame if the information is correct but misleading? Moreover, how much reduction in the number of false positives is worth an increase in false negatives?

Legislation tries to cover most of these topics in terms of performance requirements. Syringe pumps are classified as medical electrical equipment, therefore the essential requirements are specified in the “IEC 60601-2-24:2012,IDT”, particular requirements for the basic safety and essential performance of infusion pumps and controllers [16]. Section 201.12.4.4.103 of this document, specifies that the maximum infusion pressure may not cause a rupture or leak in the infusion set. Furthermore, section 201.12.4.4.104 specifies that the pump must have protection against unintended bolus and under-infusion. The Alaris GH syringe pump realizes this by an occlusion alarm after which the pressure of the IV line is released, by reversing the pump direction.

Conditions which form an exception to these regulations are defined in section 201.7.9.2.101. These exceptions are in place make the essential requirements achievable. Exceptions include: short time periods, unusual infusion liquid characteristics, the use of excessively fine needles and extreme environmental conditions. The manufacturer should specify the parameters in which the device cannot maintain the specified accuracy. For instance, the range of acceptable viscosity of liquids, back pressure, infusion rates, reaction time of the safety system, scope of the risk analysis, etc.

2.3 Multi-infusions and intravenous versus peripheral therapy

Infusion therapy can be delivered via venous and peripheral catheters. Peripheral catheters are inserted via venipuncture into a hand or arm vein [1]. Central, venous catheters are inserted directly into a major vein in the neck, chest or groin. Venous catheters allow the administration of drugs in stronger dilutions. In the ICU, substances are often administered via a central venous multi-lumen catheter, so that multiple drugs can be administered via a single catheter. This increases patient comfort and reduces infection risks due to catheter insertion [17].

A multi-infusion system is a complex infusion system, in which multiple drugs are infused via a single catheter and infusion set. Multi-infusion can be achieved by sending multiple drugs via a single lumen or by using multi-lumen catheters. However, when using a single lumen to send multiple drugs, the drugs can react with one another. This can cause the drugs to form a precipitation, leading to occlusions and/or aggregates. Unfortunately, not all drug combinations have been tested on compatibility.

2.4 IV-line occlusions

A blockage in an infusion line is often referred to as an occlusion and can be classified as either hard or soft occlusions. Causes for hard occlusion include closed stopcocks, kinked IV tubing, kinked catheters, air-locks and thrombophlebitis [10], [18]. Soft occlusions can be caused by the build-up of precipitates, such as intraluminal deposition of drugs, compression of the catheter, narrowing of the vessel lining, thrombophlebitis, resting of the catheter on a vessel wall, penetration of the catheter into extravascular tissue and perhaps even the formation of bacterial biofilms [10], [18], [19], [20].

A less obvious cause for occlusions is caused by friction between the syringe plunger and the inner lining of the syringe. At start-up and at low infusion rates, the pump must overcome the friction between the rubber plunger and the inner lining of the syringe. This initial friction can be high enough to trigger an occlusion alarm. However, in practise, this usually causes the pump to build up pressure, overshoot, and stop the infusion for a short amount of time. This behaviour is depicted in Figure 1. The amount of friction the pump must overcome is dependent on temperature and medication present in the pump.

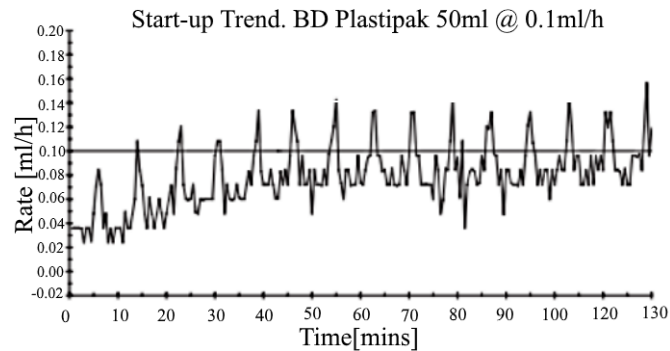


Figure 1: Start-up trend of an infusion pump, showing set and measured infusion rate over time, for a low infusion rate. The measured pressure is fluctuating around the set infusion rate, due to overshooting caused by syringe-plunger friction. [21]

The rate of the pressure rise caused by an occlusion is proportional to infusion rate and inversely related to the elasticity of the IV pathway. Environmental temperature indirectly decreases the rate of rise in pressure, as it increases the elasticity of the IV pathway. Figure 2 depicts the relative increase in pressure for a hard and a soft occlusion. Moreover, it shows the difference in pressure rise over time for a high infusion rate and stiff tubing compared to a low infusion rate with elastic tubing. During a soft occlusion, the pressure will not climb continuously as in a hard occlusion but will reach a plateau due to the increase in resistance of the tubing.

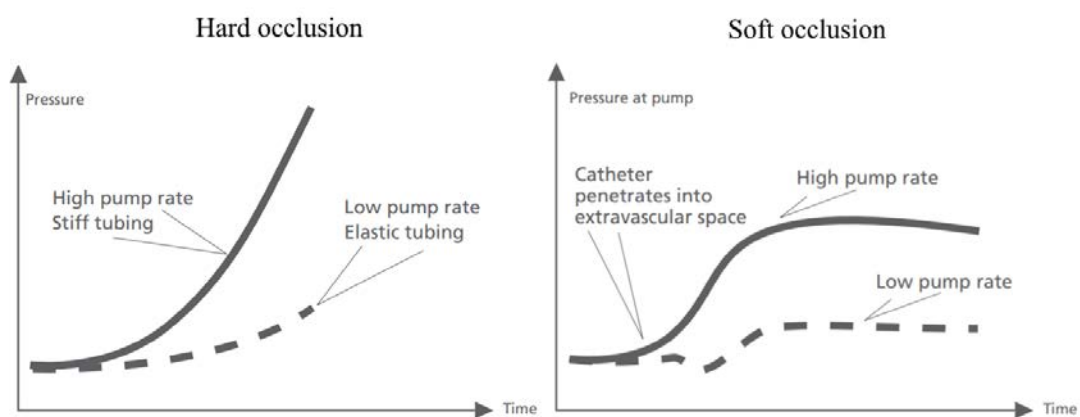


Figure 2: The relative increase in pressure over time for hard and soft occlusions. Moreover, the difference between a high infusion rate with stiff tubing versus a low infusion rate with elastic tubing is depicted for both situations. For a hard occlusion, the pressure keeps rising, whereas for a soft occlusion the pressure values reach a plateau. [18]

2.5 Occlusion implications

One of the most dangerous consequences of occlusion is extravasation [10], the passage or escape into tissue of an agent that causes blistering [3]. A less severe complication is infiltration [10], the process whereby a fluid passes into tissue [3]. Extravasation is one of the most dangerous consequences due to the long-term or permanent tissue damage it can cause [22], [23], [24]. Other implications of occlusions affecting the patient include suboptimal medication delivery, bloodstream infection and distress to the patient [12], [25]. Implications of occlusions have a significant impact on the hospital costs due to prolonged hospitalization and possible legal action [26], [27]. Prediction of occlusions will therefore have a positive impact on patient health and hospitalization costs [28].

2.6 In-line pressure monitoring

The Alaris GH is the (most widely) used syringe pump in the UMCG and is depicted in Figure 3. Syringe pumps are designed to deliver a continuous infusion of small flow rates with high accuracy and precision. A syringe can be placed in the clamp, connecting a driver to the syringe plunger. A motor moves the driver, which in turn exerts pressure on the syringe plunger. As the Alaris GH syringe pumps utilize pressure transducers to obtain occlusion information, the measurement techniques evaluated in this project are limited to those that are pressure based. In-line pressure can be determined in various ways such as, in-line measurements [29], calculated from motor power consumption [6] or calibrated to strain exerted on the motor [21].



Figure 3: A picture of the most widely used syringe pump in the UMCG: the Alaris GH. [30]

The Alaris GH utilizes a strain gauge to obtain the pressure at the syringe plunger. The electrical resistance of the strain gauge changes according to the force exerted on the motor. The force on the motor is proportional to the pressure at the syringe plunger, as they are mechanically connected via the plunger driver. When the force on the motor increases, the metal around the motor bearing is pushed outwards, exerting strain on the metal. This strain causes the metal located under the strain gauge to bend slightly, changing the resistance of the strain gauge. The resistance values are calibrated to pressure values at the syringe plunger.



Figure 4: Motor baseplate containing the motor bearing and the strain gauge used to obtain pressure values. The friction counteracting force exerted by the motor, causes strain on the metal around the motor bearings. This causes the metal, at the location of the strain gauge, to bend slightly. This bending is calibrated to pressure values at the syringe plunger. [31]

2.7 Automatic occlusion detection

Pumps that have in-line pressure monitoring, utilize a pressure threshold, at which an alarm is triggered and the pump stops. According to literature, occlusion alarm level should be set to an appropriate value based on the patient, infusion site, catheter type and infusion rate [10]. However, in the UMCG, the pressure threshold of syringe pumps is set to 400 mmHg and very rarely changed. See Appendix B for more information.

When an occlusion occurs, the pressure in the tubing distal to the patient will increase over time. The time to alarm is mainly dependent on the infusion rate, elasticity of the tubing and occlusion location. The time to alarm can vary from a few minutes up to one and a half hour. Typical time to alarm values for occlusion levels graphs are depicted in Figure 5.

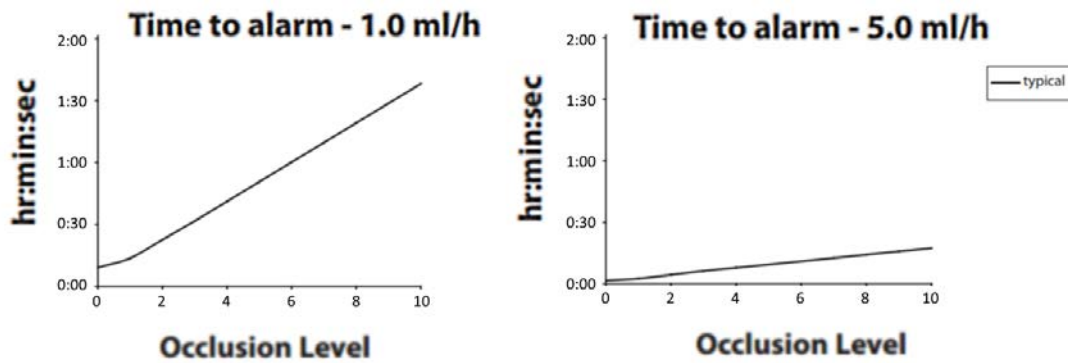


Figure 5: Typical time to alarm values for different static occlusion pressure level thresholds, according to literature. An occlusion level of 2, corresponds to a threshold of 200 mmHg and an occlusion level of 10 corresponds to a threshold of 1000 mmHg. The two graphs show that time to occlusion alarms, for a lower infusion speed are higher, and vice versa. [21]

An overview of patents registered from January 2000 till March 2017 can be seen in Table 4 in Appendix A. Most patents on occlusion detection systems for IV therapy rely on a pressure sensor placed along the IV-lines. Systems containing a syringe pump, utilize a downstream pressure sensor. Only one patent was found, registered under number US2005096593, which utilizes force measurements inside the pump, like the Alaris GH.

Most detection methods measure pressure development over time. These measurements are used to calculate averages, slopes and resistances. The patent under number US9272087 relies on giving a bolus and measuring the pressure decay over time to obtain a pressure profile. This profile is compared to a nominal profile. The differences between profiles are used as an indication of occlusion presence. Not all found methods are based on pressure measurements, for instance the patent under number US7880624 is purely based on flow measurements.

2.8 Occlusion localization

Due to the high number of IV-lines to the patients in the ICU, the lines often end up in a spaghetti-like tangle [32]. When an occlusion alarm is triggered, the nurse must locate the cause of the occlusion. With a high amount of tangled IV-lines, this can be a time-consuming task. Therefore, providing occlusion estimations will possibly speed up the process of finding occlusion causes. Based on my current knowledge, there are no systems commercially available nor patented to provide occlusion localization.

2.9 Hypothesis

Based on the previous, the following hypothesis was formulated:

A centralized system, that combines the sensor signals of multiple pumps in a multi-infusion setup, will decrease the time to occlusion alarm and provide occlusion location information.

3

CONCEPTUAL MODEL

So far, the goal and motivation of this project have been defined. A theoretical framework has been established with a corresponding hypothesis. In this chapter, an outline for the development process of the data analysis techniques and algorithms is given.

In the proposed conceptual model, depicted by Figure 6, a JAVA interface is used to control the connected devices and log data. The JAVA interface communicates with the syringe pumps and the IDA 4, from which data can be logged. The topology of the IV-lines will be entered in the JAVA interface to enable occlusion localisation.

The incoming pressure signals will be processed simultaneously by the central processing unit. Several data analysis techniques, aimed at arriving at occlusion detection and localisation, were theoretically established. Resistance slope steepness was selected to perform the occlusion detection. A method based on cross-correlation was selected to perform occlusion localization. The other techniques are mentioned in Chapter 6, future recommendations.

- Resistance slope steepness: slope steepness is a measure of the rate of change of a signal. Slope steepness can be used to reduce the time to occlusion alarm significantly, as it removes the need to wait for the pressure to rise. By converting the pressure signals to resistance, the slope steepness will be normalized with respect to flow rate. A sliding window will be used to fit a linear model and obtain slope coefficients. The sliding slope coefficients can be used in combination with a threshold or a peak detection algorithm to indicate the presence of an occlusion.
- Cross-correlation between signals: the cross-correlation between pressure signals from different pumps is a measure of their similarity. Cross-correlation is given by Equation 1 and will be calculated over an incrementing or sliding window. When an occlusion is detected by the resistance slope steepness method, cross-correlation can be used to determine which pumps share the same occlusion and which are still unobstructed. When the pumps that share an occlusion are determined and the IV-line configuration is known, the location of the occlusion can be estimated.

Equation 1: Cross-correlation of two discrete, weakly stationary, real-valued, stochastic time series.
[33]

$$xcorr(f[n], g[n]) = \sum_{m=-\infty}^{\infty} f[m]g[m+n]$$

Once an occlusion has been detected and an occlusion alarm is triggered, the occlusion localisation algorithm is activated. The localisation will be based on the IV-line topology and will look for interconnections in fluid pathways, marked as having an occlusion. The interconnections between marked fluid pathways are used to provide estimated occlusion locations.

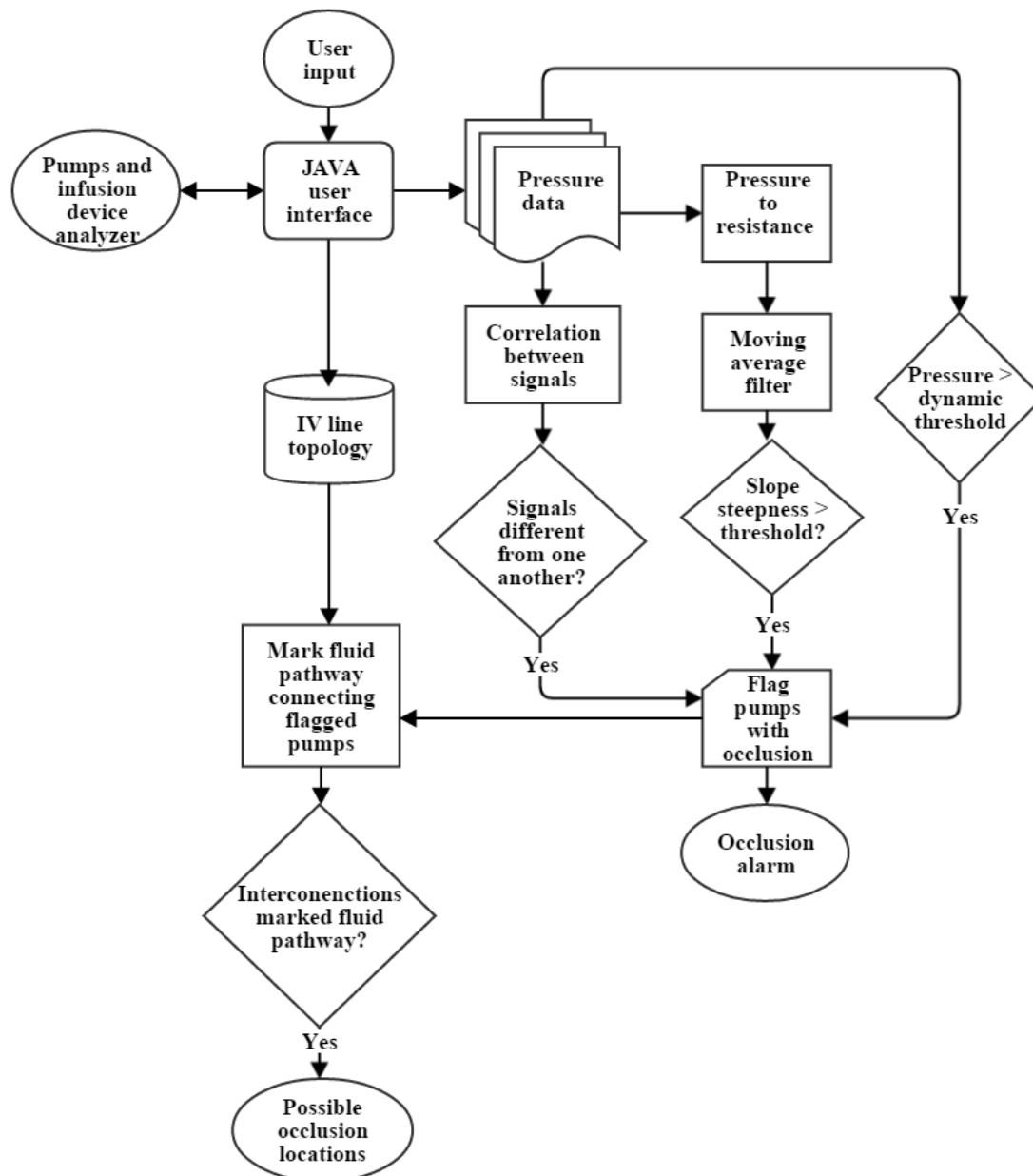


Figure 6: Conceptual model for occlusion detection and localization in multi-infusion systems. The model includes the hardware used, pump and infusion device analyzer, the software used to control the hardware, the JAVA user interface, and the basic functioning of the occlusion detection and localization algorithm. The model requires the input of one or more infusion pumps and can also log data from the infusion device analyzer. [34]

4

RESEARCH DESIGN

To test the conceptual model, a setup was created to control and log pressure data from the Alaris GH syringe pumps. To validate the pressure values from the Alaris GH sensors, the IDA 4 Infusion Device Analyser [14] was made available by the UMCG. Unfortunately, the Fluke IDA 4 does not support the logging of data. Therefore, the communication protocol for the IDA 4 was reversed engineered from the included software Hydrograph [14].

To log the data from Alaris GH syringe pumps and the IDA 4 on a synchronised time scale, a JAVA interface was developed to control and log both devices. An example of a test setup configuration is depicted in Figure 7. This test setup was connected to a computer via USB, where the devices are controlled by a JAVA interface. More information on the JAVA interface is available in Appendix C. Using the data from the test setup, an algorithm capable of occlusion detection and localization was developed.

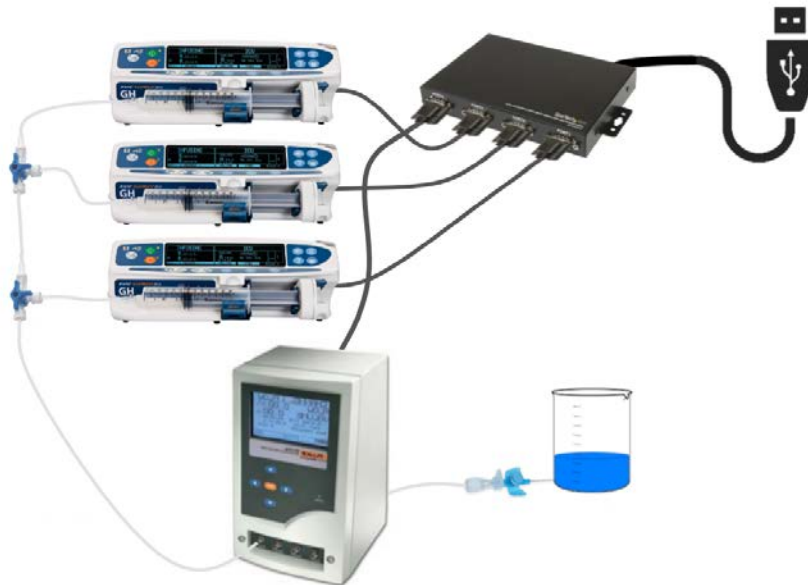


Figure 7: Schematic of an example test setup, used to obtain pressure data in a multi-infusion setting. The setup consists of the IDA 4 infusion device analyser, multiple Alaris GH infusion pumps and a waste container, connected via IV-lines and stopcocks. [35]

To validate the proper functioning of the hardware and software used in the test setup, as depicted in Figure 6 and Figure 7, all components were extensively tested. The experiments used were documented in an experiment book where materials, procedure and results were noted [36]. A summation of the findings of these experiments are listed below.

1. Calibration values IDA 4 Infusion device analyser: calibration values of the IDA 4 are in the hexadecimal format with the character 'V' representing the decimal mark. [37]
2. Update frequency of the syringe pump: the optimal command delay for a single pump is 200 ms. [38]
3. Update frequency syringe pump verification: the command delay of 200 ms performs equally well in a test setup where up to four pumps and four IDA 4 channels are logged simultaneously. [39]
4. Pump and syringe time to occlusion alarm variance: variances in time to occlusion alarm are mainly caused by syringes. [40]
5. Time to alarm for different infusion rates: time to occlusion alarm and infusion rate are inversely exponentially related. [41]
6. Validation syringe pump and IDA 4: pressure values from the syringe pump are similar to those of the IDA 4. [42]
7. Removing redundant data: the script to remove redundant data functions properly and reduces the amount of data by about 72%. [43]
8. Synchronized sampling: a shared buffer and a shared timed buffer implementation both provide synchronised sampling but the shared timed buffer provides a consistent sampling frequency. [44]

Once the test setup was validated to function properly, a resistance slope steepness occlusion detection implementation was tested in experiments 9 through 12, which are documented in the Experiment Book [45], [46]. The implementation is based on a sliding slope coefficient algorithm. From these tests, the most important data is presented in the next chapter.

5

RESULTS

In this chapter, the most important results of this project are presented. To start off with, a typical pressure time series is depicted by Figure 8. In Figure 8, the time of occlusion occurrence and occlusion alarm are marked, as well as the occlusion alarm pressure threshold. Once an occlusion alarm is triggered, the pump reverses its pump direction to a negative infusion rate, causing a steep drop in pressure and relieving pressure from the IV-line.

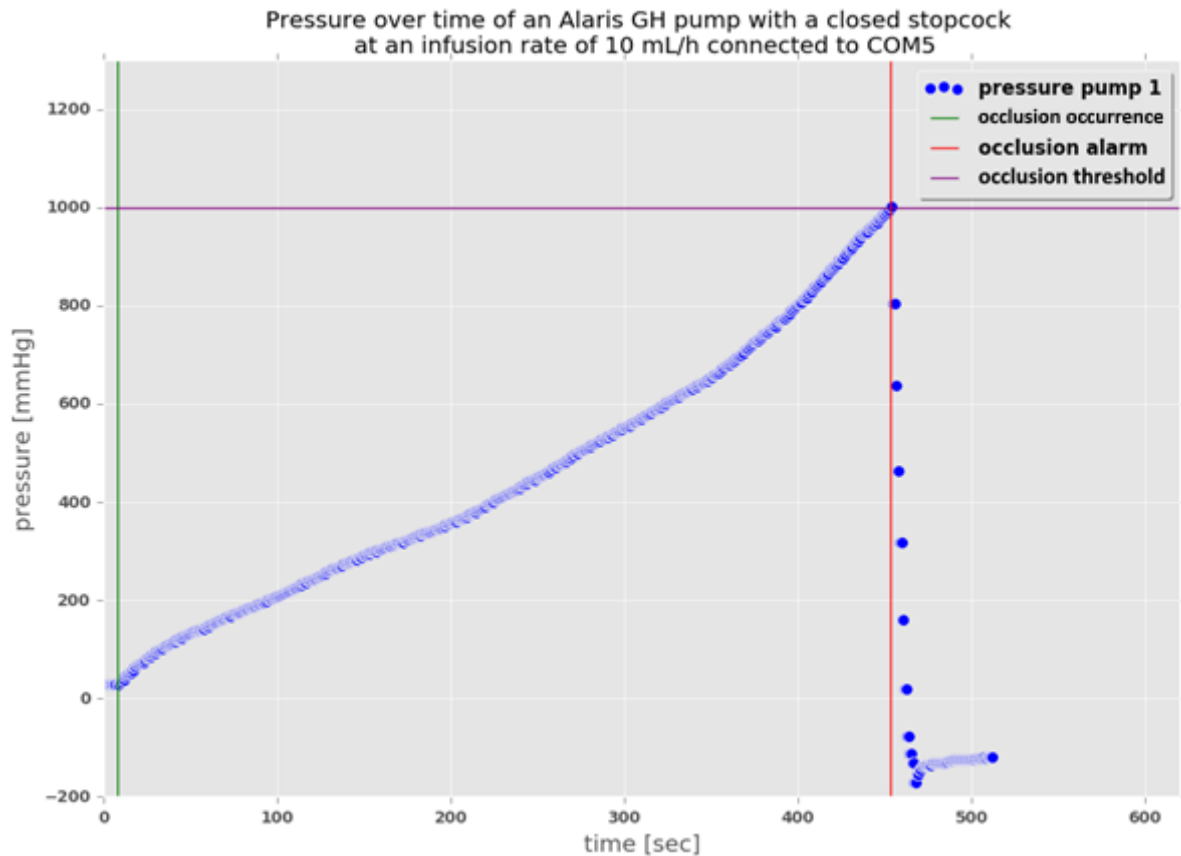


Figure 8: Example pressure time series, for a single pump and syringe, directly connected to a closed stopcock. The vertical green line represents the start of the infusion, at which point in time the pressure first starts rising. When the pressure reaches the threshold value of 1000 mmHg, indicated by the purple horizontal line, the occlusion alarm in the syringe pump is triggered. The pump then reverses its pumping direction, causing the pressure to decrease rapidly.

5.1 Multithreading and synchronised sampling

The JAVA interface relies on multithreading to be scalable without losing performance. To deal with unsynchronised sampling caused by multithreading, a shared and timed buffer was implemented. This buffer will overwrite old values and at an interval of 0.5 Hz the newest values are logged. Figure 8 depicts four pressure time series with infusion rates, demonstrating the functioning of the shared timed buffer. From Figure 8 it can be seen that values are logged at exactly the same points in time and that no redundant data is present.

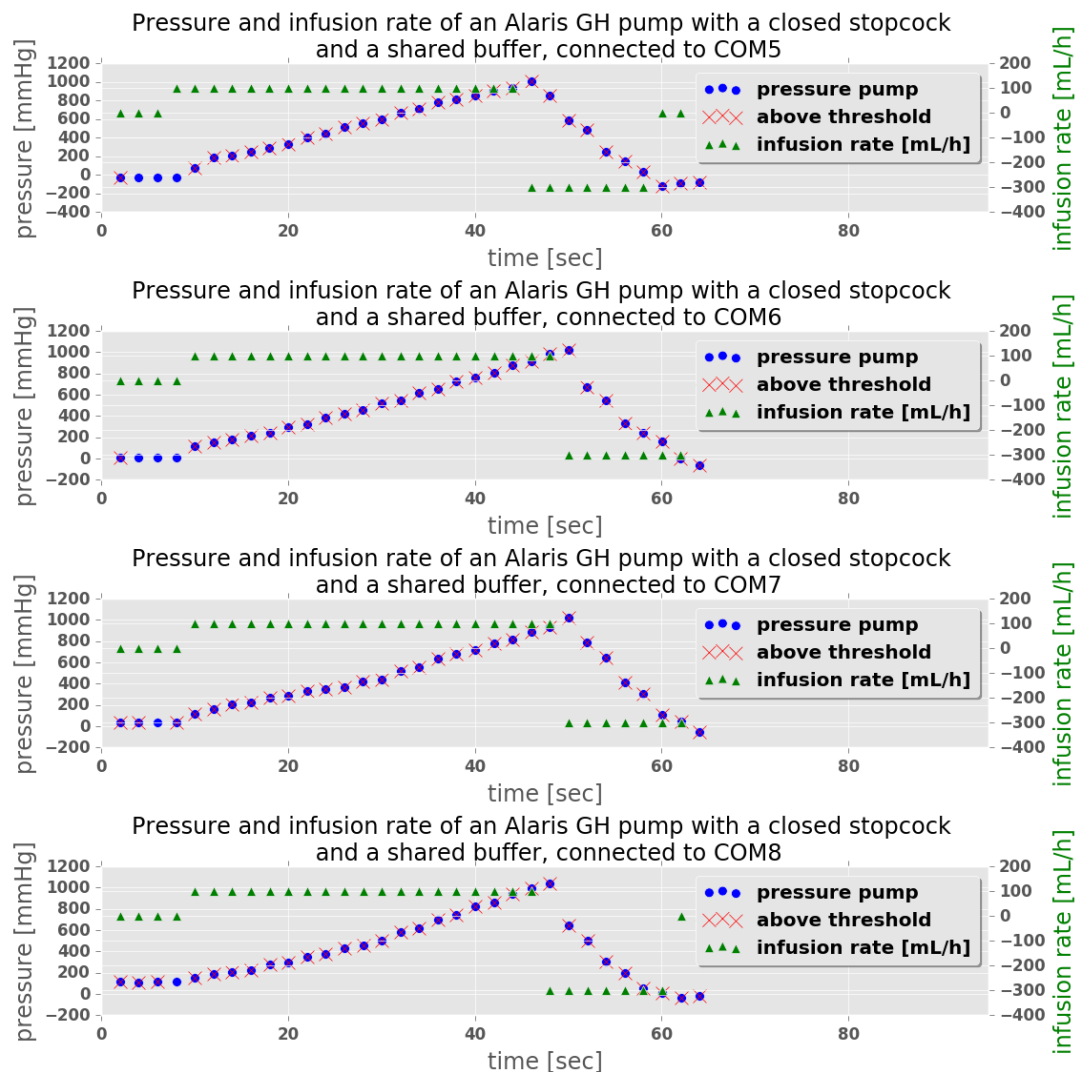


Figure 9: Demonstration of synchronised sampling by four pressure and infusion rate time series with a shared and timed buffer. Consecutive values that are different by more than a pressure threshold are marked with a red cross. Most data points are marked by a red cross, indicating low redundancy in data. The shared timed buffer results in a synchronized static sampling frequency of 0.5 Hz.

5.2 Time occlusion alarm and infusion rate

Experimental data pointed out that time to occlusion alarm was determined to be mainly dependent on infusion rate [41]. Infusion rate and time to occlusion alarm are inverse exponentially related, as depicted in Figure 10. However, the spread in time to occlusion alarm and time to occlusion alarm do not seem to share a clearly definable relationship.

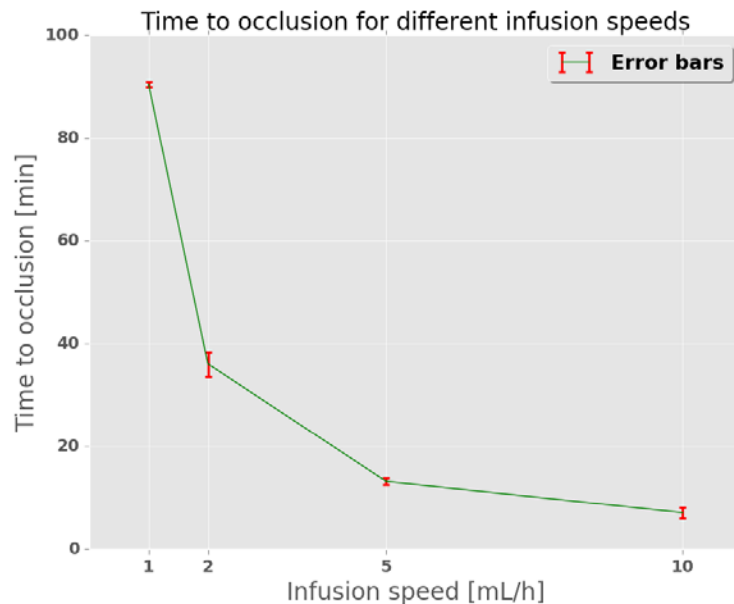


Figure 10: Time to occlusion alarm for typical infusion rates, with error bars. The error bars comprise of three data points. Infusion rate and time to occlusion alarm are inversely exponentially related. However, no clear relationship between spread in time to occlusion alarm and infusion rate is visible.

To be able to use the steepness of a curve as an indication for occlusions, the pressure data has to be normalized based on flow. This was done by dividing pressure with the flow rate, as demonstrated by Equation 2.

Equation 2: Resistance expressed as pressure over flow

$$R = \frac{P}{Q} \left[\frac{kg}{m^4 * s} \right]$$

- $R = \text{resistance} \left[\frac{kg}{m^4 * s} \right]$
- $P = \text{pressure} [mmHg]$
- $Q = \text{flow rate} \left[\frac{m^3}{s} \right]$

5.3 Resistance slope steepness and infusion rate

The principle of normalizing slope steepness for flow rate, by converting pressure to resistance, is depicted by Figure 11. Higher infusion rates result in the data becoming more compressed and reaching a lower final resistance value. As a result, the steepness of the curves has become comparable to one another.

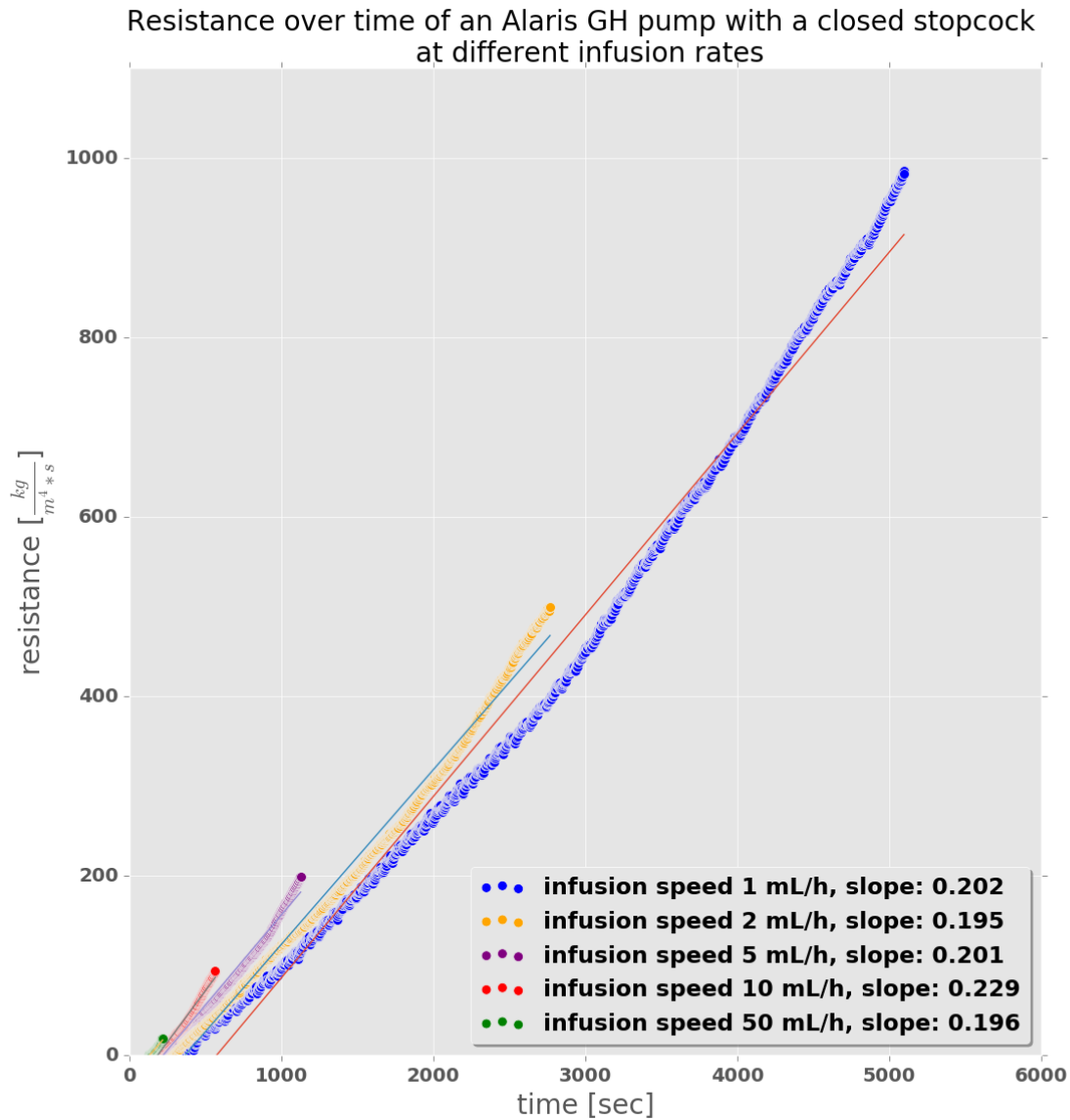


Figure 11: Resistance over time for different infusion rates, demonstrating the principle of normalizing slope steepness for flow rate. For infusion speeds 1, 2, 5, 10 and 50 mL/h, the slope coefficients are all around 0.2. The datasets were cut off at the point where they reached 1000 mmHg, at which point in time an occlusion alarm was triggered by the pump.

5.4 Test-dataset

In a setup with three pumps connected to a shared occlusion (Figure 12), the pumps were set to the same infusion rates and pressure data was recorded. The infusion rates 1, 2, 5, 10 and 50 mL/h were used. For each infusion rate the experiment was repeated three times. This leads to nine datasets per infusion rate and a total dataset of 45 time series, as shown in Table 1. This dataset is from here on referred to as the test-dataset, as it was used for initial testing and development of the slope steepness algorithm.

Table 1: Infusion rates of the test-dataset, for dataset and pump number. The pump configuration for this comprised of three pumps. A schematic of the setup is depicted in Figure 12. For each infusion rate, the experiment was repeated three times. With 15 datasets of three time series, a total of 45 time series was recorded.

dataset number	pump		
	1	2	3
1	1 mL/h	1 mL/h	1 mL/h
2	1 mL/h	1 mL/h	1 mL/h
3	1 mL/h	1 mL/h	1 mL/h
4	2 mL/h	2 mL/h	2 mL/h
5	2 mL/h	2 mL/h	2 mL/h
6	2 mL/h	2 mL/h	2 mL/h
7	5 mL/h	5 mL/h	5 mL/h
8	5 mL/h	5 mL/h	5 mL/h
9	5 mL/h	5 mL/h	5 mL/h
10	10 mL/h	10 mL/h	10 mL/h
11	10 mL/h	10 mL/h	10 mL/h
12	10 mL/h	10 mL/h	10 mL/h
13	50 mL/h	50 mL/h	50 mL/h
14	50 mL/h	50 mL/h	50 mL/h
15	50 mL/h	50 mL/h	50 mL/h

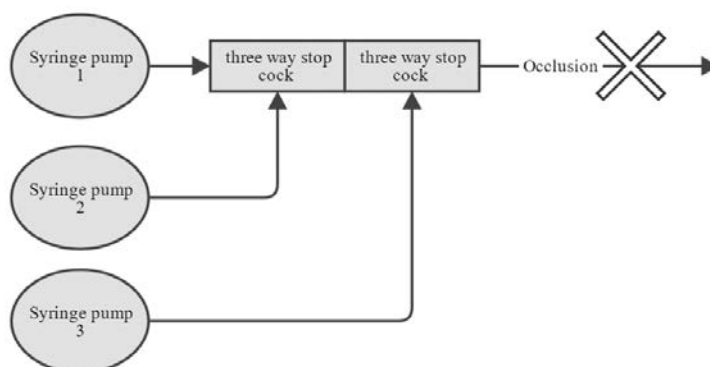


Figure 12: Schematic overview of the pump configuration used for the test-dataset. The test setup comprised of three infusion pumps, connected to three-way stopcocks via infusion lines.

5.5 Pressure and resistance slope coefficients

For each pressure time series, the slope coefficient was calculated, from the time of occlusion, to the occlusion alarm. The results are displayed by the top plot of Figure 13. Each pressure time series was then converted to resistance and the slope coefficient was calculated again, depicted in the bottom plot of Figure 13. The slope coefficients of the pressure time series are proportional to the infusion speed, whereas the slope coefficients of the resistance time series remain constant, within error margins.

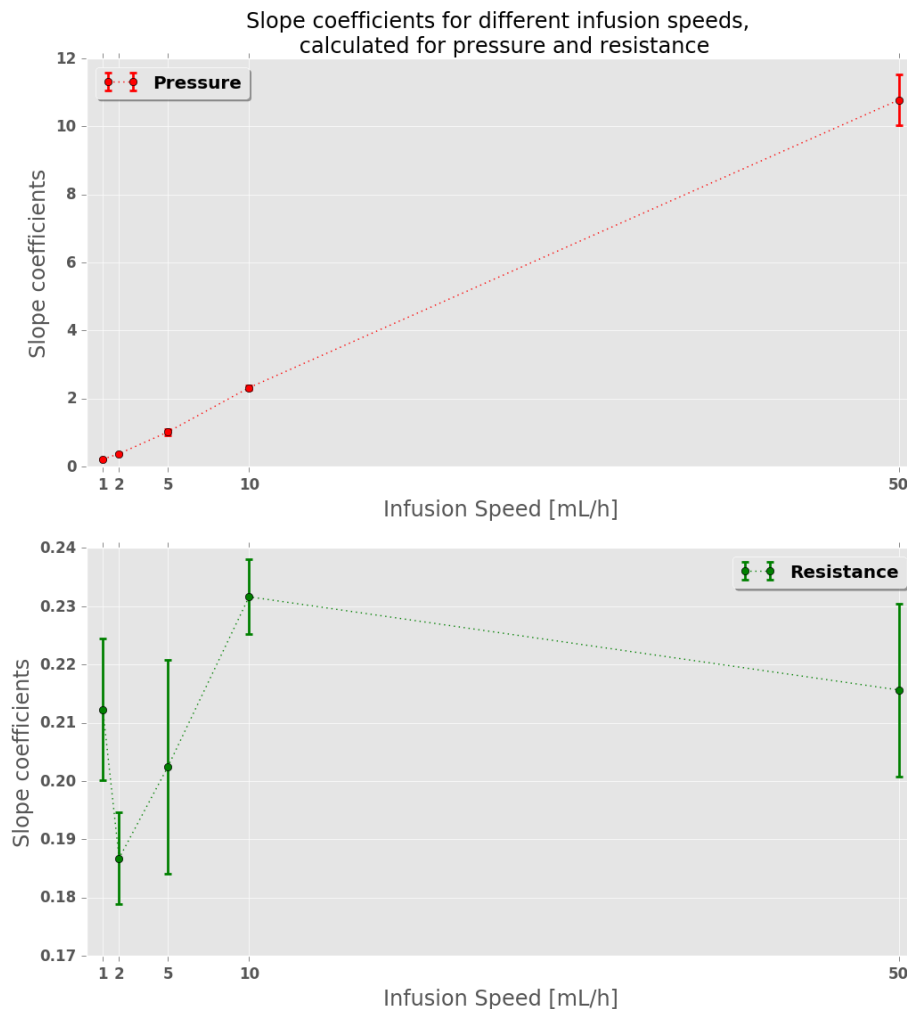


Figure 13: Difference in slope coefficients for pressure and resistance at infusion speeds 1, 2, 5, 10 and 50 mL/h. The slope coefficient were calculated from the time of occlusion to the time of occlusion alarm. The spread for each infusion rate is calculated from time series points. Slope coefficients for pressure increase linearly with infusion rate, whereas for resistance the slope coefficient remain between 0.18 and 0.24, demonstrating that for a total of 45 signals, the slope coefficients were normalized for flow rate.

5.6 Occlusion detection using sliding slope coefficients

To determine when an occlusion has occurred, a sliding slope coefficient algorithm was developed in Python. A windows size of 10 was determined to be optimal for an infusion rate of 10 mL/h in experiment 9, documented in the Experiment Book [45]. Therefore, for initial testing the algorithm calculated slope coefficients over the window with size 10. However, the pressure time series contain small fluctuations, causing the slope coefficients to fluctuate. Therefore, the resistance time series is moving average filtered, before running the sliding slope coefficient algorithm. This concept is demonstrated by Figure 14. In Figure 14 the point in time where an occlusion occurs is marked by a vertical green line. From this point in time, the slope coefficients increase from a small value to about 0.2, indicating an occlusion.

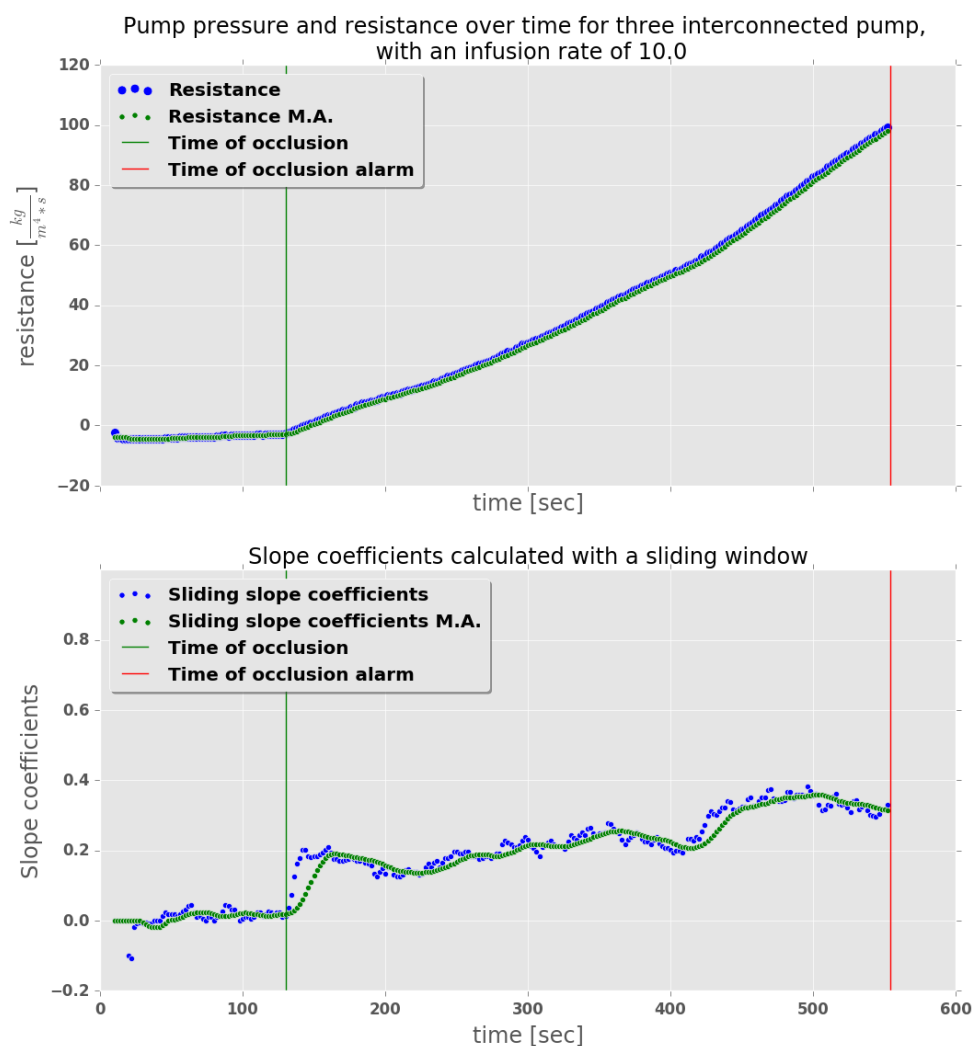


Figure 14: Demonstration of the output from the occlusion detection algorithm based on sliding slope coefficients. The top graph shows resistance over time (blue dots) and the same time series moving average filtered (green dots). The second plot shows the slope coefficients, calculated from the resistance time series in the top plot. The sliding window size was 10. After the occlusion occurs (vertical green line), an increase in slope coefficients is observed, indicating an occlusion. Moreover, the sliding slope coefficients from the moving average filtered time series contain less fluctuations.

A problem with the sliding slope coefficient algorithm, that utilizes a static window size of 10, occurs at infusion rates lower than 10 mL/h. The slower increase in pressure, causes fluctuations in the signal to be relatively smaller. This means that fluctuations are larger with respect to the increase in pressure, compared to higher infusion rates. This causes a large spread in sliding slope coefficients, making the point in time of occlusion hard to distinguish. This phenomenon is demonstrated by Figure 15.

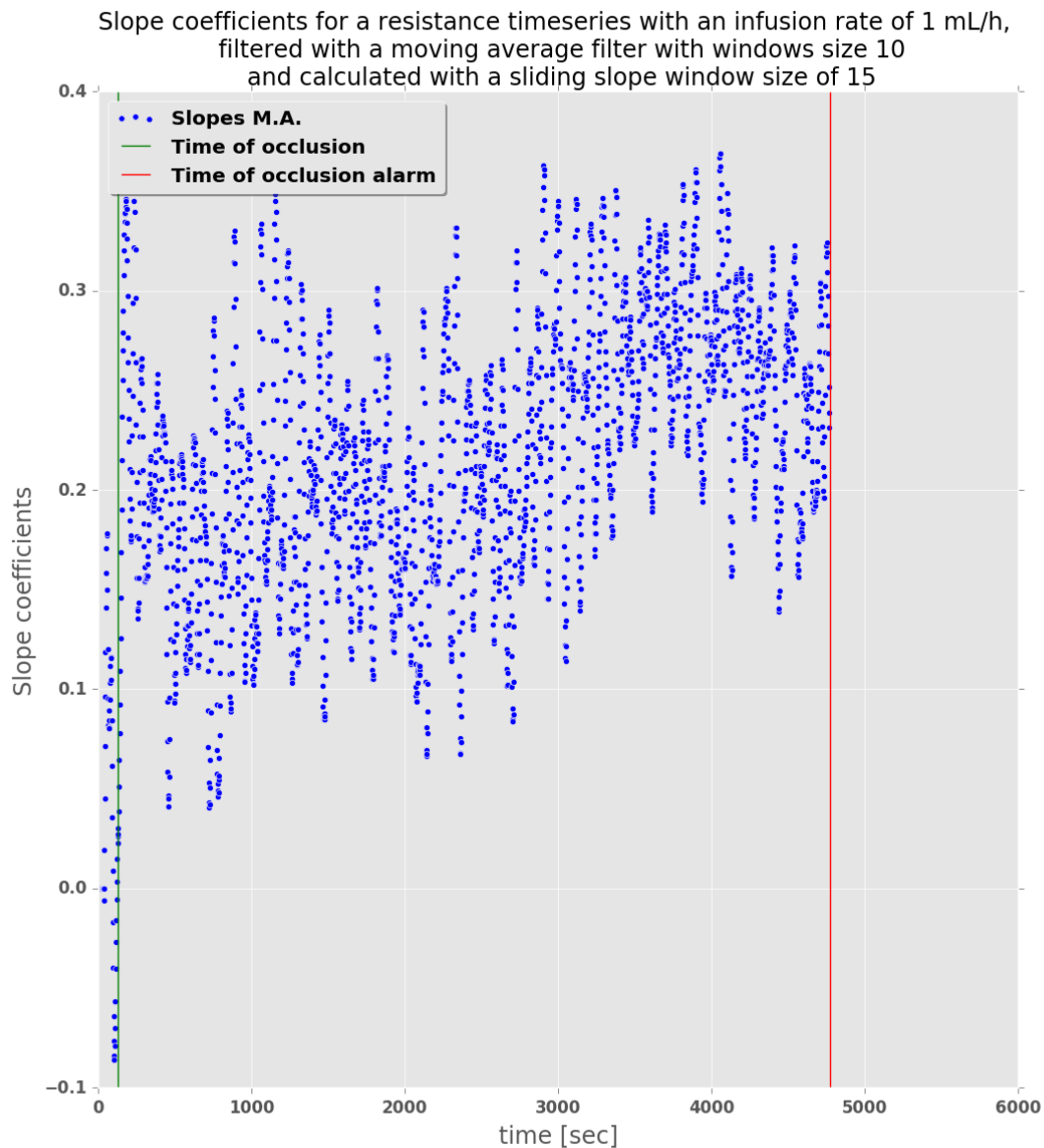


Figure 15: A large spread in sliding slope coefficients, caused by pressure fluctuations at an infusion speed of 1 mL/h. The sliding slope coefficients were calculated over a window size of 10 samples from a moving average filtered resistance time series. However, moving average filtering did not smooth the resistance time series enough to get rid of the pressure fluctuations. The large spread makes the point of occlusion (green vertical line) hard to distinguish.

5.7 Dynamic window size

To reduce the spread in sliding slope coefficient for low infusion rates, a dynamic window size was implemented. By varying the window size for various infusion rates and visually inspecting the resulting time series, window sizes were selected for various infusion rates. The evaluated infusion rates were 1, 2, 5, 10 and 50 mL/h as documented in experiment 11 in the Experiment Book [47]. From the selected window sizes, the model that fitted these values best was determined to be:

$$windowSize = \frac{100}{InfusionRate}$$

In Figure 16 the selected window sizes are plot against their corresponding infusion rates. Moreover, the model is also plotted in this graph.

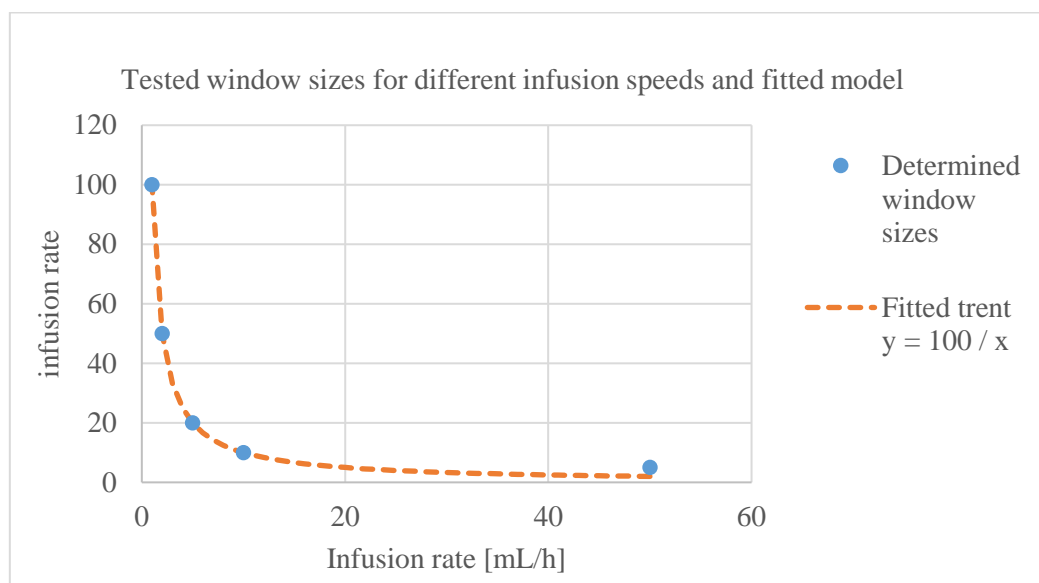


Figure 16: Determined window sizes for infusion rate 1, 2, 5, 10 and 50 mL/h (blue dots) with a fitted trend line (orange-striped line). The fitted trend can be described with the equation $windowSize = 100 / InfusionRate$. The equation will be used to calculate window sizes for the sliding slope coefficient algorithm dynamically, based on infusion rate.

For high infusion rates the model outputs low window sizes. However, a window containing less than 5 samples was determined to output inconsistent values. Therefore, in the sliding slope with dynamic window size algorithm, the minimum window size is set to 5.

The implementation of a dynamic window size in the sliding slope algorithm lead to the reduction in spread of outputted slope coefficients for low infusion rates. The top plot in Figure 17 shows the standard deviation of sliding slope coefficients for a static (top plot) and dynamic (bottom plot) window size. The standard deviation was calculated over the whole slope coefficient time series. In Figure 17, it can be seen that for a static window size the spread in sliding slope coefficients is large, indicating that the time of occlusion will be hard to distinguish. For a dynamic window size, the standard deviations remain more constant, indicating that the time of occlusion will be easier to recognize.

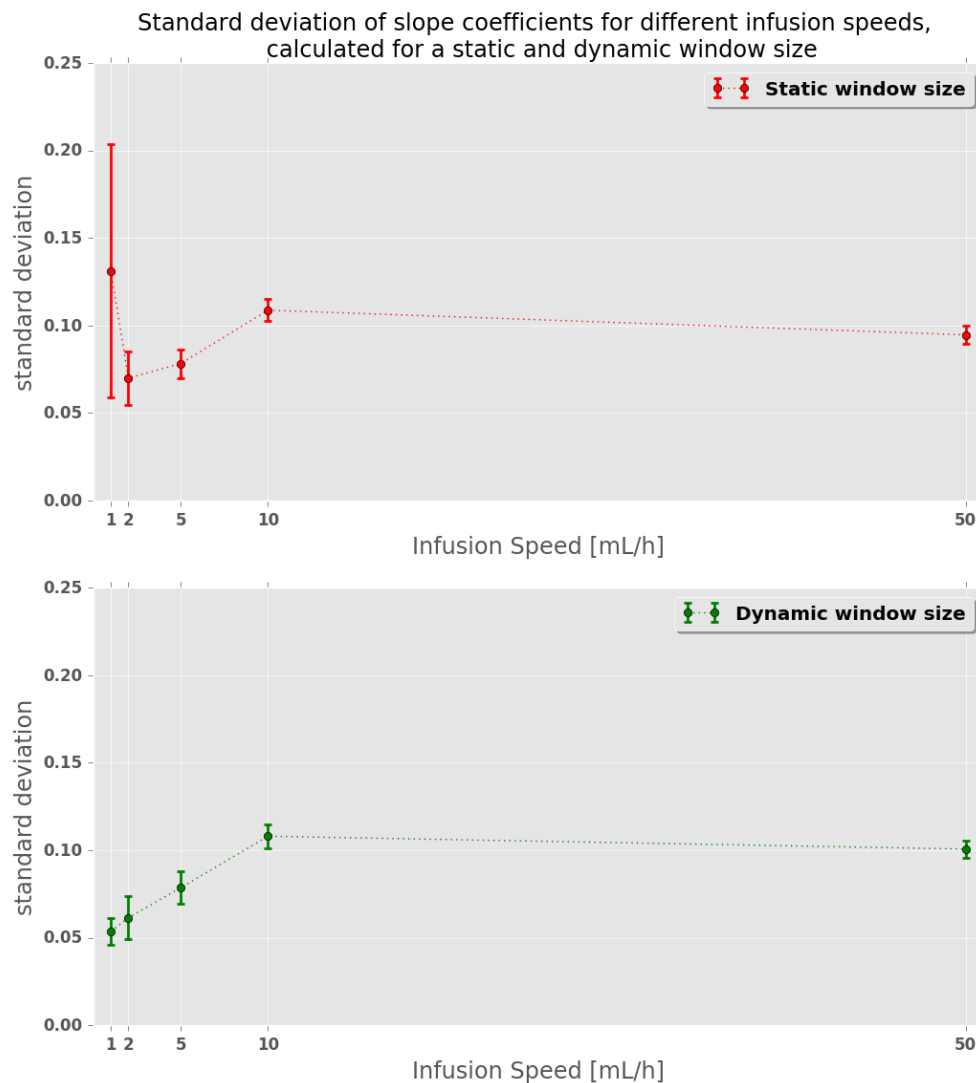


Figure 17: Demonstration of the reduction in sliding slope coefficient spread by using a dynamic window size. Both graphs depict standard deviations of slope coefficients time for infusion rates 1, 2, 5, 10 and 50 mL/h. The spread of each data point is calculated from nine time series. The top plot shows the standard deviations for a static window size. For lower infusion speeds, the spread becomes higher. A high spread indicates large fluctuations, meaning that the time of occlusion alarm will be harder to distinguish, compared to lower infusion speeds. The bottom plot shows standard deviations for a dynamic window size. The standard deviation remains fairly constant for all infusion speeds. This indicates that the fluctuation will be lower, compared to a static window size, making the time of occlusion easier to distinguish.

A problem encountered with the dynamic window size, was that for low infusion rates and a large window size, the algorithm waited for the entire window to fill before calculating the first slope coefficient. For example, at an infusion rate of 1 mL/h, a window size of 100 is calculated. With a sampling frequency of 0.5 Hz, the window will take 198 seconds to fill. Therefore, an initially incrementing window size was implemented. The initial window size is set to 5, and the size will increment till it reaches the calculated window size, at which point in time it becomes a sliding window. This concept is demonstrated by Figure 18.

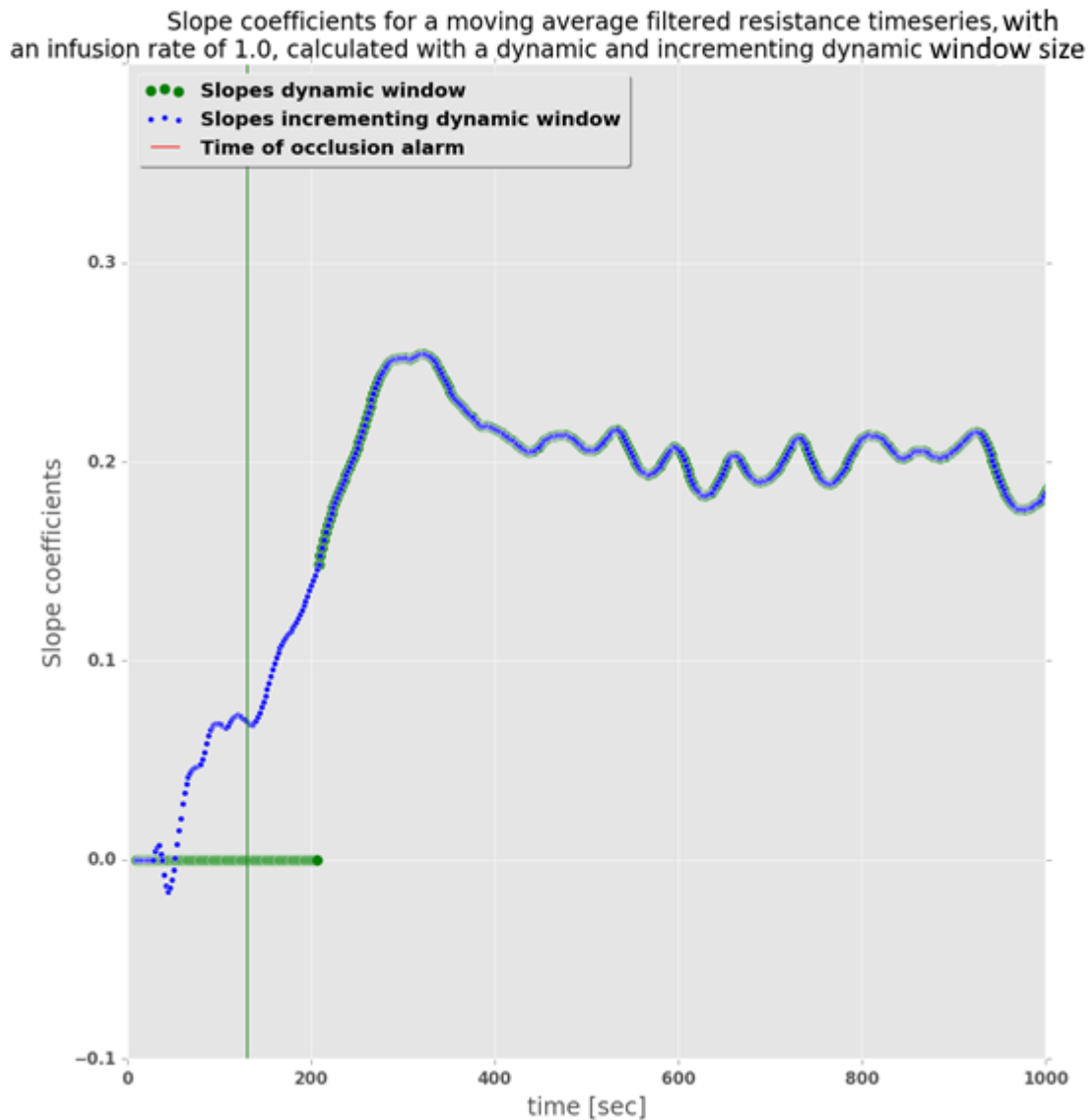


Figure 18: The difference between a sliding dynamic window (green dots) and initially incrementing, sliding window (blue dots). The sliding slope coefficients were calculated from a resistance time series with an infusion rate of 1 mL/h. For the dynamic window, the initial 198 seconds contain zero-values slope coefficients, as the window is not yet full. For the initially incrementing window size, only the first 10 seconds with 5 data points are zero-valued.

5.8 Sliding slope coefficient threshold

To determine the threshold, at which point in time the sliding slope coefficient is marked, the following equation is used:

Equation 3: Equation used to calculate the threshold for the sliding slope coefficient algorithm.

$$Threshold = \frac{average(afterOcclusion) - average(baseline)}{2}$$

This principle is demonstrated by Figure 19, where the average baseline and after occlusion are marked. The threshold lays exactly in the middle and was determined to be 0.09 for the test dataset.



Figure 19: Demonstration of the threshold used for occlusion detection using sliding slope coefficients. The top graph show resistance over time, split up into before (blue dots) and after (green dots) the occlusion. The bottom graph shows the corresponding sliding slope coefficients, also split up into before, labelled baseline, and after, labelled occlusion, the occlusion. From the test-dataset of 45 signals, average slopes baseline and slopes occlusion values were calculated. From these values, the threshold is calculated, using Equation 3.

5.9 Sliding slope coefficient algorithm implementation

Figure 20 depicts a flowchart of the sliding slope coefficient algorithm, used to determine the presence of an occlusion. The input of the algorithm is a pressure time series and infusion rate. From the infusion rate a window size is calculated. The pressure time series is iterated over with a sliding window. This will allow the algorithm to function real-time, once implemented in a centralized processing unit. The algorithm first waits for ten samples, the minimum window size. If the calculated window size is smaller than the number of samples available, an incrementing window is initially used. Then, once the number of samples is equal or higher than the calculated window size, a sliding window is used. Then, the pressure window is converted to resistance. A linear model is fit over the window and the slope coefficient is noted. However, for the incrementing window, the slope coefficient is set to zero if the pressure time series window contains negative values to prevent start-up issues. If the slope coefficient is higher than 0.09, an occlusion alarm is triggered and the algorithm is stopped.

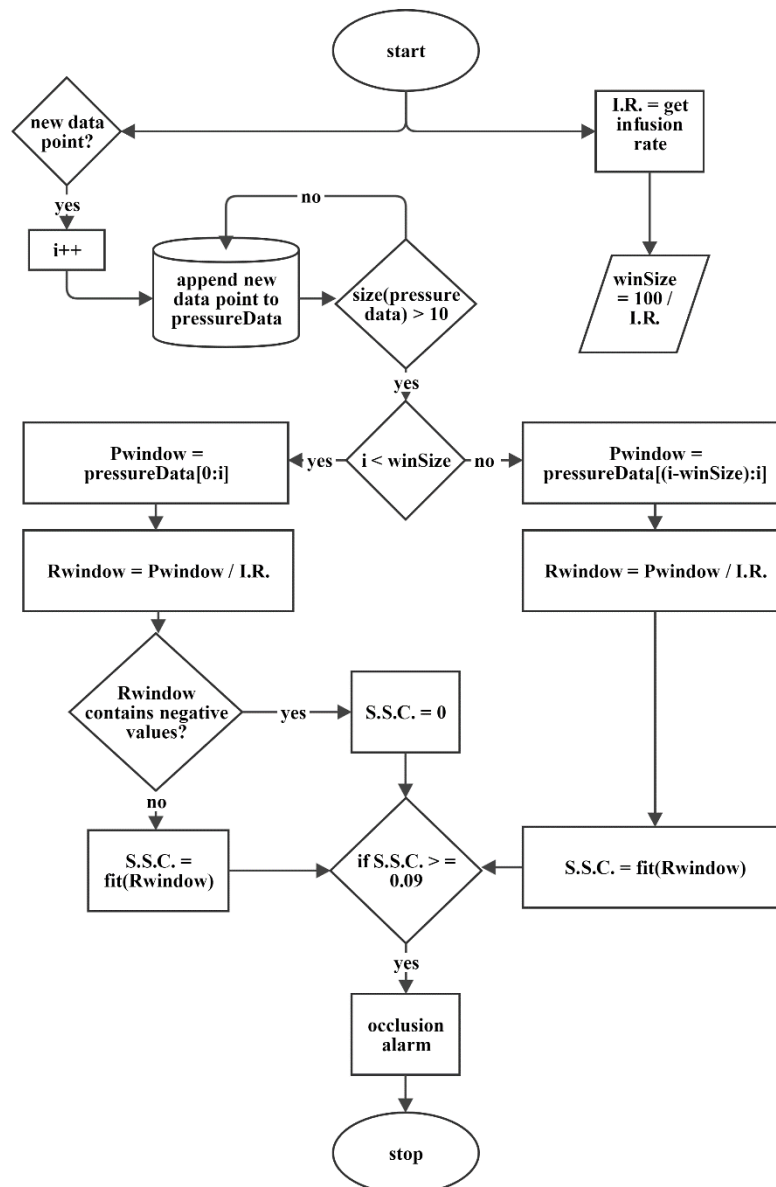


Figure 20: A flowchart of the sliding slope coefficient algorithm, used to determine the presence of occlusions, based on the steepness of a resistance time series curve. The algorithm requires a single pressure time series as input and determines if an occlusion has occurred. Once the algorithm is executed, every new data point is appended to a pressure time series (pressureData). The window size (winSize) is calculated from the infusion rate (I.R.). The algorithm waits until the pressure time series consists of more than 10 samples. Once the pressure time series is more than 10 samples long, a check is done whether the calculated window size can be filled with the pressure time series. If the calculated window size cannot yet be filled, an incrementing window is used. The pressure time series window (Pwindow) is converted to a resistance time series window (Rwindow). If the incrementing window contains negative values, the slope coefficient is set to zero to prevent start-up problems. Then, a linear model is fit over the resistance time series window and the sliding slope coefficient is checked to be above 0.09. If the slope coefficient is higher than 0.09, the occlusion alarm is triggered and the algorithm stops. If the calculated window size can be filled with samples, a sliding window is used. Again, the pressure time series window is converted to resistance and a linear model is fit over the window. If the sliding slope coefficient is larger than 0.09, the occlusion alarm is triggered and the algorithm stops.

The functioning of the algorithm depicted in Figure 20, is demonstrated by Figure 21. In the top plot the resistance over time is depicted. In the middle plot, the sliding slope coefficients over time are depicted. The bottom plot depicts pressure over time. For all plots, the time of occlusion occurrence and pump alarm are marked. For bottom plot the time of occlusion detection is marked as well. The occlusion threshold (horizontal yellow line, middle plot) is determined from the 45 time series in the test-dataset. The occlusion detection (vertical yellow line bottom plot) is determined by the sliding slope coefficient algorithm and is faster in determining occurrence of the occlusion compared to the alarm from the pump.

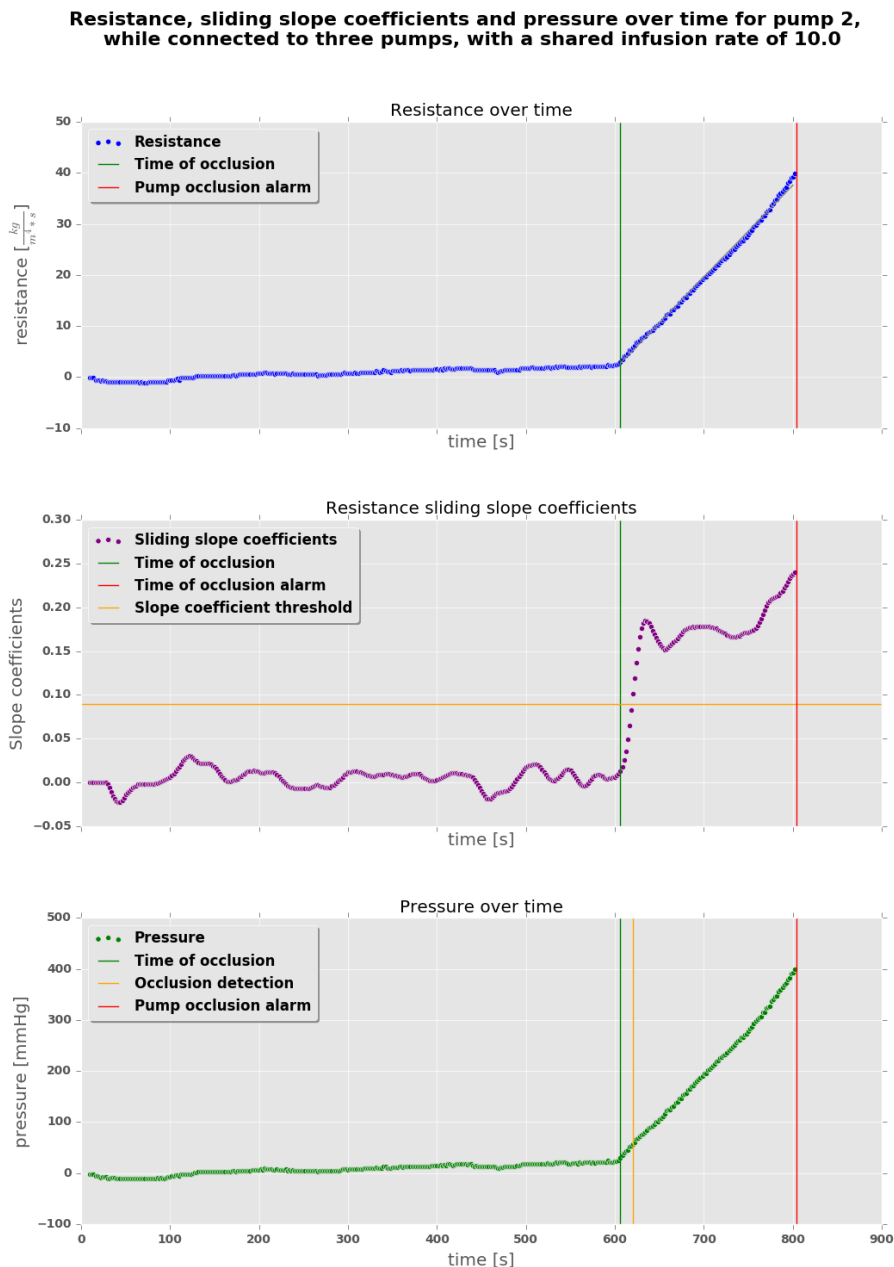


Figure 21: Output of the sliding slope coefficient algorithm depicted in Figure 20. The top graph depicts a resistance time series and the bottom graph the corresponding sliding slope coefficients time series. The locations of the start of occlusion (green line), occlusion detection (yellow line) and occlusion alarm (red line) are marked.

5.10 Sliding slope coefficient algorithm validation

To benchmark the sliding slope coefficient algorithm, a validation-dataset was created. This dataset is aimed at capturing a wide variety of pump configurations and infusion speeds. Three pump configurations were included in the dataset. These configurations are depicted by Figure 22.

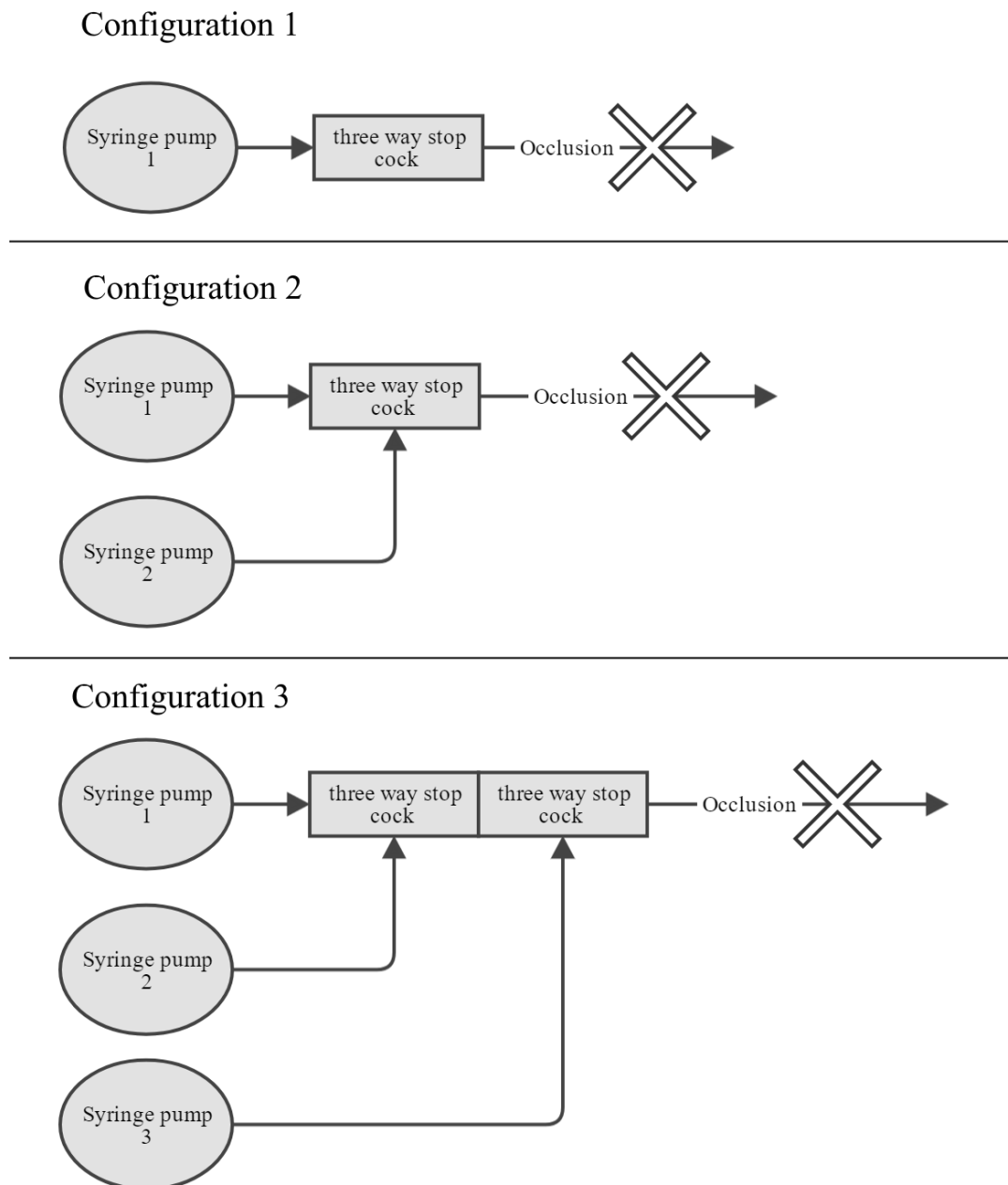


Figure 22: Schematic overview of pump configurations included in the validation-dataset. [48]

The three configurations depicted in Figure 22, were logged for combinations of infusion speeds 1, 5, 10 and 50 mL/h. An overview of the 16 datasets, comprising of 34 time series is given by Table 2.

Table 2: Infusion rates of the validation-dataset, for pump configuration, time series number and pump number. For configurations 1 and 2, not all pumps were used, leading to empty entries are marked by an ‘X’. For configurations 2 and 3, the last two time series comprise of pumps with different infusion speeds.

configuration	time series number	pump		
		1	2	3
1	1	1 mL/h	X	X
	2	5 mL/h	X	X
	3	10 mL/h	X	X
	4	50 mL/h	X	X
2	5	1 mL/h	1 mL/h	X
	6	5 mL/h	5 mL/h	X
	7	10 mL/h	10 mL/h	X
	8	50 mL/h	50 mL/h	X
	9	1 mL/h	50 mL/h	X
	10	5 mL/h	10 mL/h	X
3	11	1 mL/h	1 mL/h	1 mL/h
	12	5 mL/h	5 mL/h	5 mL/h
	13	10 mL/h	10 mL/h	10 mL/h
	14	50 mL/h	50 mL/h	50 mL/h
	15	1 mL/h	10 mL/h	50 mL/h
	16	5 mL/h	5 mL/h	10 mL/h

Using the 16 time series in the validation-dataset, the sliding slope coefficient algorithm was benchmarked. From the 34 time series, the algorithm incorrectly marked the occlusion point in time for one time series. For the other 33 the location was correctly marked, with an average decrease in time to occlusion detection of 86%. The average time to pump alarm and average time to occlusion alarm are presented in Table 3. The complete results of the benchmarking on the validation dataset is given in Appendix D.

Table 3: Overview of the benchmarking results for the sliding slope coefficient algorithm on the validation-dataset. The infusion speed(s) for each dataset are given, with average time to occlusion detection and pump alarm. The last columns give the average decrease, expressed as a percentage and as a factor.

Pump configuration	Infusion speed(s)	Average time to occlusion detection [s]	Average time to pump alarm [s]	Average decrease [%]	Factor decrease
1	1	96.04	2555.69	96.24	26.61
	5	24.02	420.18	94.28	17.49
	10	16.03	204.12	92.15	12.73
	50	5.99	19.99	70.04 *	3.34 *
2	1	88.04	2451.74	96.41	27.85
	5	24.01	484.19	95.04	20.17
	10	11.01	204.08	94.61	18.54
	50	12.00	30.00	60.02	2.50
	1, 50	22.05	68.05	67.60 **	3.09 **
	5, 10	22.00	280.08	92.15	12.73
3	1	86.75	1816.78	95.23	20.94
	5	24.68	398.16	93.80	16.14
	10	14.66	198.05	92.60	13.51
	50	10.01	34.03	70.58	3.40
	1, 10, 50	30.01	88.02	65.91	2.93
	5, 5, 10	20.68	268.10	92.29	12.96

* Deviant value due to 8 second error in time of occlusion occurrence, caused by a delay in the logging of the first IDA 4 value

** Deviant value due to missing data point as the algorithm incorrectly marked the time of occlusion before the occurrence of the occlusion

5.11 Occlusion localization

After an occlusion has been detected, cross-correlation can be used to determine which pumps share the occlusion. This principle is demonstrated by Figure 23 and Figure 24. When two pumps share an occlusion, both their pressure signals will increase. Therefore, the pressure time series will be similarly shaped. By cross-correlating the signals from the pump that has detected the occlusion with the signals from other pumps, a high correlation will be found for pumps that share the occlusion.

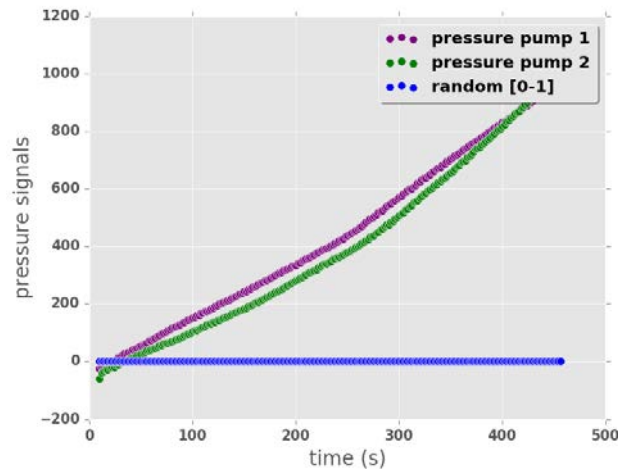


Figure 23: This graph contains three time series: two pressure time series, recorded by two pumps that have a shared occlusion, and one time series with random values between zero and one. It is expected that the two pressure time series share a high cross-correlation and random with the pressure time series a lower correlation.

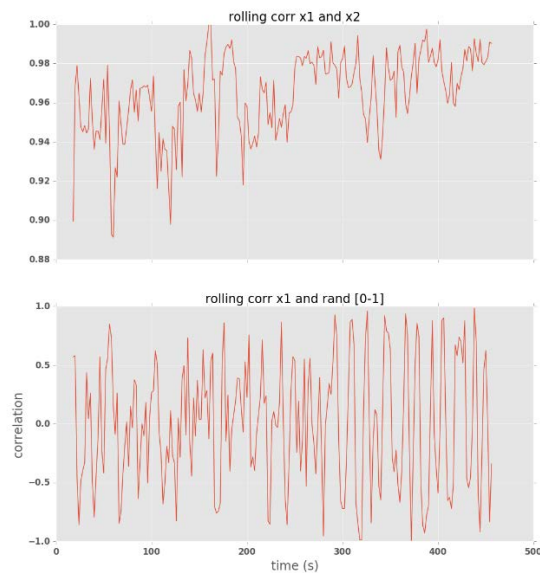


Figure 24: Rolling correlation values for pressure time series depicted in Figure 23. x_1 and x_2 are pressure signals 1 and 2, respectively, and have a very high correlation between 0.9 and 0.99. x_1 and the random signal between zero and one, have highly variant correlation between -1 and 1.

6

DISCUSSION, CONCLUSION & RECOMMENDATIONS

The conclusions drawn from this project will be presented and discussed in this chapter. Moreover, recommendation will be given for future steps.

6.1 Conclusion

To determine a method for occlusion detection and localisation in a centralized system, both literature and applied research were conducted. The causes for hard occlusions in infusions systems include closed stopcocks, kinked IV tubing, kinked catheters, air-locks and thrombophlebitis [10], [18]. Nurses from the ICU indicated that closed stopcocks were the most frequent cause for occlusions (appendix B).

The creation of a centralized processing unit was achieved using the serial connection on the Alaris GH syringe pumps and a RS-232 hub connected to a computer. The syringe pumps were controlled and logged using a JAVA interface in which multiple pumps can be logged simultaneously. With each connected pump a new thread is created (also called multithreading) to make the interface scalable. Data is sampled with a frequency of 0.5 Hz, as was determined to be optimal in experiment 3 in the Experiment Book for a multi-pump setup, when connected via a RS-232 hub [39]. Synchronised sampling was achieved with the implementation of a shared and timed buffer, of which the proper functioning is demonstrated in experiment 8 in the Experiment book [44].

Time to occlusion alarm was successfully reduced with the sliding slope coefficient algorithm depicted in Figure 20. However, this was not achieved by combining the signals from multiple pumps but by using resistance slope steepness instead of pressure. A validation-dataset of 30 signals was created, in which a variety of pump configurations and infusion speeds were included (Table 2). Benchmarking on the validation-dataset resulted in a reduction of time to occlusion alarm by 86% on average.

A method for occlusion localization that combines the pressure sensor information from multiple pumps was theoretically established but requires further testing. This method requires a digitized map of the fluid pathway, which will have to be entered manually. Figure 24 demonstrates that rolling cross-correlation can be used to match pumps that share an occlusion. When both the infusion pumps that share an occlusion and the fluid pathway are known, fluid pathway in which the occlusion most likely has occurred can be marked.

To conclude, a centralized processing unit in which multiple pressure signals from Alaris GH syringe pumps are logged, was successfully developed. Although the work presented here has not yet combined pressure signals from multiple pumps, groundwork for the exploration of this principle has been laid. A new algorithm for automatic occlusion detection that utilizes a single signal was successfully implemented and reduced the time to occlusion alarm by 86% on average. A reduction in time to occlusion alarm will result in increased patient safety by limiting suboptimal drug delivery. Future implications of the algorithm include the reduction of false alarms and the detection of soft occlusions, leading to decreased alarm fatigue and increased patient comfort. Moreover, a method for occlusion localization was theoretically established but requires further testing.

6.2 Discussion

When the same experiment was repeated multiple times, a spread in time to pump occlusion alarm was observed. The two main suspected factors were pump and syringe variances. By repeating the same experiment for a combination of pumps and syringes, it was determined that pump variances were insignificant whereas syringe variances were significant in experiment 4 in the Experiment Book [40]. The variances are likely caused by manufacturing margins, causing differences in syringe-plunger friction.

Testing indicated a reduction in time to occlusion detection for the sliding slope coefficient algorithm when compared to the current pump occlusion alarm. However, as is, the algorithm will also increase the number of false positives. On the validation-dataset of 30 time series, one occlusion was incorrectly determined (Figure 42, Appendix D). For one more time series the threshold was almost reached, while no occlusion was present (Figure 33, Appendix D). Syringe-plunger friction causes start-up fluctuations leading to large sliding slope coefficients. Moreover, initial pressure values are often negative, causing a steep rise in pressure once the pressure increases to more realistic values. Negative pressure values are an incorrect result of the Alaris GH measurement method that utilizes a strain gauge, calibrated to pressure values. The issue of large initial sliding slope coefficients might be solved by creating more restrictions on initial data, such as negative pressure value restrictions on the sliding window or limits on the initial sliding slope coefficient values.

The flow rate of the Alaris GH syringe pumps is regulated by turning off and on the pump motor. In some situation this can cause a repeated overshoot throughout the time series. This phenomena is clearly visible at an infusion rate of 50 mL/h (Figure 39, Figure 43, Figure 54, Figure 55 and Figure 58 in appendix D) but does not seem to occur in all 50 mL/h time series (Figure 31 and Figure 53 in appendix D). This causes the sliding slope coefficient to be abnormally large. This did not cause incorrect detection of occlusion on the validation-dataset but might on a larger dataset.

In one situation (Figure 31, appendix D) the time of occlusion occurrence was marked 8 seconds late. The occlusion is caused by the starting of an occlusion test on IDA 4. When the test is started, the data from the IDA 4 is logged. The time of occlusion was marked when the first IDA 4 data point was logged. In this case, a delay is introduced causing the occlusion location to be marked late by 8 seconds. The delay is most likely caused by internal delay by the IDA 4, as well as the RS-232 connection in combination with the shared and timed buffer.

6.3 Recommendations

The sliding slope coefficient algorithm is currently threshold based. I recommend investigating a standard deviation, sliding window based, peak detection algorithm as a solution to current start-up issues. To further improve the performance of the algorithm, I recommend creating a larger database in which more pump configurations and infusion speeds are included as well as different fluid viscosities. The sliding slope algorithm seems to detect occlusion slower for situations where different infusion speeds are used for pumps that have a shared occlusion. Therefore I recommend that these situations are extensively analysed. By evaluating the behaviour of the algorithm in more situations, parameters such as the sliding slope threshold, initial window size and dynamic window size can be tweaked to make the algorithm more robust.

Before deciding on a final design for the implementation of an occlusion detection and localization algorithm, I advise to first investigate other possible implementations. Below two suggestions are made. Furthermore, a dynamic pressure threshold can be used as safeguard in the first series of implemented occlusion detection modules. A pressure threshold will ensure that the number of false positives is kept to a minimum.

- Cross-correlation between measured and modelled signals: the cross-correlation between a modelled output, without occlusions, and a measured signal, is a measure of difference between measured and expected. The model will be based on the syringe pumps' flow rate, resistance and topology of its fluid pathways. By creating a large dataset of pressure signals without occlusions, normal pressure ranges can be obtained for flow rates and IV line configurations. Using these ranges, the model can be tweaked to output realistic values.
- Autocorrelation between historical data: the correlation between incoming data and time shifted data can be used as a measure of change over time. When no present is occurring, it is expected that the autocorrelation for a signal is close to 1, indicating a strong correlation. However, when an occlusion occurs, the correlation of that signal with a time shifted version of itself, will decrease, indicating a weaker correlation.

Equation 4: Autocorrelation function for discrete, weakly stationary, real-valued, stochastic time series [49]

$$acorr(f[n], l) = \sum_{m=-\infty}^{\infty} f[m]f[m-l]$$

To start implementing the occlusion localization, a dataset should be created in which more complex pump configurations are included. Rolling cross-correlation time series should be calculated, as in Figure 24, and classified as having a shared occlusion or not. Then a method of automatically placing signals in one or the other class has to be developed. If the two classes (shared occlusion and no occlusion) are separable by a threshold then a thresholding method can be used. I suspect however that this won't work based on Figure 24. Time series that are dissimilar have a rolling cross-correlation time series that jumps up and down more compared to a two similar time series. Therefore, a method that calculates the standard deviation over the cross-correlation time series using an incrementing window might be used to differentiate the two classes.

BIBLIOGRAPHY

- [1] F. Halderman, "Selecting a vascular access device," *Nursing*, vol. 30, no. 11, pp. 59-61, 2000.
- [2] M. N. Winslow, L. Trammell and D. Camp-Sorrell, "Selection of vascular access devices and nursing care.," *Seminars in Oncology Nursing*, vol. 11, no. 3, pp. 73-167, 1995.
- [3] J. S. Mosby, *Mosby's Medical Dictionary*, Philadelphia, Pennsylvania: Elsevier Health Sciences, 2013.
- [4] Health Canada Population and Public Health, "Preventing infections associated with indwelling intravascular access devices," *Canada communicable disease report*, vol. I, no. 8, pp. 1-32, 12 1997.
- [5] N. P. O'grady, M. Alexander, L. A. Burns, E. P. Dellinger, J. Garland, S. O. Heard, P. A. Lipsett, H. Masur, L. A. Mermel, M. L. Pearson and others, "Guidelines for the Prevention of Intravascular Catheter-related Infections," *Clinical Infectious Diseases*, vol. 52, no. 9, pp. e162-e193, 2011.
- [6] R. A. Peterfreund and J. H. Philip, "Critical parameters in drug delivery by intravenous infusion," *Expert opinion on drug delivery*, vol. 10, no. 8, pp. 1095-1108, 2013.
- [7] B. Décaudin, S. Dewulf, D. Lannoy, N. Simon, A. Secq, C. Barthélémy, B. Debaene and P. Odou, "Impact of multiaccess infusion devices on in vitro drug delivery during multi-infusion therapy," *Anesthesia & Analgesia*, vol. 109, no. 4, pp. 1147-1155, 2009.
- [8] R. P. Dellinger, M. M. Levy, A. Rhodes, D. Annane, H. Gerlach, S. M. Opal, J. E. Sevransky, C. L. Sprung, I. S. Douglas, R. Jaeschke and others, "Surviving Sepsis Campaign: international guidelines for management of severe sepsis and septic shock," *Intensive care medicine*, vol. 39, no. 2, pp. 165-228, 2012.
- [9] E. Rivers, B. Nguyen, S. Havstad, J. Ressler, A. Muzzin, B. Knoblich, E. Peterson and M. Tomlanovich, "Early goal-directed therapy in the treatment of severe sepsis and septic shock," *New England Journal of Medicine*, vol. 345, no. 19, pp. 1368-1377, 2001.
- [10] S. M. Gouveia, "In-line pressure monitoring in IV infusions: benefits for patients and nurses," *British Journal of Nursing*, vol. 19, no. 25, pp. S28-S33, 2016.
- [11] C. Claunch, "Top 10 Health Technology for 2011," *Health Devices*, vol. 39, no. 11, pp. 389-390, 2010.
- [12] Thames Valley Cancer Network, "guidelines on treatment of extravastion thames valley cancer cytotoxic drugs," 2014.

- [13 Fluke, “IDA 4 Plus Infusion Device Analyzer Operational Manual,” Fluke Biomedical,
] Carson, 2003.
- [14 Fluke , “IDA 4 Plus Graphics Software Hydrograph,” Fluke Biomedical, Carson, 2005.
]
- [15 F. Doesburg, “Developing a System for Integrated Automated Control of Multiple
] Infusion Pumps: The Multiplex Infusion System,” University of Groningen, 2013.
- [16 N. Normalisatie-instituut, “NEN-EN-IEC 60601-2-24,” *Medical electrical equipment -
] Part 2-24*, 2015.
- [17 S. Fletcher, “Catheter-related bloodstream infection,” *Continuing Education in
] Anaesthesia, Critical Care & Pain*, vol. 5, no. 2, pp. 49-51, 2005.
- [18 B. Butterfield, “Monitoring and Detection of IV line occlusions,” *Research Fellow. Alaris
] Medical Systems*, vol. 1, no. 1, pp. 1-3, 2010.
- [19 J. L. Baskin, C.-H. Pui, U. Reiss, J. A. Wilimas, M. L. Metzger, R. C. Ribeiro and S. C.
] Howard, “Management of occlusion and thrombosis associated with long-term indwelling
central venous catheters,” *The Lancet*, vol. 374, no. 9684, pp. 159-169, 2009.
- [20 J. Arai, Y. Mouri and Y. Miyamoto, “Detection of peripherally inserted central catheter
] occlusion by in-line pressure monitoring,” *Pediatric Anesthesia*, vol. 12, no. 7, pp. 621-
624, 2002.
- [21 Cardinal Health, Inc., “Alaris® GH Syringe Pump Directions For Use,” Cardinal Health,
] Inc., 2006.
- [22 D. Doellman, L. Hadaway, S. Al-Benna, C. O’Boyle and J. Holley, “Extravasation
] Injuries in Adults,” *ISRN Dermatology*, vol. 32, no. 4, pp. 203-211, 2009.
- [23 C. Lake and C. Beecroft, “Extravasation injuries and accidental intra-arterial injection,”
] *Continuing Education in Anaesthesia, Critical Care & Pain*, vol. 10, no. 4, pp. 109-113,
2010.
- [24 B. Reynolds, “Neonatal extravasation injury: case report,” *Infant*, vol. 3, no. 6, pp. 230-
] 232, 2007.
- [25 C. M. Rowan, K. E. Miller, A. L. Beardsley, S. S. Ahmed, L. A. Rojas, T. L. Hedlund, R.
] H. Speicher and M. E. Nitu, “Alteplase use for malfunctioning central venous catheters
correlates with catheter-associated bloodstream infections,” *Pediatric Critical Care
Medicine*, vol. 14, no. 3, pp. 306-309, 2013.
- [26 J. Thigpen, “Peripheral intravenous extravasation: nursing procedure for initial
] treatment,” *Neonatal Network*, vol. 26, no. 6, pp. 379-384, 2007.
- [27 S. Masoorli, “Pediatrics: small children at high risk,” *Journal of the Association of
] Vascular Access*, vol. 8, no. 3, pp. 42-43, 2003.

- [28 J. Wolf, L. Tang, J. E. Rubnitz, R. C. Brennan, D. R. Shook, D. C. Stokes, P. Monagle,
] N. Curtis, L. J. Worth, K. Allison and others, “Monitoring central venous catheter
resistance to predict imminent occlusion: a prospective pilot study,” *PloS one*, vol. 10, no.
8, p. e0135904, 2015.
- [29 Elveflow, “Microfluidic Inline Pressure Sensor,” 2016. [Online]. Available:
] [http://www.elveflow.com/microfluidic-flow-control-products/microfluidic-flow-control-
module/mfp-microfluidic-inline-pressure-sensor/](http://www.elveflow.com/microfluidic-flow-control-products/microfluidic-flow-control-module/mfp-microfluidic-inline-pressure-sensor/). [Accessed 7 3 2017].
- [30 M. Medikal, “Alaris GH - General Syringe Pump,” *Tüm Hakları Saklıdır*.
]
- [31 M. Wessels, “Picture of motor baseplate of the Alaris GH, containing the motor bearing
] and strain gauge,” *Photograph*, 2017.
- [32 D. M. Raymer and D. E. Smith, “Spontaneous Knotting of an agitated string,”
] *Proceedings of the National Academy of Sciences*, vol. 104, no. 42, pp. 16432-16437,
2007.
- [33 R. Bracewell, “Pentagram Notation for Cross Correlation,” McGraw-Hill, New York,
] 1965.
- [34 M. Wessels, “Conceptual model of the occlusion detection and localisation algorithm,”
] *Gliffy.com*, 2017.
- [35 M. Wessels, “Schematic of an example test setup,” *Paint.net*, 2017.
]
- [36 M. Wessels, “Experiment book - Occlusion detection and localisation,” 2017.
]
- [37 M. Wessels, “Experiment 1 - Calibration values IDA 4 infusion device analyzer,”
] *Experiment Book - Occlusion detection and localization*, pp. 12-17, 2017.
- [38 M. Wessels, “Experiment 2 - Update frequency of the Alaris GH syringe pump,”
] *Experiment Book - Occlusion detection and localization*, pp. 18-24, 2017.
- [39 M. Wessels, “Experiment 3 - Update frequency Alaris GH verification,” *Experiment Book*
] *- Occlusion detection and localization*, pp. 25-30, 2017.
- [40 M. Wessels, “Experiment 4 - Pump and syringe time to occlusion alarm variance,”
] *Experiment Book - Occlusion detection and localization*, pp. 31-37, 2017.
- [41 M. Wessels, “Experiment 5 - Time to alarm for different infusion speeds,” *Experiment*
] *Book - Occlusion detection and localization*, pp. 38-42, 2017.
- [42 M. Wessels, “Experiment 6 - Validation Alaris GH and IDA 4,” *Experiment Book -*
] *Occlusion detection and localization*, pp. 43-48, 2017.

- [43 M. Wessels, “Experiment 7 - Removing redundant data,” *Experiment Book - Occlusion detection and localization*, pp. 48-52, 2017.
- [44 M. Wessels, “Experiment 8 - Synchronised sampling,” *Experiment Book - Occlusion detection and localization*, pp. 53-57, 2017.
- [45 M. Wessels, “Experiment 9 - Sliding slope detection and moving average window size,” *Experiment Book - Occlusion detection and localization*, pp. 58-64, 2017.
- [46 M. Wessels, “Experiment 12 - Occlusion detection by resistance slope steepness thresholding,” *Experiment Book - Occlusion detection and localization*, pp. 83-91, 2017.
- [47 M. Wessels, “Experiment 11 - Sliding slope coefficient variances and infusion speed,” *Experiment Book - Occlusion detection and localization*, pp. 71-82, 2017.
- [48 M. Wessels, “Validation-dataset configurations,” *gliffy.com*, 2017.
- [49 P. Dunn, “Measurement and Data Analysis for Engineering and Science,” McGraw–Hill, New York, 2005.
- [50 Google, “Google Scholar,” [Online]. Available: <https://scholar.google.nl/>. [Accessed 6 3 2017].
- [51 Espacenet, “Smart search,” [Online]. Available: https://worldwide.espacenet.com/help?locale=en_EP&topic=smartsearch&method=handleHelpTopic. [Accessed 6 3 2017].
- [52 D. Halbert, “Fluid line occlusion detection system and methods”. United States Patent 9,272,087, 2016.
- [53 S. Keith, “System and method for detecting occlusions in a medication infusion system using pulsewire pressure signals”. United States Patent 61,713,096, 2014.
- [54 S. A. Denis and S. Williams, “Occlusion detection method”. United States Patent US2013238261, 2013.
- [55 K. Geoffrey, “Infusion device occlusion detection system”. US Patent US2014276537, 2014.
- [56 B. Pope, “Syringe Pump Rapid Occlusion Detection System”. United States Patent 8182461, 2012.
- [57 J. L. Favreau, “Occlusion detection using pulse-width modulation and medical device incorporating same”. United States Patent 0253420, 2013.
- [58 J. A. DelCastilio and A. Yardimci, “System and method for detecting occlusion using flow sensor output”. United States Patent 0177148, 2009.

- [59 R. D. Butterfield, “Upstream Occlusion Detection”. United States Patent 6358225, 2002.
]
- [60 L. S. Wood and S. M. Gullo, “IV vesicants: How to avoid extravasation,” *Am J Nurs*, pp. 42-45, 1993.
]
- [61 A. Margulies, Y. Wengström and A. Margulies, “European oncology nursing society extravasation guidelines,” *European Journal of Oncology Nursing*, vol. 12, no. 4, pp. 357-361, 2008.
]
- [62 L. Olivier, D. Kendoff, U. Wolfhard, D. Nast-Kolb, M. N. Yazici and H. Esche, “Modified syringe design prevents plunger-related contamination—results of contamination and flow-rate tests,” *Journal of Hospital Infection*, vol. 53, no. 2, pp. 140-143, 2003.
]
- [63 F. Doesburg and W. Bult, “Van medicatie verenigbaarheid tot multiplex infusie,” p. 10, 2015.
]
- [64 R. L. Mott and J. A. Untener, *Toegepaste Stromingsleer*, Pearson Benelux B.V., 2014.
]
- [65 R. Snijder, “Physical causes of dosing errors in patients receiving multi-infusion therapy,” *Utrecht University*, 2016.
]
- [66 M. Wessels, “Experiment 10 - Pressure and resistance slope steepness during occlusion,” *Experiment Book - Occlusion detection and localization*, pp. 65-70, 2017.
]

APPENDIX A

PATENT RESEARCH ON IV-LINE OCCLUSION

DETECTION SYSTEMS

Research method

The search engines used in this patent research were Google Scholar [50] and Espacenet Smart Search [51]. The search terms used were a combination of: 'IV', 'intravenous', 'occlusion', 'detection'. Results older than January 2000 were considered but filtered out due to outdated hardware. The following is list of found patents with a summary system and methods.

Patents

2016, Fluid Line Occlusion Detection System And Methods [52]

Summary Occlusion detection system and method for volumetric IV pumps. Utilizes at least one pressure sensor along a downstream fluid line. The method revolves around giving a bolus and measuring the pressure decay to calibrate the system.

2016, System and method for detecting occlusions in a medication infusion system using pulsewise pressure signals [53]

Summary: Occlusion detection system and method that measures the pressure of a medication fluid path using a downstream fluid detector. Compares the minimum pressure of the current interval to a predetermined threshold pressure. This threshold is based on a calculation taking into account peak pressure and minimum pressure of the previous interval. The system registers an occlusion if the current minimum pressure is less than the threshold.

2015, Occlusion detection method [54]

Summary: Occlusion detection method for volumetric Iv pumps using an upstream and downstream occlusion sensor. Includes automatic detection of changes made to the system, such as changes of patient or IV-lines. If the system detects changes, it will recalibrate its baselines. The occlusion detection is based on a pressure slope and running averages of pressure.

2014, Infusion device occlusion detection system [55]

Summary: Syringe pump device with occlusion detection. Measures residual sum values and loads them into a running weighted average filter. If the output of this filter is higher than the nominal filter output by a threshold difference, the system sounds an occlusion alarm.

2012, Syringe pump rapid occlusion detection system [56]

Summary: A syringe pump system and method for detecting occlusions. The system utilizes a force measurement, which it compares to a predetermined relationship. The occlusion detection method is based on determining the slope of the measurements and whether the measurements are steady state.

2012, Occlusion detection using pulse-width modulation and medical device incorporating same [57]

Summary: A system design for a volumetric IV pump, which utilizes the duty cycle send to the motor as an indication of occlusions. When an occlusion occurs, the motor needs to work harder, resulting in the control unit increasing the duty cycle. The duty cycle is compared to historical data to determine occlusions.

2011, System and method for detecting occlusion using flow sensor output [58]

Summary: System and method for detecting occlusion in a volumetric IV pump setup. The system uses a downstream flow sensor. An occlusion is registered if the filtered flow output is below a threshold. The filter consists of a ten second backwards moving average filter. The patent includes a second, more sophisticated method. An FFT of the flow sensor signal is computed. The threshold is set to the signal strength of normal pumping.

2002, Upstream occlusion detection system [59]

Summary: Method for detecting occlusion in a volumetric IV pump setup. Utilizes a downstream pressure sensor to detect upstream occlusion. The pressure threshold for an occlusion alarm is based on the pressure difference between the pump and the downstream sensor.

Results

An overview of patents registered from January 2000 till March 2017 can be seen in Table 2. Most patents on occlusion detection systems for IV therapy rely on a pressure sensor placed along the IV-lines. Systems containing a syringe pump, utilize a downstream pressure sensor. Systems containing a volumetric pump can also utilize an upstream pressure sensor. There is one patent registered under number US2005096593 that utilizes force measurements inside the pump, like the Alaris GH.

Most detection methods measure pressure development over time. These measurements are used to calculate averages, slopes and resistances. The patent under number US9272087 relies on giving a bolus and measuring the pressure decay over time to obtain a pressure profile. This profile it compared to a nominal profile. The differences between profiles are used as an indication of occlusion presence. Not all found methods are based on pressure measurements, the patent under number US7880624 is purely based on flow measurements.

Table 4: Patent title, number, year, type of sensor and short description of detection method for occlusion detection systems between 2000 and March 2017. A more detailed description is available in Appendix A.

Patent Title	Patent Number	Year	Sensor description	Detection method
Fluid Line Occlusion Detection System And Methods	US9272087 B2	2016	Downstream pressure	Give bolus and measure pressure decay
Occlusion detection method	US2013238261	2015	Upstream and downstream pressure	Pressure slope and running average of pressure compared to threshold
System and method for detecting occlusions in a medication infusion system using pulsewise pressure signals	US2017035965	2014	Downstream pressure	Compare minimum pressure of current interval to threshold
Infusion device occlusion detection system	US2014276537	2014	Downstream pressure	Weighted average of residual sum values of pressure compared to nominal filter output
Syringe pump rapid occlusion detection system	US2005096593 A1	2012	Force measurement inside pump	Compare force measurement to a predetermined relationship
Occlusion detection using pulse-width modulation and medical device incorporating same	US9344024 B2	2012	Duty cycle send to motor	Duty cycle is compared to historical duty cycles.
System and method for detecting occlusion using flow sensor output	US7880624 B2	2011	Downstream flow	Filtered flow output below a threshold
Upstream occlusion detection system	WO1997007843 A1	2002	Downstream pressure sensor	Pressure difference between pump pressure and downstream pressure compared to threshold

APPENDIX B

INTERVIEWS ADULT INTENSIVE CARE NURSES

Questions asked

To gain insight into the use of the Alaris GH syringe pump, interviews were held with the people who use them most, namely the nurses. On the 21st of March 2017, five nurses of the Adult Intensive Care were asked the following questions:

1. What are common infusion rates for syringe pumps?
2. What steps do you take in after an occlusion alarm sounds?
3. Do you change the threshold pressure for an occlusion alarm?
4. What occlusion causes have you encountered?
5. Do you think it would be useful to have a system that provides occlusion locations?
6. Approximately how many occlusion alarms do you encounter per week?
7. How many of those are false alarms?

Interview answers

Interviewee 1

1. 0.5 to 10 ml/h
2. Stop the pump, check for the cause, fix the cause, start the pump
3. Almost never, however after an occlusion alarm went off the pressure threshold is automatically increased
4. Nine out of ten times a stopcock is closed, however sometimes a precipitation decreases the lumen to the extent that an occlusion alarm is triggered. Precipitations can for instance be caused by a patient coughing, due to the increase in blood pressure, blood is forced into the IV-line
5. No, it would not save me that much time.
6. Two times per week
7. None that I recall

Interviewee 2

1. 1 to 10 ml/h
2. Stop the pump, check the IV-line for kinks or closed stopcocks, start the pump
3. Never
4. Kink in IV-line, precipitations due to medicine reacting
5. I do not think it would save a lot of time since there are not many occlusion alarms
6. Once a week
7. Once a month

Interviewee 3

1. Minimally 3 ml/h
2. Stop the pump, check for closed stopcocks and straighten the line start the pump. If the alarm goes off again, flush the IV-line, start the pump
3. Yes, when two lines are infused with a large difference in infusion rate, I put the pressure threshold up to 700 mmHg instead of 400 mmHg
4. Kink in IV-line, closed stopcock, multiple lines with large difference in infusion rate
5. Maybe, not a lot of the alarms are occlusion alarms
6. Four times a week
7. Once a week or more

Interviewee 4

1. 0.5-100 ml/h
2. Look for an obvious cause for the occlusion and fix it. If I do not see the cause immediately, I reset the infusion pump and start it again.
3. Yes, when multiple lines are linked together
4. Kink in the IV-line, closed stopcock, patient lying on the IV-line
5. I do not think the system would be useful we do not spend a lot of time on finding the cause for the occlusion
6. Twice a week
7. Almost never

Interviewee 5

1. Under 10 ml/l
2. Stop the pump, look for cause, fix it, start the pump again
3. No
4. Stopcock, kinked IV-line, multiple lines with different infusion rate
5. During some situation where critical medicines are delivered, it could save precious time
6. Twice a week
7. None

Summation of interview results

The answers given by the nurses to each question can be summarized as:

1. Most persons indicated an infusion rate between 0.5 to 100 ml/h
2. Stop the pump, check for the cause (mainly closed stopcocks and kinked IV-lines). If the cause is not obvious immediately, some start the pump again to see if the alarm goes off again. If the alarm goes off again, some flush the IV-line
3. Answers range from almost never to never. Some change the pressure threshold when two pump with a large difference in infusion rates are connected. Most are not aware that the pressure threshold is increased when an alarm went off and the pump is started again.
4. Closed stopcock, kinked IV-line, precipitation/coagulation, lines with large difference in infusion rates that are connected
5. Most think it would not save a lot of time as they think that there are not many occlusion alarms and they do not spend a lot of time on solving occlusions. However, in time pressuring situation, for example when the patient is heavily reliant of the infused drug, it could save valuable time
6. From one up to four times a week
7. From never up to once a week or more

APPENDIX C

JAVA INTERFACE FOR COMMUNICATING AND CONTROLLING THE ALARIS GH AND THE IDA 4

JAVA user interface

The JAVA interface used to communicate with and control the Alaris GH syringe pumps and the IDA 4 infusion device analyser, is an extensive program that relies on a serial connection between the devices. The interface was developed by Frank Doesburg and is extended upon to provide the functionality required for this project. The user interface itself is depicted by Figure 25.

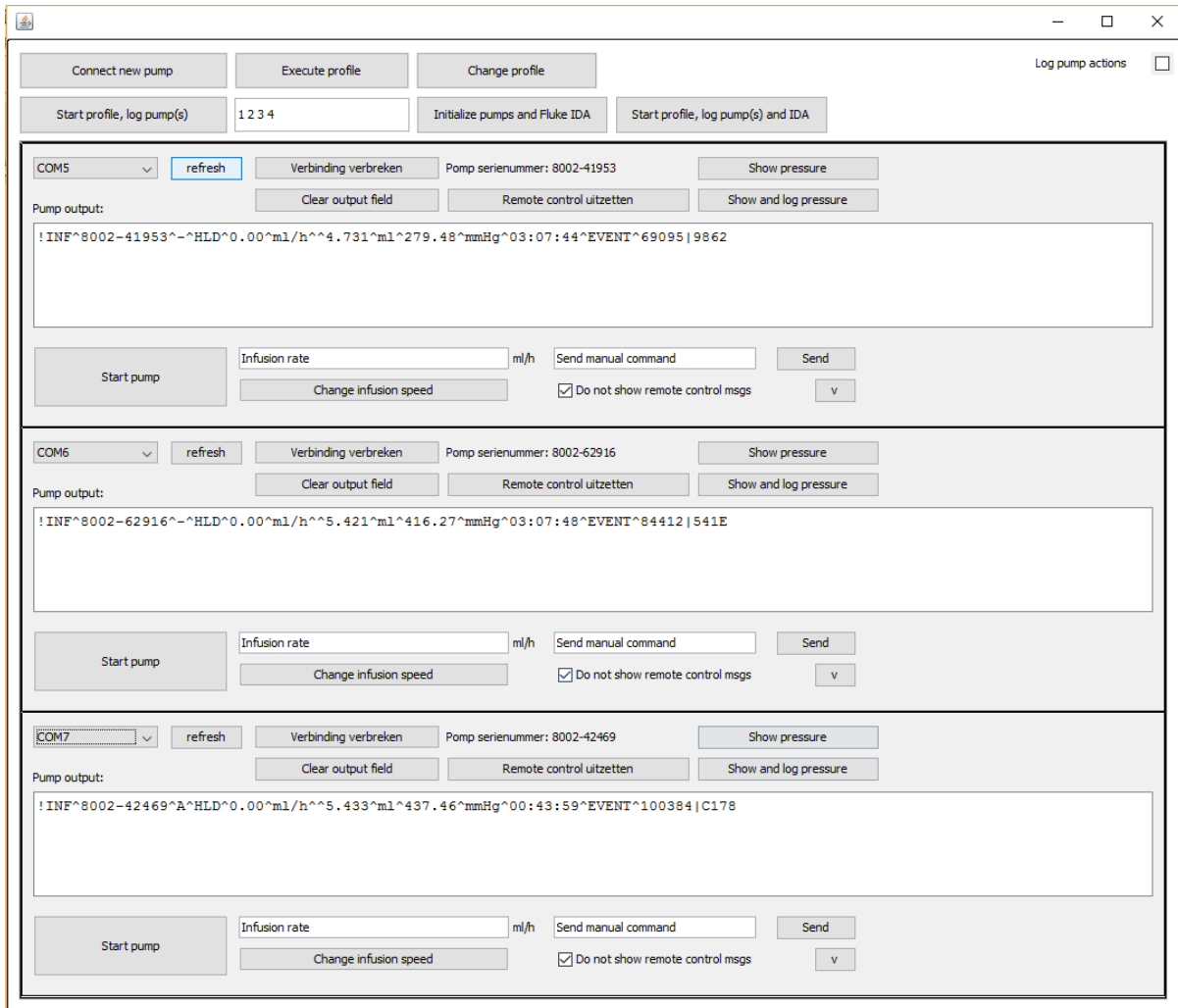


Figure 25: Image of the JAVA user interface, while three pumps are connected.

The interface already had functionality to communicate via serial and control the syringe pumps. However, functionality was added to control the IDA 4 and log data. The interface mainly consists of three classes, the GUI, IDA 4 controller and pump controller, as depicted by Figure 26. The GUI communicates with the IDA 4 and pump controller classes and can create multiple pump controller instances with operate in parallel via threading. Data acquired from the controller classes is send to the GUI, where it is stored in a buffer and written to a text file with frequency of 0.5 Hz.

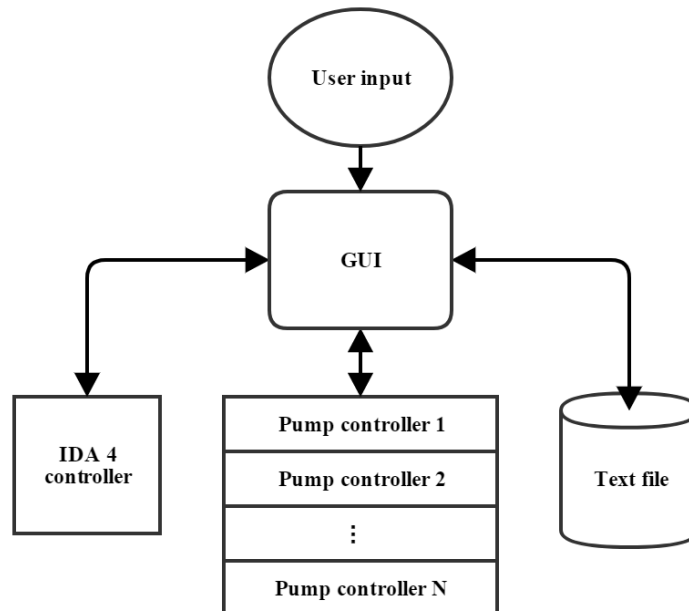


Figure 26: Simplified overview of the functioning of the JAVA interface, used to control and log data from the Alaris GH syringe pump and the IDA 4 infusion device analyser.

APPENDIX D

BENCHMARK RESULTS OF THE SLIDING SLOPE COEFFICIENT ALGORITHM USING THE VALIDATION- DATASET

Summary of the performance

In this appendix you will find the complete results of the performance of the sliding slope coefficient algorithm on the validation-dataset. To start off with, **Error! Reference source not found.** provides an overview of the averages results, sorted on configuration and infusion speed.

Table 5: Overview of the benchmarking results for the sliding slope coefficient algorithm on the validation-dataset. The infusion speed(s) for each dataset are given, with average time to occlusion detection and pump alarm. The last columns give the average decrease, expressed as a percentage and as a factor.

Pump configuration	Infusion speed(s)	Average time to occlusion detection [s]	Average time to pump alarm [s]	Average decrease [%]	Factor decrease
1	1	96.04	2555.69	96.24	26.61
	5	24.02	420.18	94.28	17.49
	10	16.03	204.12	92.15	12.73
	50	5.99	19.99	70.04 *	3.34 *
2	1	88.04	2451.74	96.41	27.85
	5	24.01	484.19	95.04	20.17
	10	11.01	204.08	94.61	18.54
	50	12.00	30.00	60.02	2.50
	1, 50	22.05	68.05	67.60 **	3.09 **
	5, 10	22.00	280.08	92.15	12.73
3	1	86.75	1816.78	95.23	20.94
	5	24.68	398.16	93.80	16.14
	10	14.66	198.05	92.60	13.51
	50	10.01	34.03	70.58	3.40
	1, 10, 50	30.01	88.02	65.91	2.93
	5, 5, 10	20.68	268.10	92.29	12.96

* Deviant value due to 8 second error in time of occlusion occurrence, caused by a delay in the logging of the first IDA 4 value

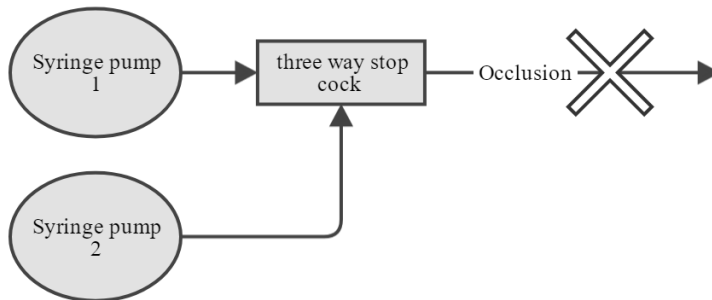
** Deviant value due to missing data point as the algorithm incorrectly marked the time of occlusion before the occurrence of the occlusion

An overview of the three pump configurations used in the validation dataset is depicted below and will be referred to later.

Configuration 1



Configuration 2



Configuration 3

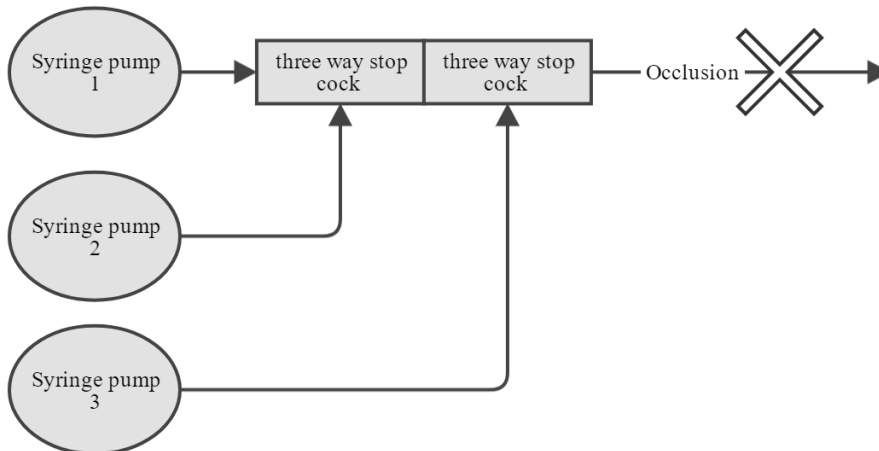


Figure 27: schematic overview of pump configurations, included in the validation-dataset. [48]

Table 6: Complete overview of the performance results of the sliding slope coefficient algorithm on the validation dataset. The ‘X’ marks missing data due to detection of occlusion before occlusion occurrence.

Configuration 1							
Pump number	Infusion rate [mL/h]	Time of occlusion [s]	Occlusion detection [s]	Occlusion alarm pump [s]	Time to detection [s]	Time to pump alarm [s]	Decrease [%]
1	1	606.24	702.28	3161.93	96.04	2555.69	96.24
1	5	616.28	640.30	1036.46	24.02	420.18	94.28
1	10	612.28	628.31	816.40	16.03	204.12	92.15
1	50	618.26	624.25	638.25	5.99	19.99	70.04 *
Configuration 2							
Pump number	Infusion rate [mL/h]	Time of occlusion [s]	Occlusion detection [s]	Occlusion alarm pump [s]	Time to detection [s]	Time to pump alarm [s]	Decrease [%]
1	1	618.21	694.24	3069.93	76.03	2451.72	96.90
2	1	618.21	718.25	3069.96	100.04	2451.75	95.92
1	5	618.21	640.22	1102.40	22.01	484.19	95.45
2	5	618.24	644.25	1102.43	26.01	484.19	94.63
1	10	608.27	618.27	812.35	10.00	204.08	95.10
2	10	608.27	620.29	812.35	12.02	204.08	94.11
1	50	608.24	618.24	638.24	10.00	30.00	66.67
2	50	608.24	622.23	638.24	13.99	30.00	53.37
1	1,50	610.22	208.07	678.27	X	X	X
2	1,50	610.22	632.27	678.27	22.05	68.05	67.60
1	5,10	608.24	628.24	888.32	20.00	280.08	92.86
2	5,10	608.24	632.23	888.32	23.99	280.08	91.43
Configuration 3							
Pump number	Infusion rate [mL/h]	Time of occlusion [s]	Occlusion detection [s]	Occlusion alarm pump [s]	Time to detection [s]	Time to pump alarm [s]	Decrease [%]
1	1	610.22	680.28	2426.99	80.06	1816.77	95.59
2	1	610.22	688.30	2426.99	88.08	1816.77	95.15
3	1	610.22	692.33	2427.03	92.11	1816.81	94.93
1	5	602.20	618.21	1000.36	26.01	398.16	93.47
2	5	602.20	614.21	1000.36	22.01	398.16	94.47
3	5	602.20	618.21	1000.36	26.01	398.16	93.47
1	10	606.23	612.23	804.30	16.00	198.07	91.92
2	10	606.26	610.25	804.30	13.99	198.04	92.94
3	10	606.26	610.25	804.30	13.99	198.04	92.94
1	50	610.22	610.22	644.25	10.00	34.03	70.61
2	50	610.22	610.22	644.25	10.00	34.03	70.61
3	50	610.22	610.25	644.25	10.03	34.03	70.53
1	1,10,50	616.23	646.26	704.27	40.03	88.04	54.53
2	1,10,50	616.26	614.25	704.27	7.99	88.01	90.92
3	1,10,50	616.26	648.27	704.27	42.01	88.01	52.27
1	5,5,10	608.24	618.24	876.34	20.00	268.10	92.54
2	5,5,10	608.24	618.24	876.34	20.00	268.10	92.54
3	5,5,10	608.24	620.29	876.34	22.05	268.10	91.78

* Deviant value due to 8 [s] error in time of occlusion occurrence, caused by a delay in the logging of the first IDA 4 value

Results configuration 1

Resistance, sliding slope coefficients and pressure over time for pump 1, with an infusion rate of 1.0

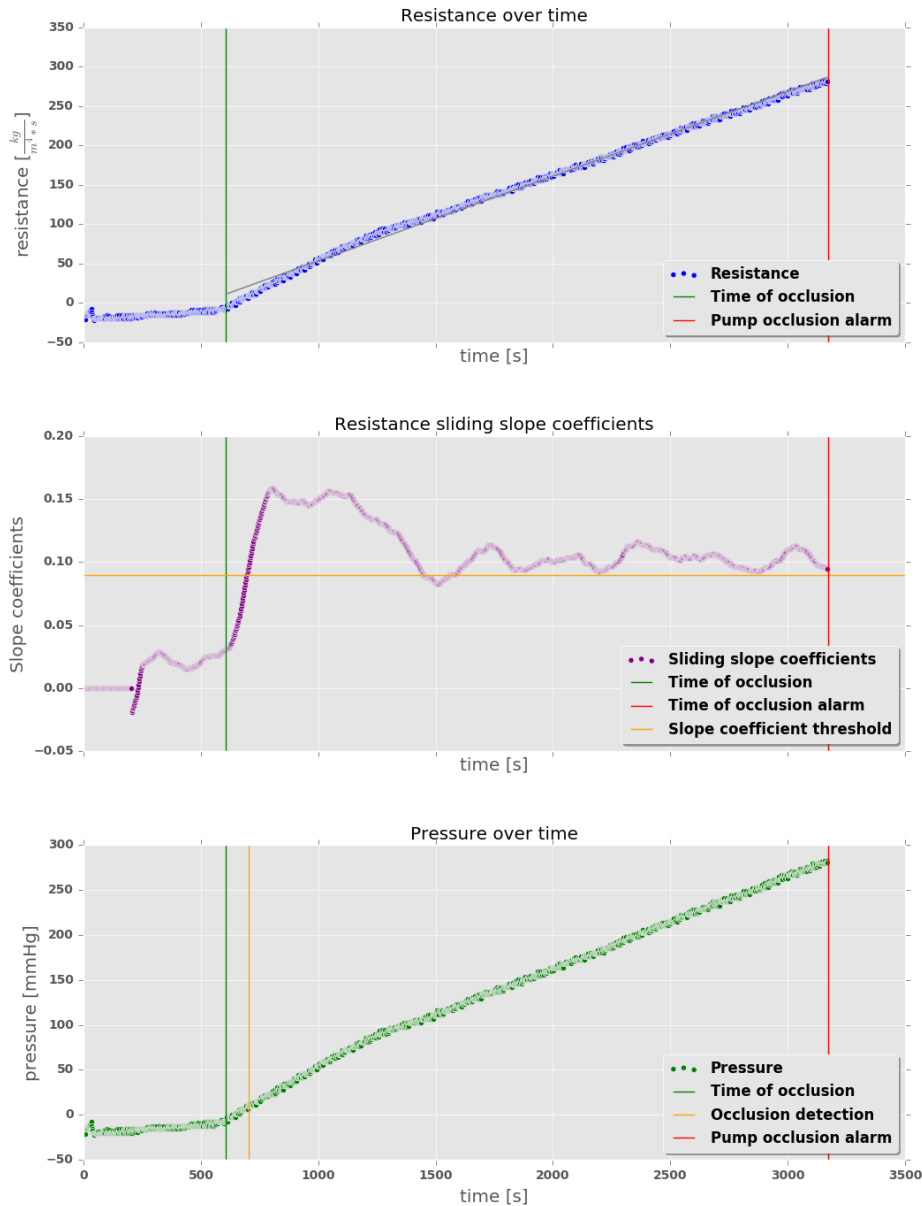


Figure 28: Resistance, sliding slope coefficients and pressure over time for configuration 1 (Figure 28) and an infusion rate of 1 mL/h. At an infusion speed of 1 mL/h the pressure rises slowly, meaning that fluctuation in pressure caused by the pumping mechanism and friction from the syringe plunger are relatively large. This causes the sliding slope coefficients to vary. For all three plots the time of occlusion (vertical green line) and the time of pump occlusion alarm (vertical red line) have been marked. From the resistance time series (top plot) sliding slope coefficients have been calculated (middle plot). As the resistance values are negative at first, the sliding slope coefficients are zero. Then, once the window is converted from an incrementing to a sliding window, sliding slope coefficients are calculated. The horizontal yellow line indicates the occlusion threshold of 0.09. In the bottom plot, the yellow vertical line indicates the time of occlusion detection by the sliding slope coefficient algorithm. These plots show that the algorithm is much faster, especially at lower infusion speeds.

Resistance, sliding slope coefficients and pressure over time for pump 1, with an infusion rate of 5.0

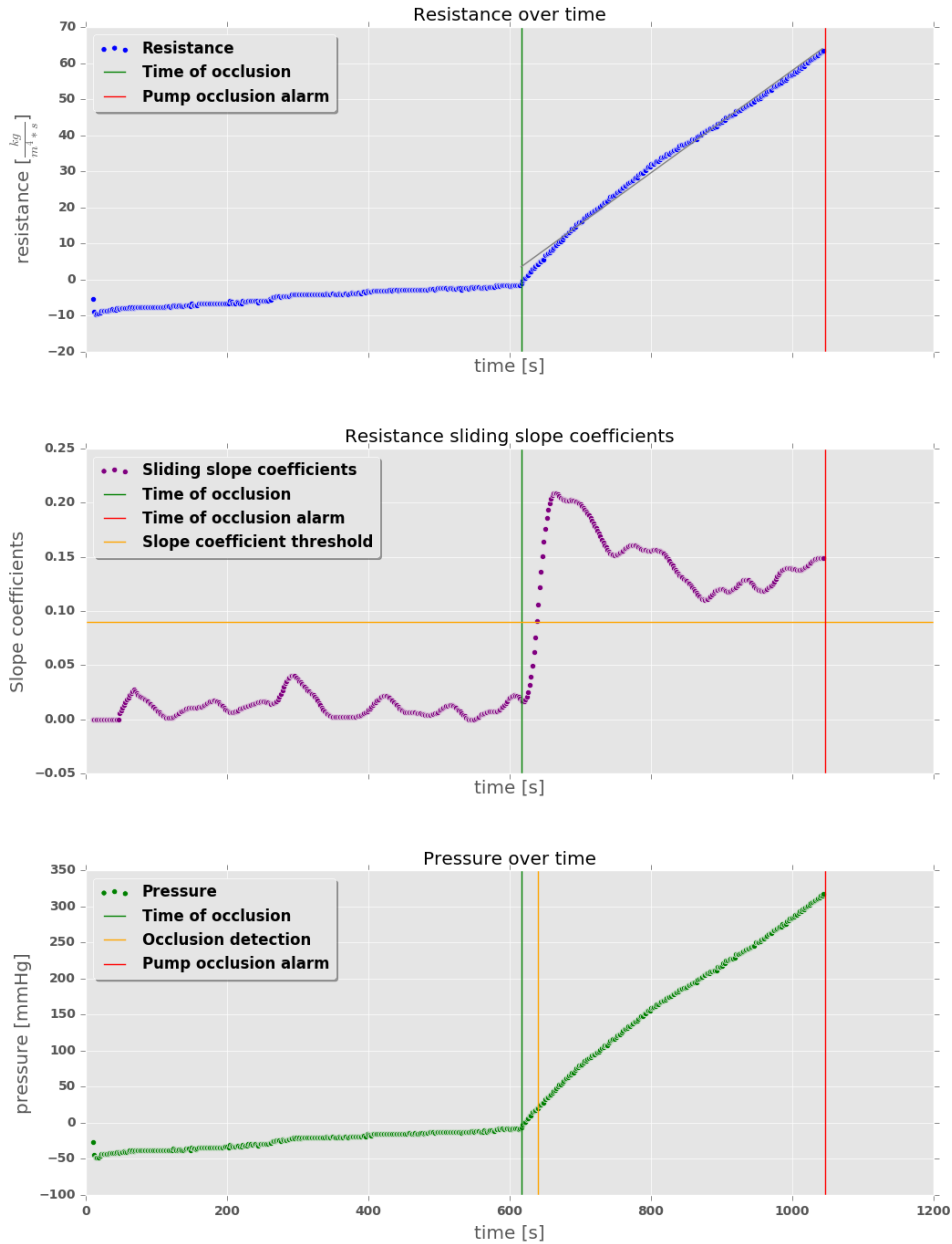


Figure 29 Resistance, sliding slope coefficients and pressure over time for configuration 1 (Figure 28) and an infusion rate of 5 mL/h. For all three plots the time of occlusion (vertical green line) and the time of pump occlusion alarm (vertical red line) have been marked. From the resistance time series (top plot) sliding slope coefficients have been calculated (middle plot). As the resistance values are negative at first, the sliding slope coefficients are zero. In this time series the first data point is around -5, then jumps to -10, after which it start increasing. Initially large slope coefficients when no occlusion has yet occurred is solved by setting the slope coefficient to zero. Then, once the window is converted from an incrementing to a sliding window, sliding slope coefficients are calculated. In the middle plot, the horizontal yellow line indicates the occlusion threshold of 0.09. In the bottom plot, the yellow vertical line indicates the time of occlusion detection by the sliding slope coefficient algorithm, when the coefficient first reaches the threshold.

Resistance, sliding slope coefficients and pressure over time for pump 1, with an infusion rate of 10.0

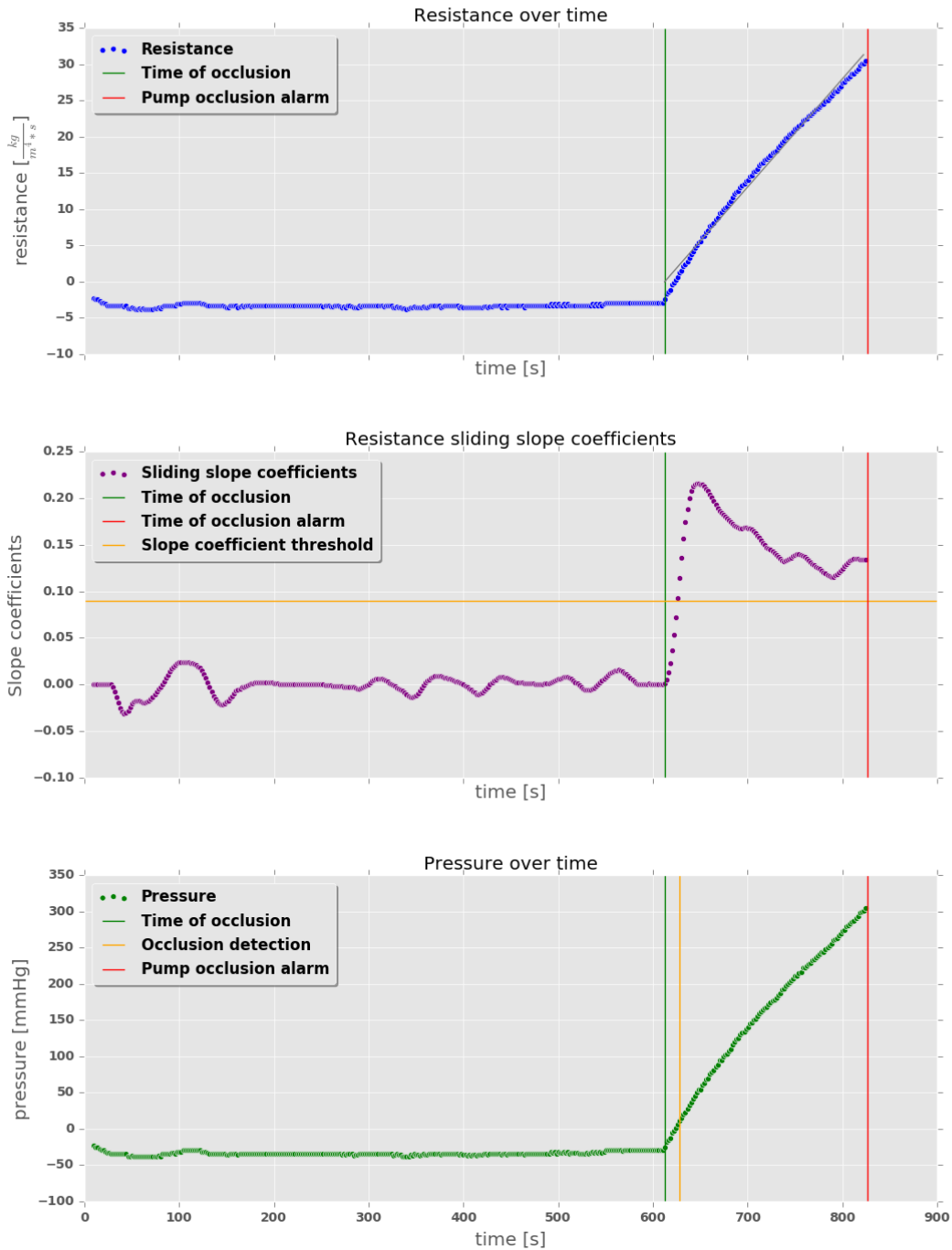


Figure 30: Resistance, sliding slope coefficients and pressure over time for configuration 1 (Figure 28) and an infusion rate of 10 mL/h. For all three plots the time of occlusion, vertical green line, and the time of pump occlusion alarm, vertical red line, have been marked. From the resistance time series (top plot) sliding slope coefficients have been calculated (middle plot). In the middle plot, the horizontal yellow line marks the occlusion threshold of 0.09. In the bottom plot, the yellow vertical line indicates the time of occlusion detection by the sliding slope coefficient algorithm.

Resistance, sliding slope coefficients and pressure over time for pump 1, with an infusion rate of 50.0

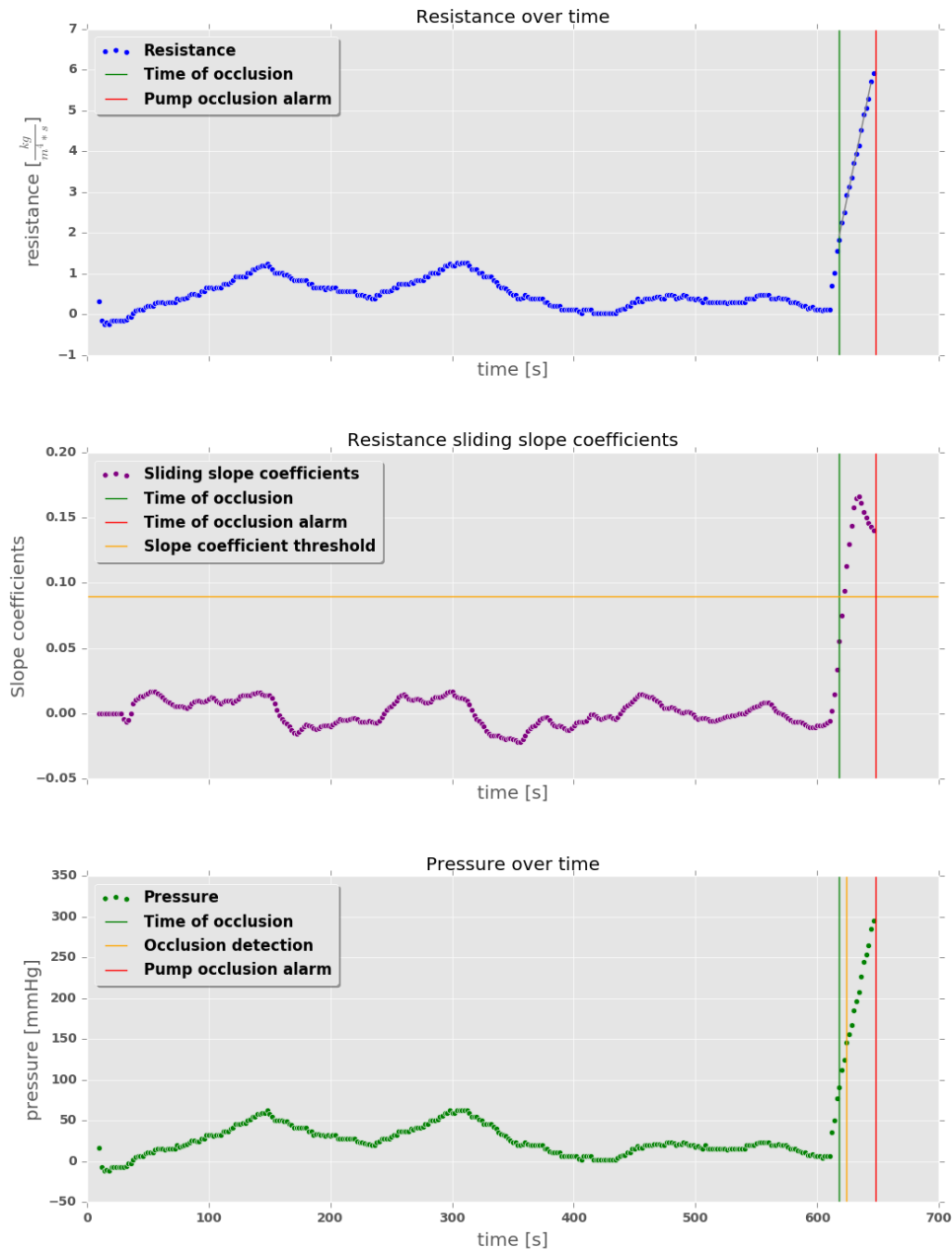


Figure 31: Resistance, sliding slope coefficients and pressure over time for configuration 1 (Figure 28) and an infusion rate of 50 mL/h. For all three plots the time of occlusion (vertical green line) and the time of pump occlusion alarm (vertical red line) have been marked. However, the fast rise in pressure reveals that in this case the method of marking the time of occlusion is inaccurate. The occlusion is caused by starting of an occlusion test on IDA 4. When the test is started, the data from the IDA 4 is logged. The time of occlusion was marked when the first IDA 4 data point was logged. In this case, a delay is introduced causing the occlusion location to be marked late by 8 seconds. From the resistance time series (top plot) sliding slope coefficients have been calculated (middle plot). In the middle plot, the horizontal yellow line indicates the occlusion threshold of 0.09. In the bottom plot, the yellow vertical line indicates the time of occlusion detection by the sliding slope coefficient algorithm, when the coefficient first reaches the threshold.

Results configuration 2

Resistance, sliding slope coefficients and pressure over time for pump 1, while connected to one other pump, with a shared infusion rate of 1.0

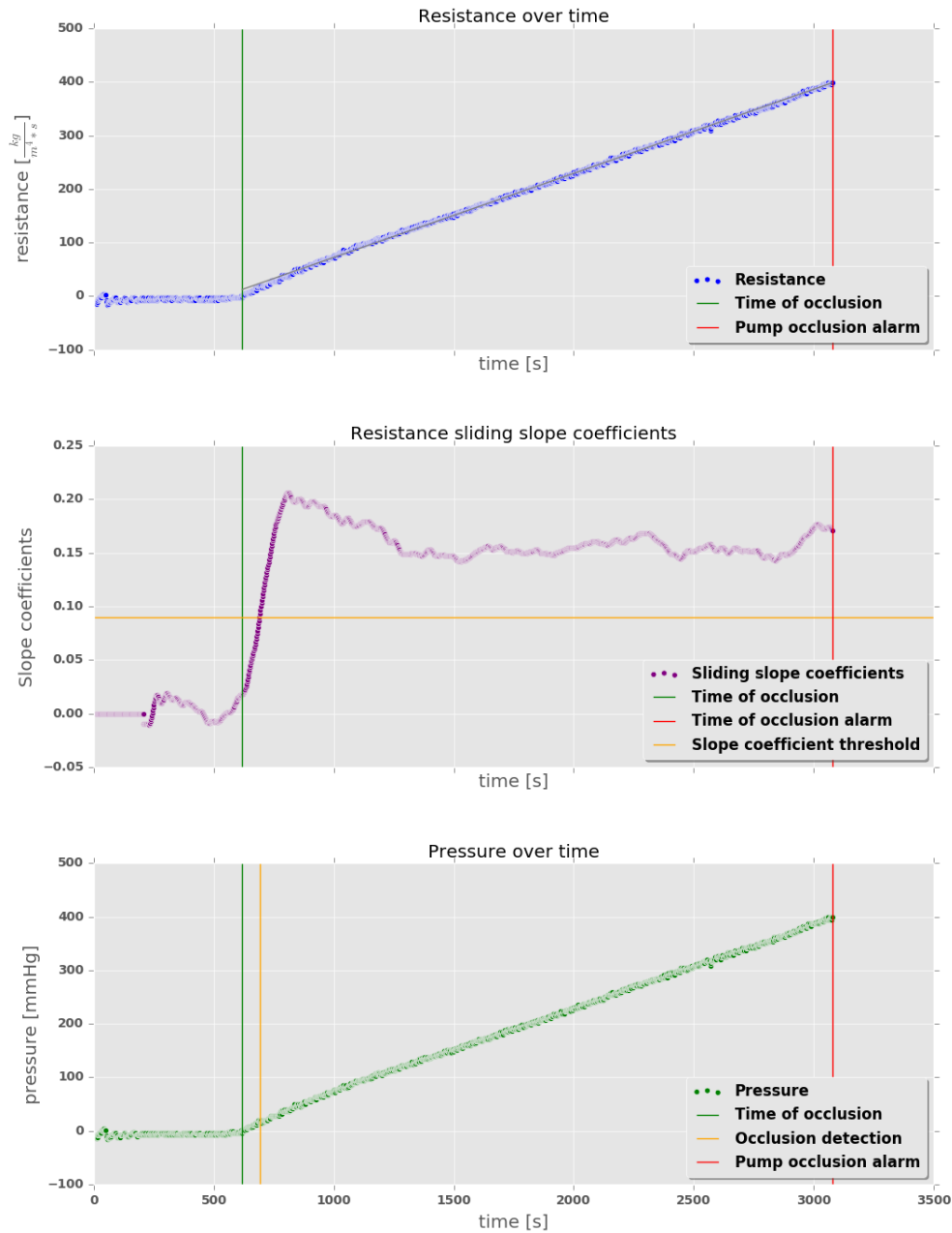


Figure 32: Resistance, sliding slope coefficients and pressure over time for pump 1 in configuration 2 (Figure 28) and an infusion rate of 1 mL/h. For all three plots the time of occlusion (vertical green line) and the time of pump occlusion alarm (vertical red line) have been marked. In the resistance and pressure time series, oscillating behaviour can be observed at start-up (the first 150 seconds). From the resistance time series (top plot) sliding slope coefficients have been calculated (middle plot). In the middle plot, the horizontal yellow line indicates the occlusion threshold of 0.09. In the bottom plot, the yellow vertical line indicates the time of occlusion detection by the sliding slope coefficient algorithm, when the coefficient first reaches the threshold.

Resistance, sliding slope coefficients and pressure over time for pump 2, while connected to one other pump, with a shared infusion rate of 1.0

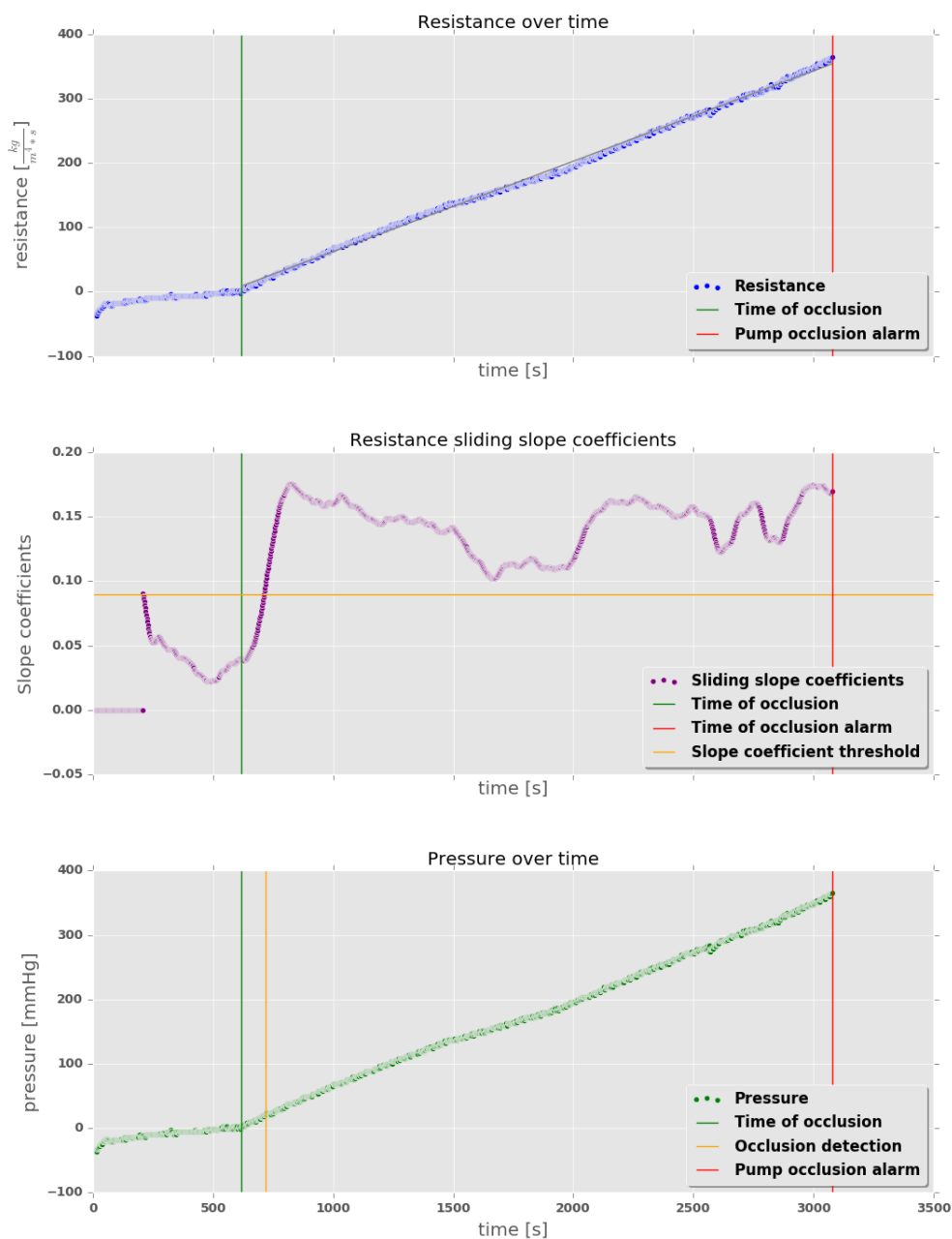


Figure 33: Resistance, sliding slope coefficients and pressure over time for pump 2 in configuration 2 (Figure 28) and an infusion rate of 1 mL/h. For all three plots the time of occlusion (vertical green line) and the time of pump occlusion alarm (vertical red line) have been marked. From the resistance time series (top plot) sliding slope coefficients have been calculated (middle plot). In the middle plot, the horizontal yellow line indicates the occlusion threshold of 0.09. A steep rise in pressure is observed during start-up, as the initial pressure is negative at first and therefore quickly rises to a non-zero pressure. The sliding slope coefficients jump to a high value as the algorithm switches from an incrementing to a sliding window. For the incrementing window, only non-negative values are allowed. This causes the first sliding slope coefficients to almost reach the threshold. In the bottom plot, the yellow vertical line indicates the time of occlusion detection by the sliding slope coefficient algorithm, when the coefficient first reaches the threshold.

Resistance, sliding slope coefficients and pressure over time for pump 1, while connected to one other pump, with a shared infusion rate of 5.0

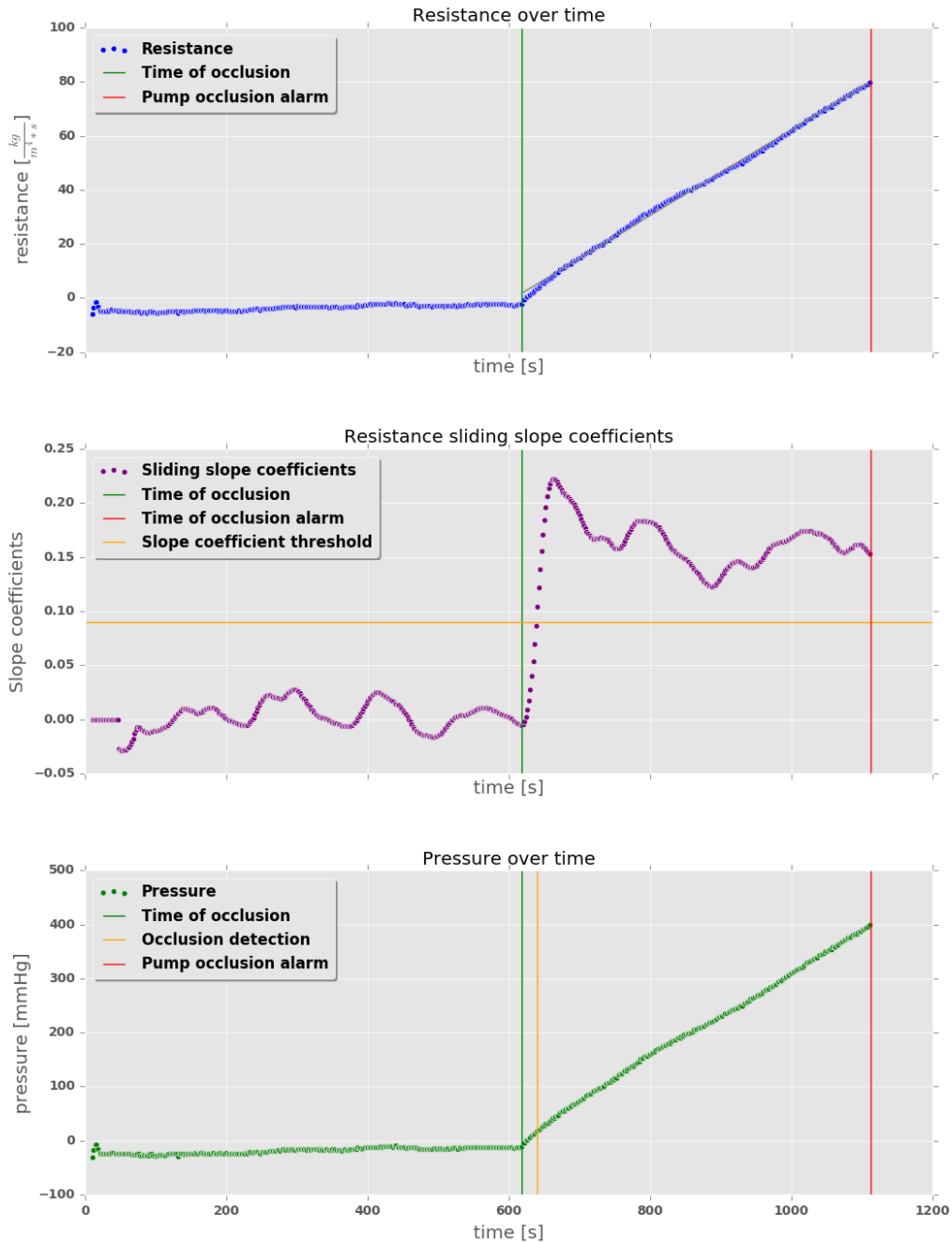


Figure 34: Resistance, sliding slope coefficient and pressure over time for pump 1 in configuration 2 (Figure 28) and an infusion rate of 5 mL/h. For all three plots the time of occlusion (vertical green line) and the time of pump occlusion alarm (vertical red line) have been marked. From the resistance time series (top plot) sliding slope coefficients have been calculated (middle plot). The sliding slope coefficient oscillate as the resistance time series oscillate due to the syringe-plunger friction. In the middle plot, the horizontal yellow line indicates the occlusion threshold of 0.09. In the bottom plot, the yellow vertical line indicates the time of occlusion detection by the sliding slope coefficient algorithm, when the coefficient first reaches the threshold.

Resistance, sliding slope coefficients and pressure over time for pump 2, while connected to one other pump, with a shared infusion rate of 5.0

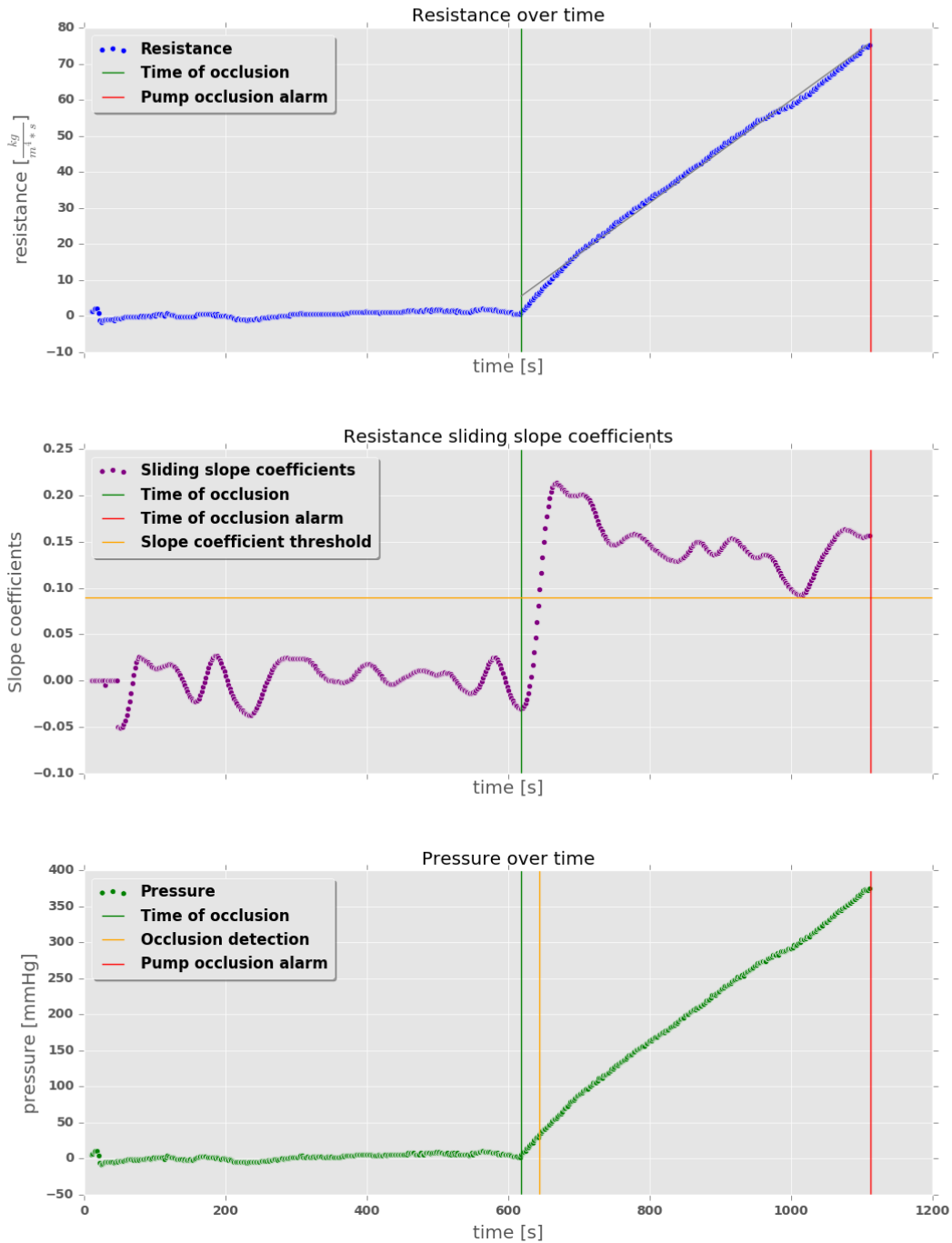


Figure 35: Resistance, sliding slope coefficient and pressure over time for pump 2 in configuration 2 (Figure 28) and an infusion rate of 5 mL/h. For all three plots the time of occlusion (vertical green line) and the time of pump occlusion alarm (vertical red line) have been marked. From the resistance time series (top plot) sliding slope coefficients have been calculated (middle plot). The sliding slope coefficient oscillate as the resistance time series oscillate due to the syringe-plunger friction. In the middle plot, the horizontal yellow line indicates the occlusion threshold of 0.09. In the bottom plot, the yellow vertical line indicates the time of occlusion detection by the sliding slope coefficient algorithm, when the coefficient first reaches the threshold.

Resistance, sliding slope coefficients and pressure over time for pump 1, while connected to one other pump, with a shared infusion rate of 10.0

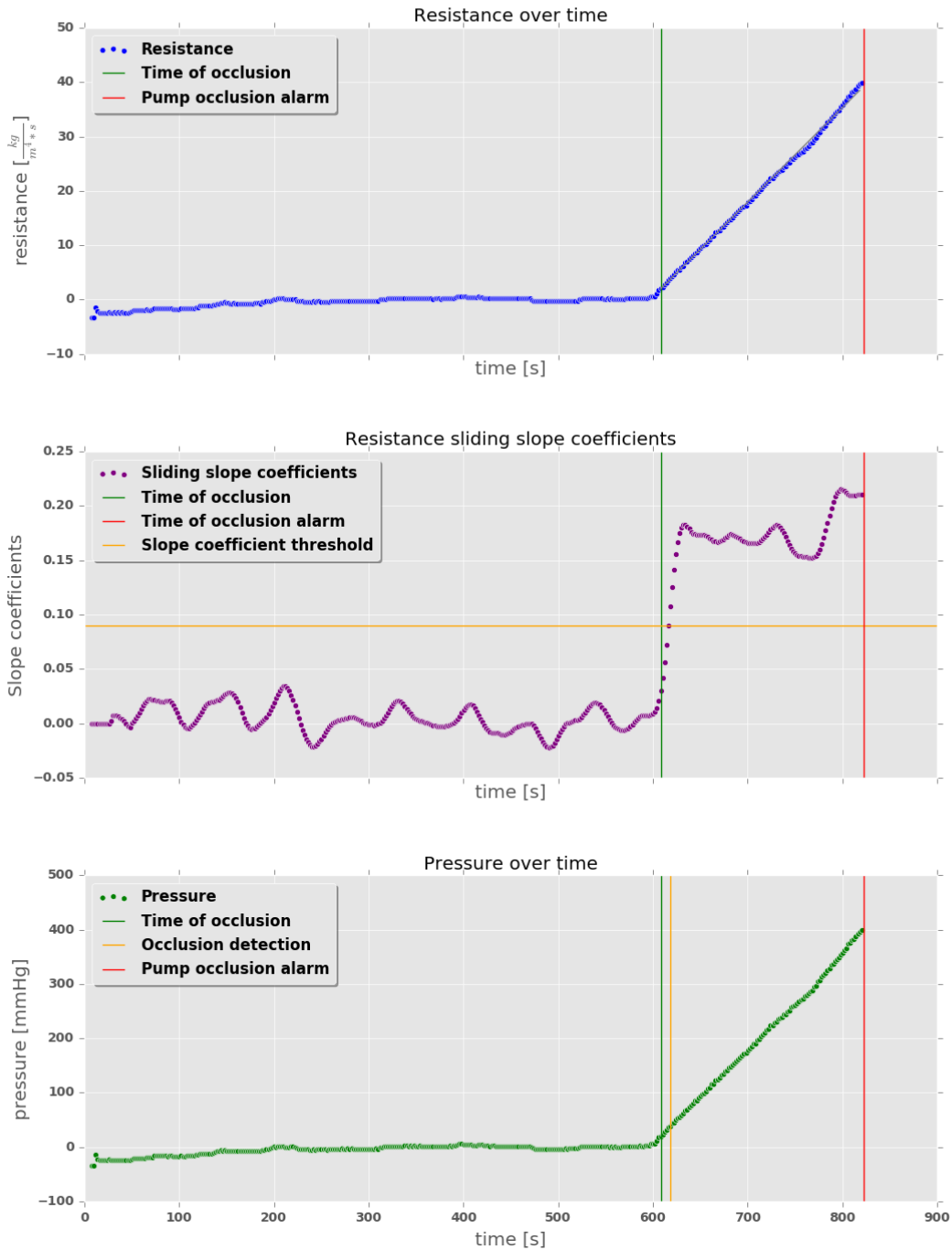


Figure 36: Resistance, sliding slope coefficient and pressure over time for pump 1 in configuration 2 (Figure 28) and an infusion rate of 10 mL/h. For all three plots the time of occlusion (vertical green line) and the time of pump occlusion alarm (vertical red line) have been marked. From the resistance time series (top plot) sliding slope coefficients have been calculated (middle plot). The sliding slope coefficient oscillate as the resistance time series oscillate due to the syringe-plunger friction. In the middle plot, the horizontal yellow line indicates the occlusion threshold of 0.09. In the bottom plot, the yellow vertical line indicates the time of occlusion detection by the sliding slope coefficient algorithm, when the coefficient first reaches the threshold.

Resistance, sliding slope coefficients and pressure over time for pump 2, while connected to one other pump, with a shared infusion rate of 10.0

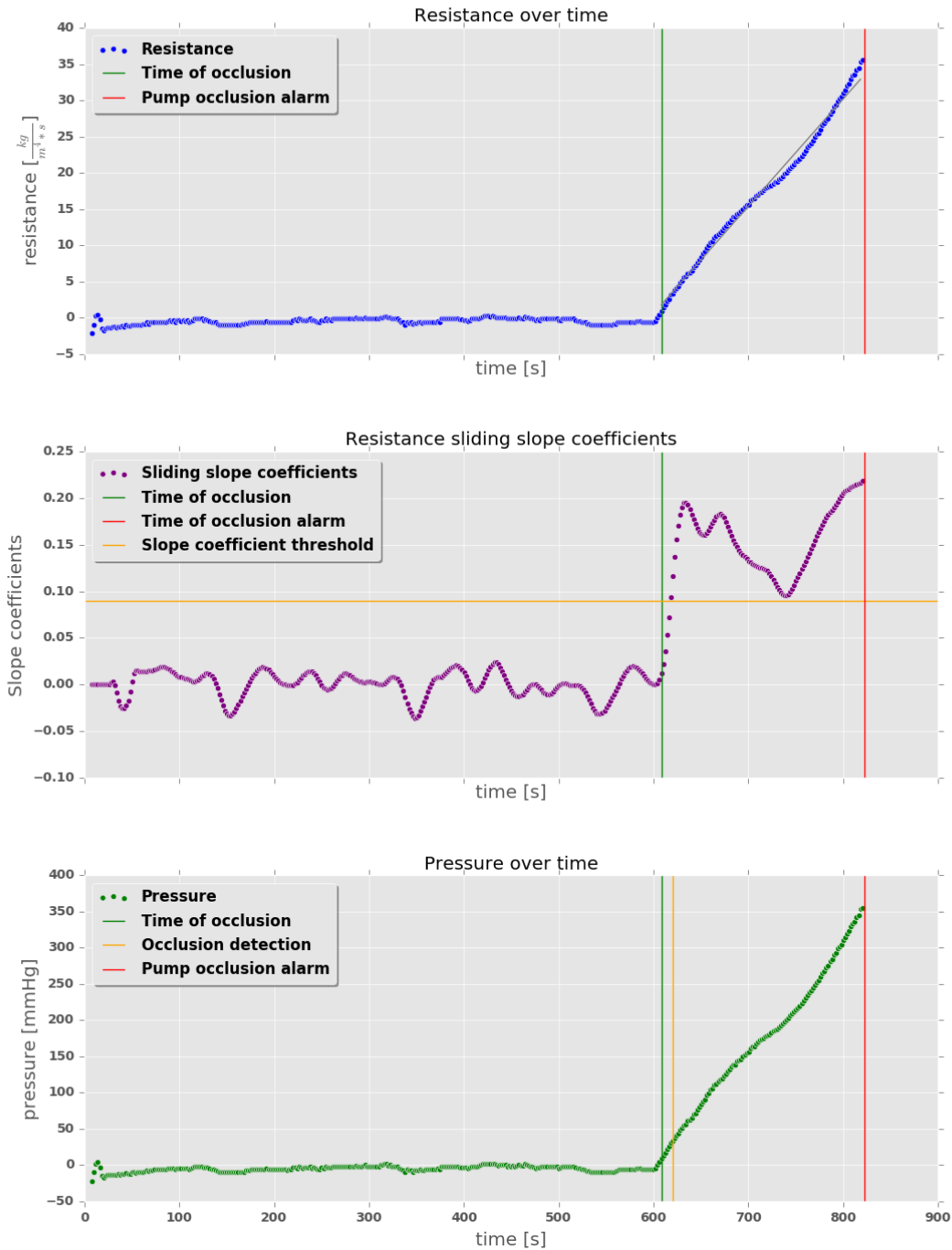


Figure 37: Resistance, sliding slope coefficient and pressure over time for pump 2 in configuration 2 (Figure 28) and an infusion rate of 10 mL/h. For all three plots the time of occlusion (vertical green line) and the time of pump occlusion alarm (vertical red line) have been marked. From the resistance time series (top plot) sliding slope coefficients have been calculated (middle plot). In the middle plot, the horizontal yellow line indicates the occlusion threshold of 0.09. In the bottom plot, the yellow vertical line indicates the time of occlusion detection by the sliding slope coefficient algorithm, when the coefficient first reaches the threshold.

Resistance, sliding slope coefficients and pressure over time for pump 1, while connected to one other pump, with a shared infusion rate of 50.0

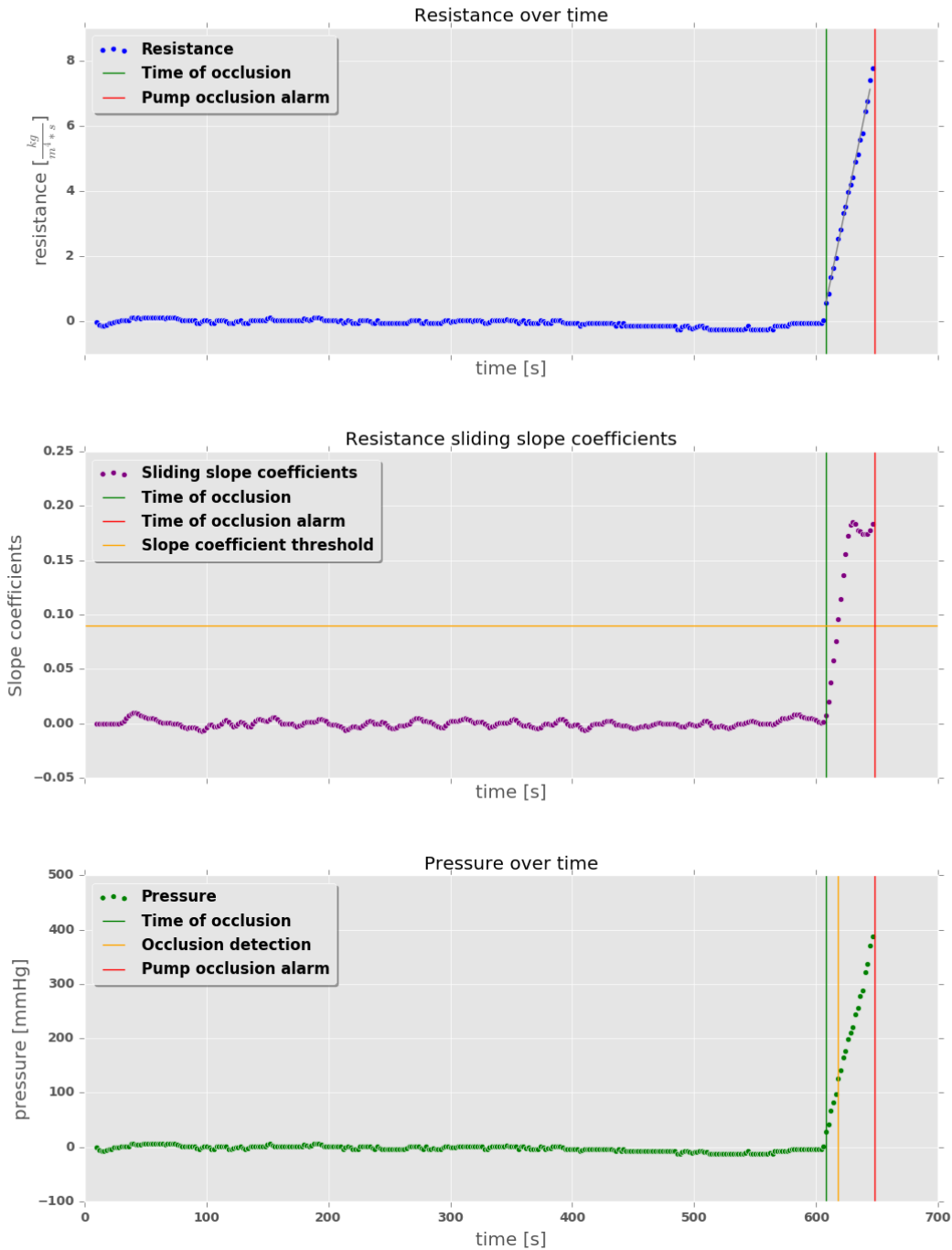


Figure 38: Resistance, sliding slope coefficient and pressure over time for pump 1 in configuration 2 (Figure 28) and an infusion rate of 50 mL/h. For all three plots the time of occlusion (vertical green line) and the time of pump occlusion alarm (vertical red line) have been marked. From the resistance time series (top plot) sliding slope coefficients have been calculated (middle plot). In the middle plot, the horizontal yellow line indicates the occlusion threshold of 0.09. In the bottom plot, the yellow vertical line indicates the time of occlusion detection by the sliding slope coefficient algorithm, when the coefficient first reaches the threshold.

Resistance, sliding slope coefficients and pressure over time for pump 2, while connected to one other pump, with a shared infusion rate of 50.0

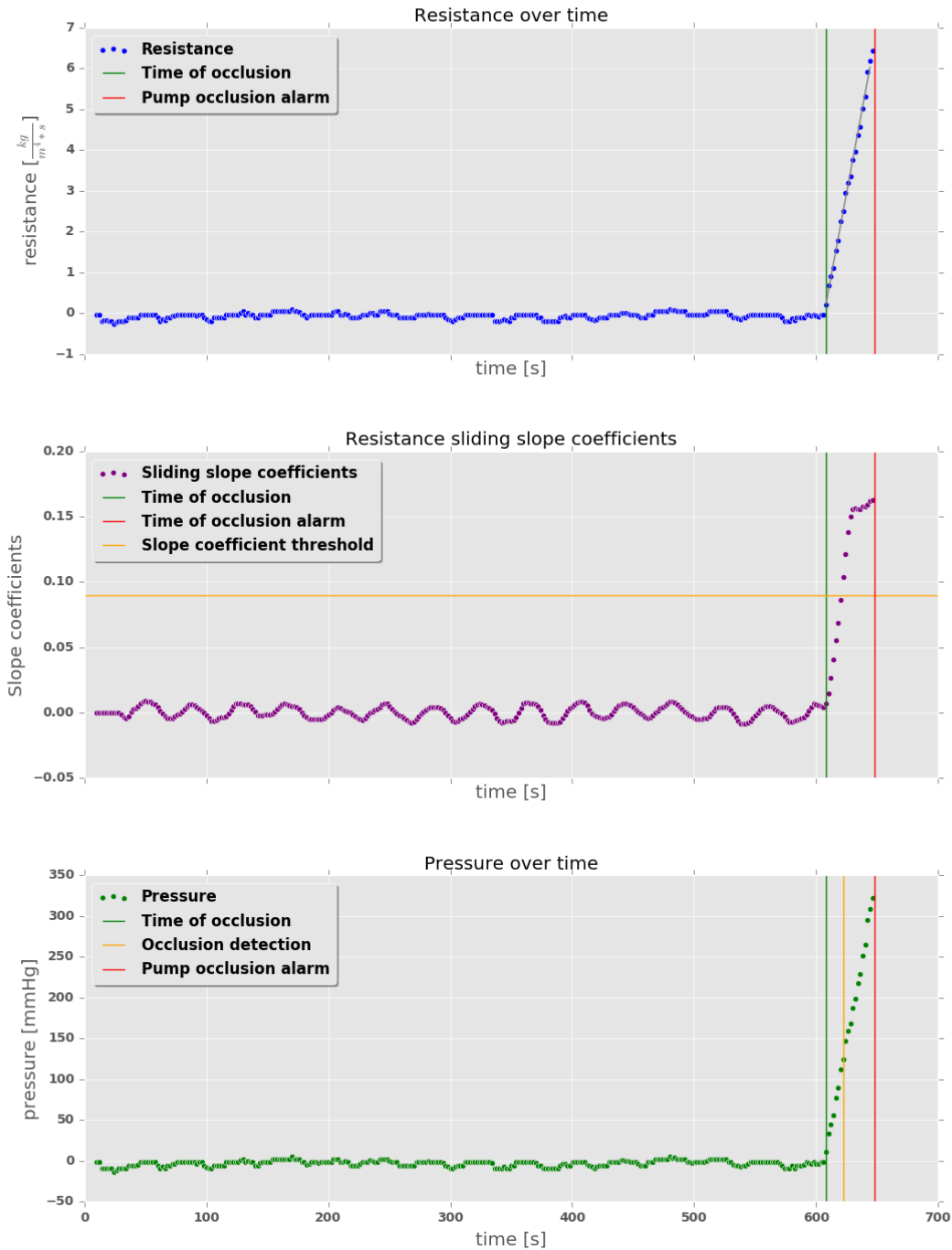


Figure 39: Resistance, sliding slope coefficient and pressure over time for pump 2 in configuration 2 (Figure 28) and an infusion rate of 50 mL/h. For all three plots the time of occlusion (vertical green line) and the time of pump occlusion alarm (vertical red line) have been marked. From the resistance time series (top plot) sliding slope coefficients have been calculated (middle plot). In the middle plot, the horizontal yellow line indicates the occlusion threshold of 0.09. In the bottom plot, the yellow vertical line indicates the time of occlusion detection by the sliding slope coefficient algorithm, when the coefficient first reaches the threshold.

Resistance, sliding slope coefficients and pressure over time for pump 1, while connected to one other pump with infusion rates 5 and 10 mL/h. For this pump the infusion rate is: 5.0 mL/h

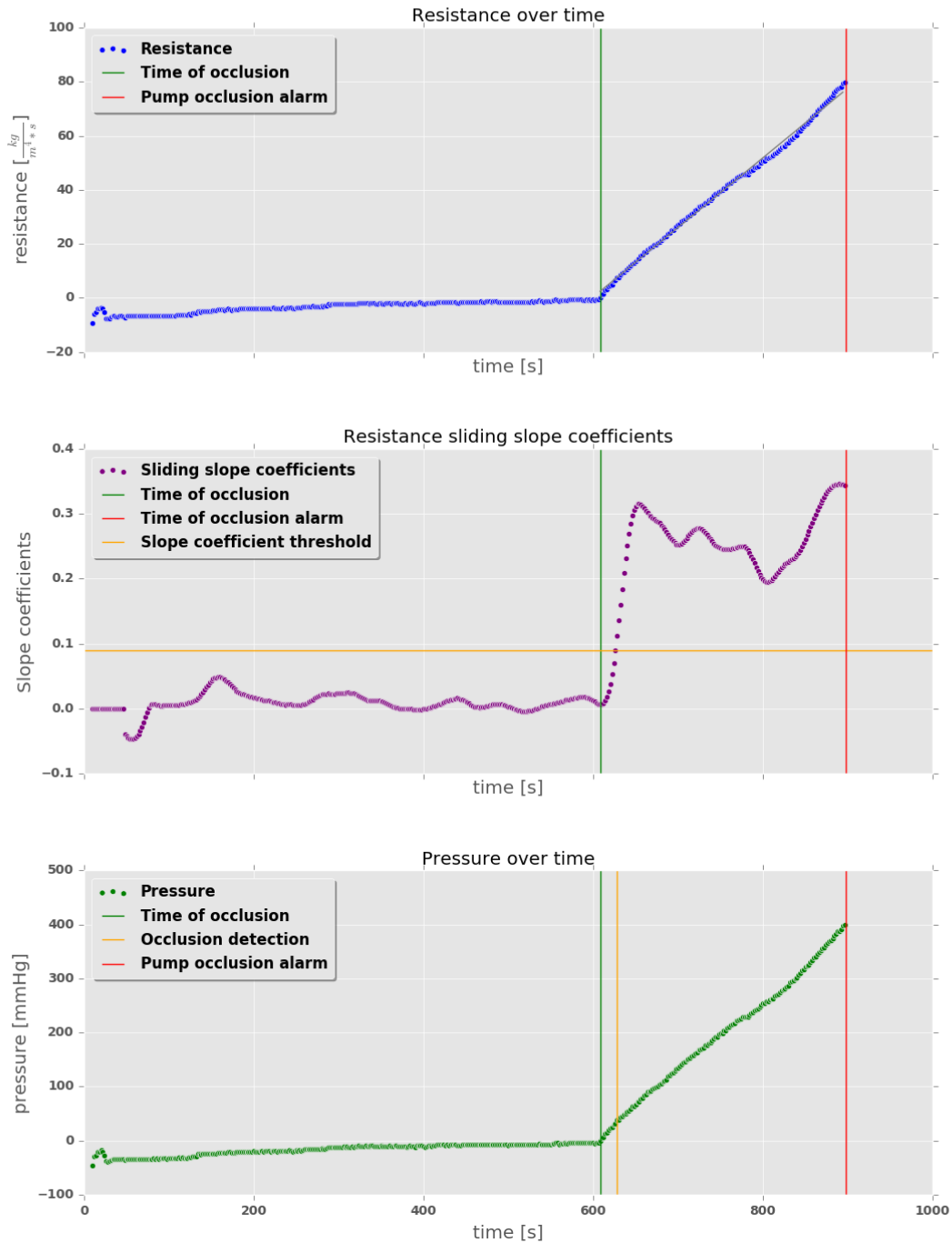


Figure 40: Resistance, sliding slope coefficient and pressure over time for pump 1 in configuration 2 (Figure 28) with an infusion rate of 5 mL/h. In this situation two pumps with infusion rates 5 and 10 mL/h were connected to each other. For all three plots the time of occlusion (vertical green line) and the time of pump occlusion alarm (vertical red line) have been marked. From the resistance time series (top plot) sliding slope coefficients have been calculated (middle plot). In the middle plot, the horizontal yellow line indicates the occlusion threshold of 0.09. In the bottom plot, the yellow vertical line indicates the time of occlusion detection by the sliding slope coefficient algorithm, when the coefficient first reaches the threshold.

Resistance, sliding slope coefficients and pressure over time for pump 2, while connected to one other pump with infusion rates 5 and 10 mL/h. For this pump the infusion rate is: 10.0 mL/h

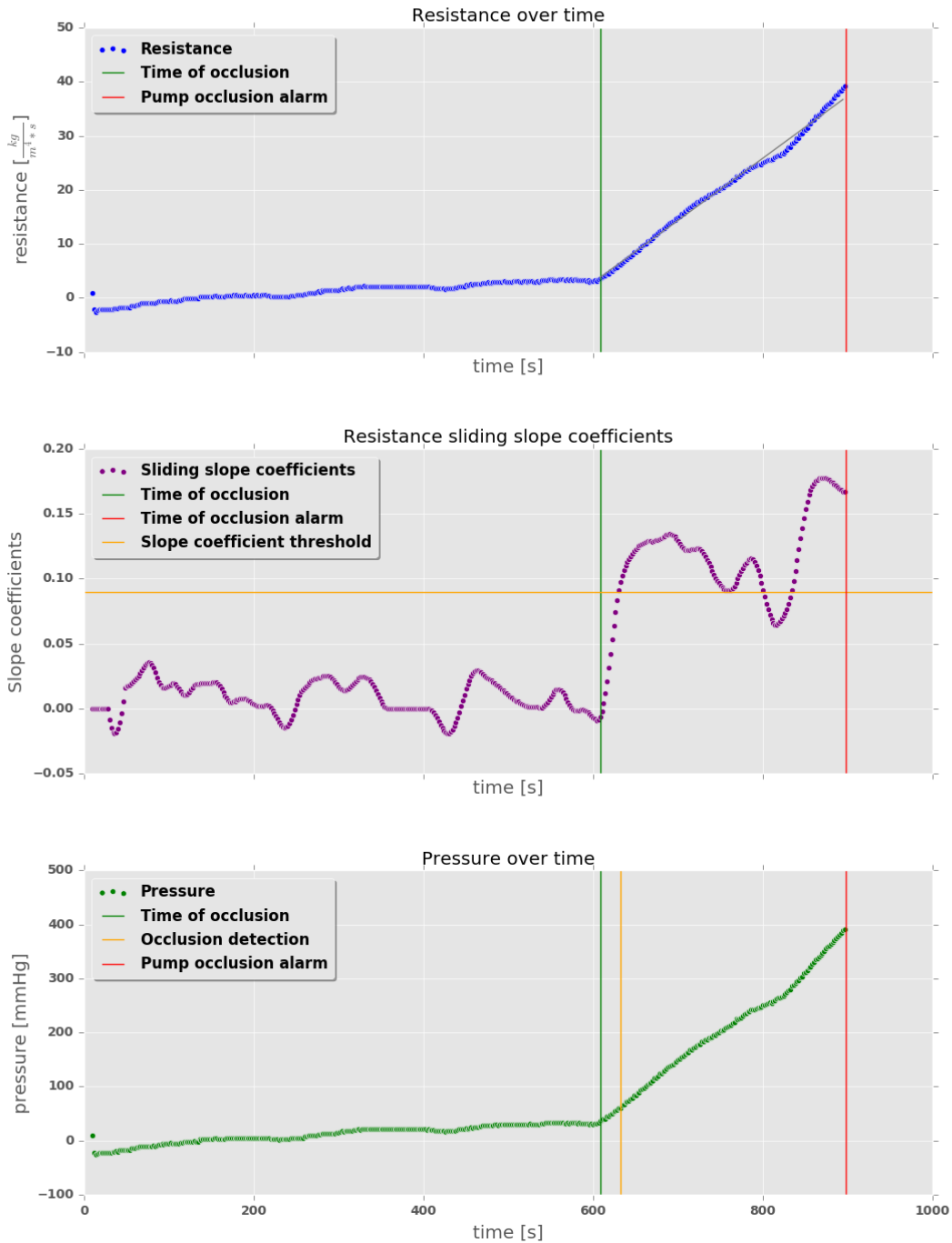


Figure 41: Resistance, sliding slope coefficient and pressure over time for pump 2 in configuration 2 (Figure 28) with an infusion rate of 10 mL/h. In this situation two pumps with infusion rates 5 and 10 mL/h were connected to each other. For all three plots the time of occlusion (vertical green line) and the time of pump occlusion alarm (vertical red line) have been marked. From the resistance time series (top plot) sliding slope coefficients have been calculated (middle plot). In the middle plot, the horizontal yellow line indicates the occlusion threshold of 0.09. In the bottom plot, the yellow vertical line indicates the time of occlusion detection by the sliding slope coefficient algorithm, when the coefficient first reaches the threshold.

Resistance, sliding slope coefficients and pressure over time for pump 1, while connected to one other pump with infusion rates 1 and 50 mL/h. For this pump the infusion rate is: 1.0 mL/h

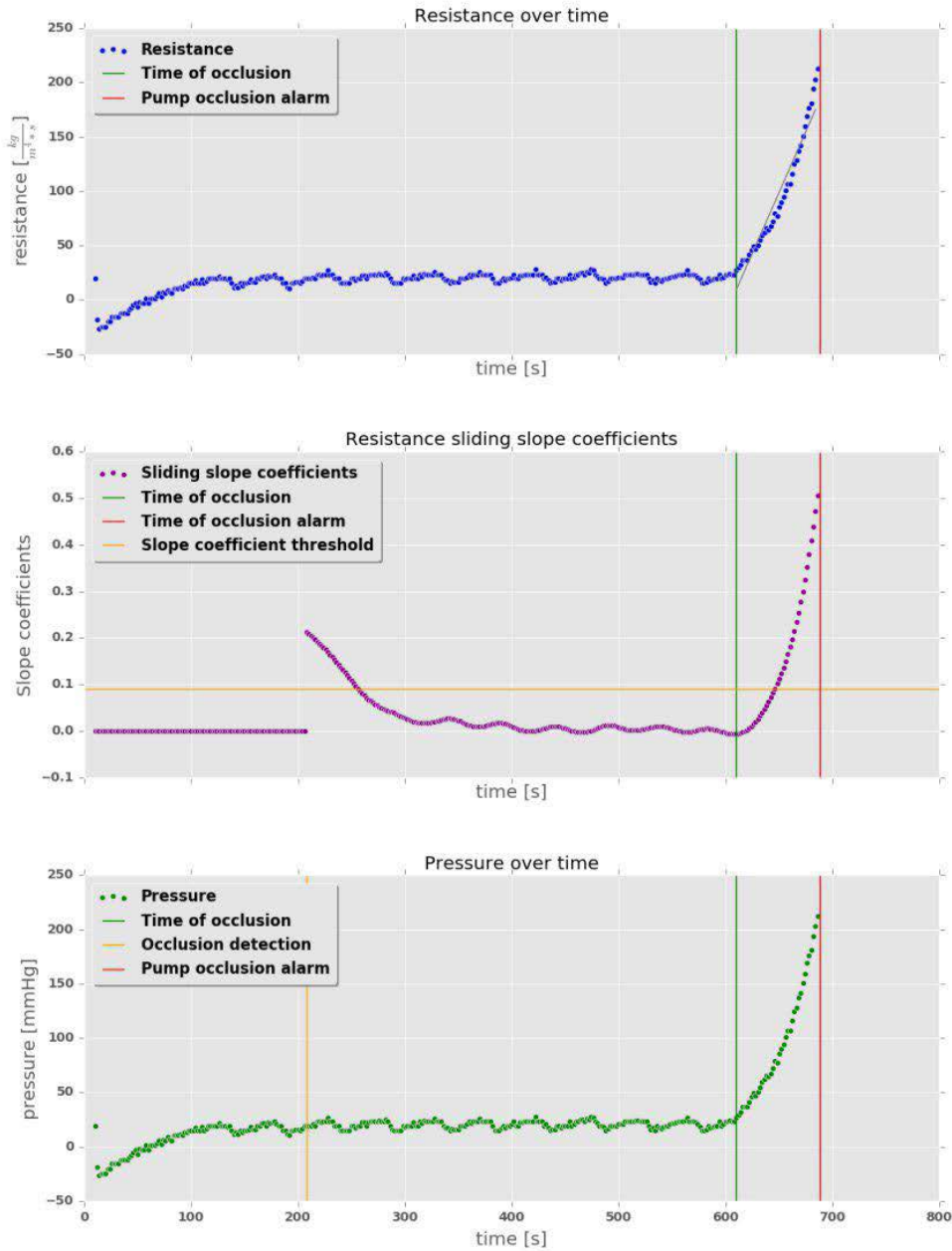


Figure 42: Resistance, sliding slope coefficient and pressure over time for pump 1 in configuration 2 (Figure 28) with an infusion rate of 1 mL/h. In this situation two pumps with infusion rates 1 and 50 mL/h were connected to each other. For all three plots the time of occlusion (vertical green line) and the time of pump occlusion alarm (vertical red line) have been marked. From the resistance time series (top plot) sliding slope coefficients have been calculated (middle plot). The sliding slope coefficients jump to a high value as the algorithm switches from an incrementing to a sliding window. For the incrementing window, only non-negative values are allowed. In the middle plot, the horizontal yellow line indicates the occlusion threshold of 0.09. In the bottom plot, the yellow vertical line indicates the time of occlusion detection by the sliding slope coefficient algorithm, when the coefficient first reaches the threshold. In this situation the occlusion is detected incorrectly, as the initial sliding slope coefficient exceeds the threshold. This high sliding slope coefficient is caused by the initially negative values that quickly rise to non-negative values at this relatively high infusion rate.

Resistance, sliding slope coefficients and pressure over time for pump 2, while connected to one other pump with infusion rates 1 and 50 mL/h. For this pump the infusion rate is: 50.0 mL/h

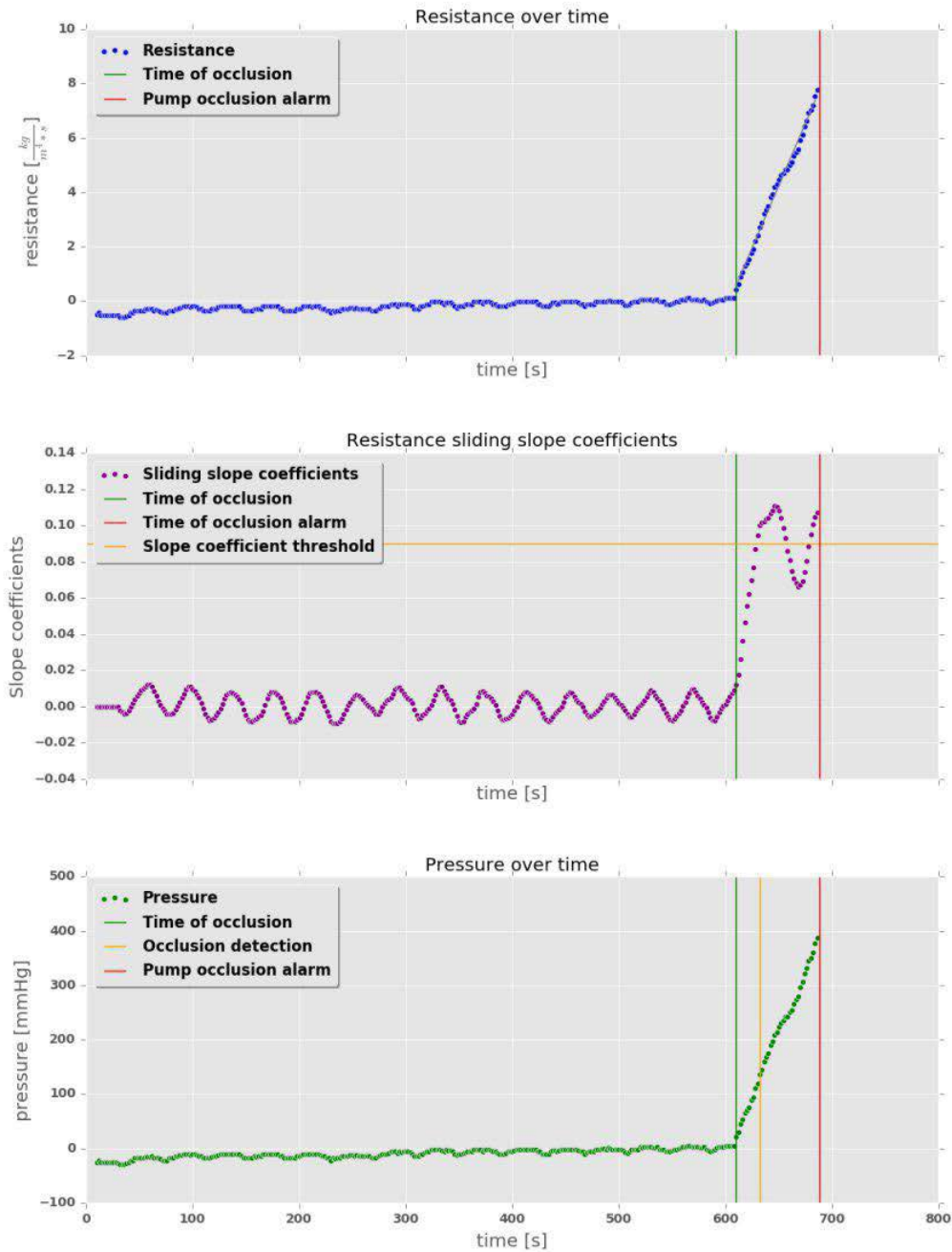


Figure 43: Resistance, sliding slope coefficient and pressure over time for pump 1 in configuration 2 (Figure 28) with an infusion rate of 50 mL/h. In this situation two pumps with infusion rates 51 and 50 mL/h were connected to each other. For all three plots the time of occlusion (vertical green line) and the time of pump occlusion alarm (vertical red line) have been marked. From the resistance time series (top plot) sliding slope coefficients have been calculated (middle plot). At this relatively high infusion rate, pressure time series contains fluctuations throughout the signal due to continuous overshooting of the pump mechanism. In the middle plot, the horizontal yellow line indicates the occlusion threshold of 0.09. In the bottom plot, the yellow vertical line indicates the time of occlusion detection by the sliding slope coefficient algorithm, when the coefficient first reaches the threshold.

Results configuration 3

Resistance, sliding slope coefficients and pressure over time for pump 1, while connected to three pumps, with a shared infusion rate of 1.0

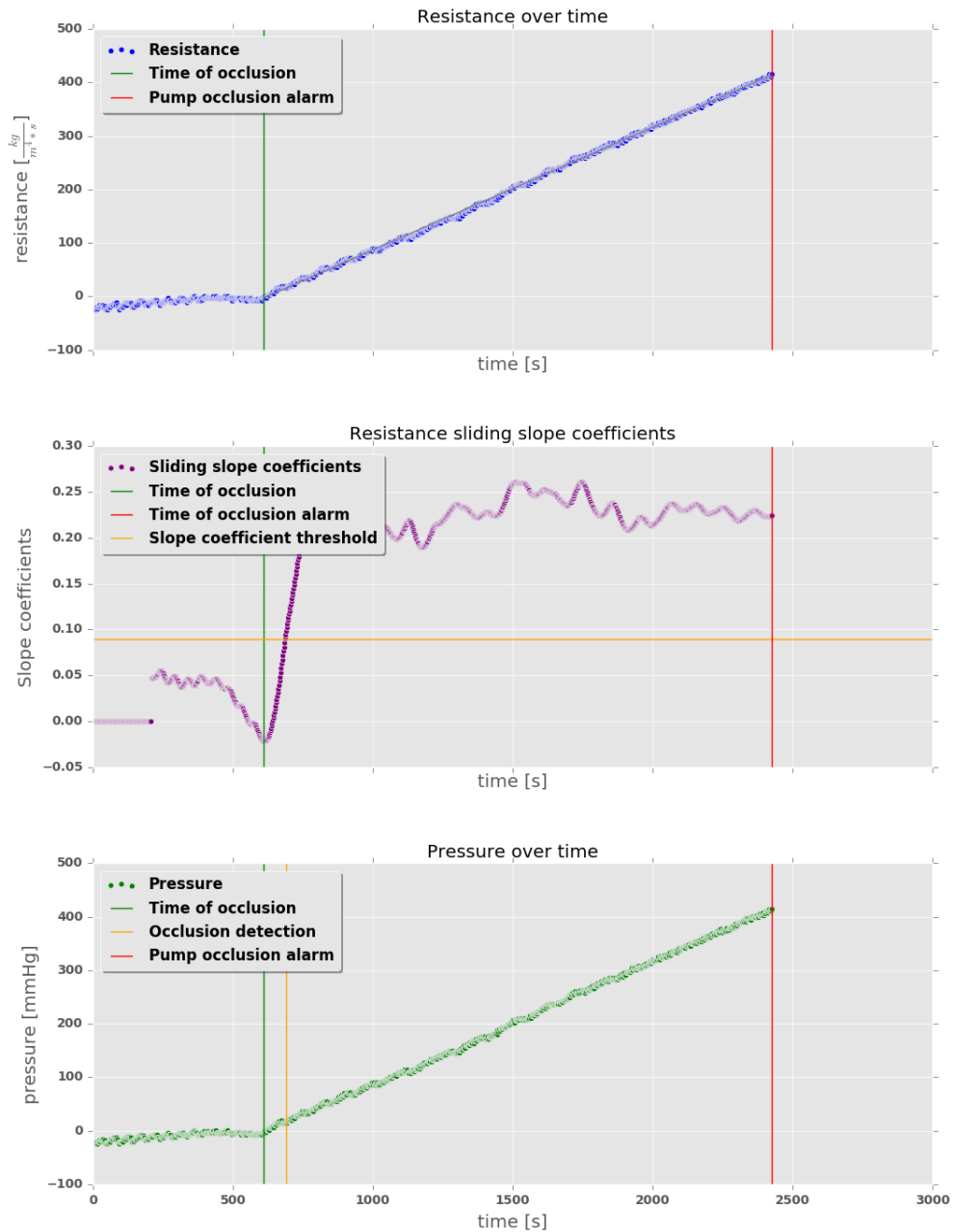


Figure 44: Resistance, sliding slope coefficient and pressure over time for pump 1 in configuration 3 (Figure 28) with an infusion rate of 1 mL/h. For all three plots the time of occlusion (vertical green line) and the time of pump occlusion alarm (vertical red line) have been marked. From the resistance time series (top plot) sliding slope coefficients have been calculated (middle plot). In the middle plot, the horizontal yellow line indicates the occlusion threshold of 0.09. In the bottom plot, the yellow vertical line indicates the time of occlusion detection by the sliding slope coefficient algorithm, when the coefficient first reaches the threshold.

Resistance, sliding slope coefficients and pressure over time for pump 2, while connected to three pumps, with a shared infusion rate of 1.0

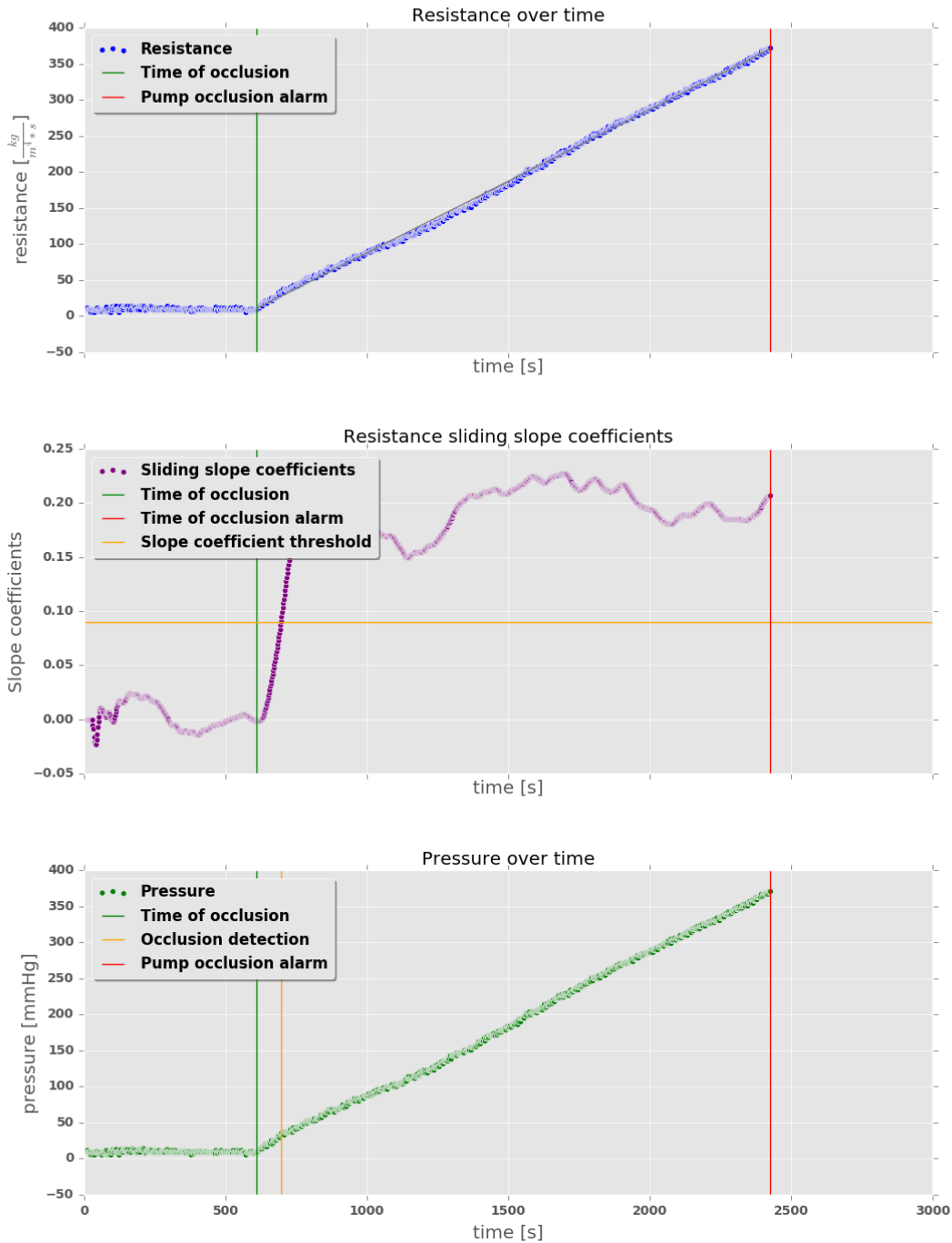


Figure 45: Resistance, sliding slope coefficient and pressure over time for pump 2 in configuration 3 (Figure 28) with an infusion rate of 1 mL/h. For all three plots the time of occlusion (vertical green line) and the time of pump occlusion alarm (vertical red line) have been marked. From the resistance time series (top plot) sliding slope coefficients have been calculated (middle plot). In the middle plot, the horizontal yellow line indicates the occlusion threshold of 0.09. In the bottom plot, the yellow vertical line indicates the time of occlusion detection by the sliding slope coefficient algorithm, when the coefficient first reaches the threshold.

Resistance, sliding slope coefficients and pressure over time for pump 3, while connected to three pumps, with a shared infusion rate of 1.0

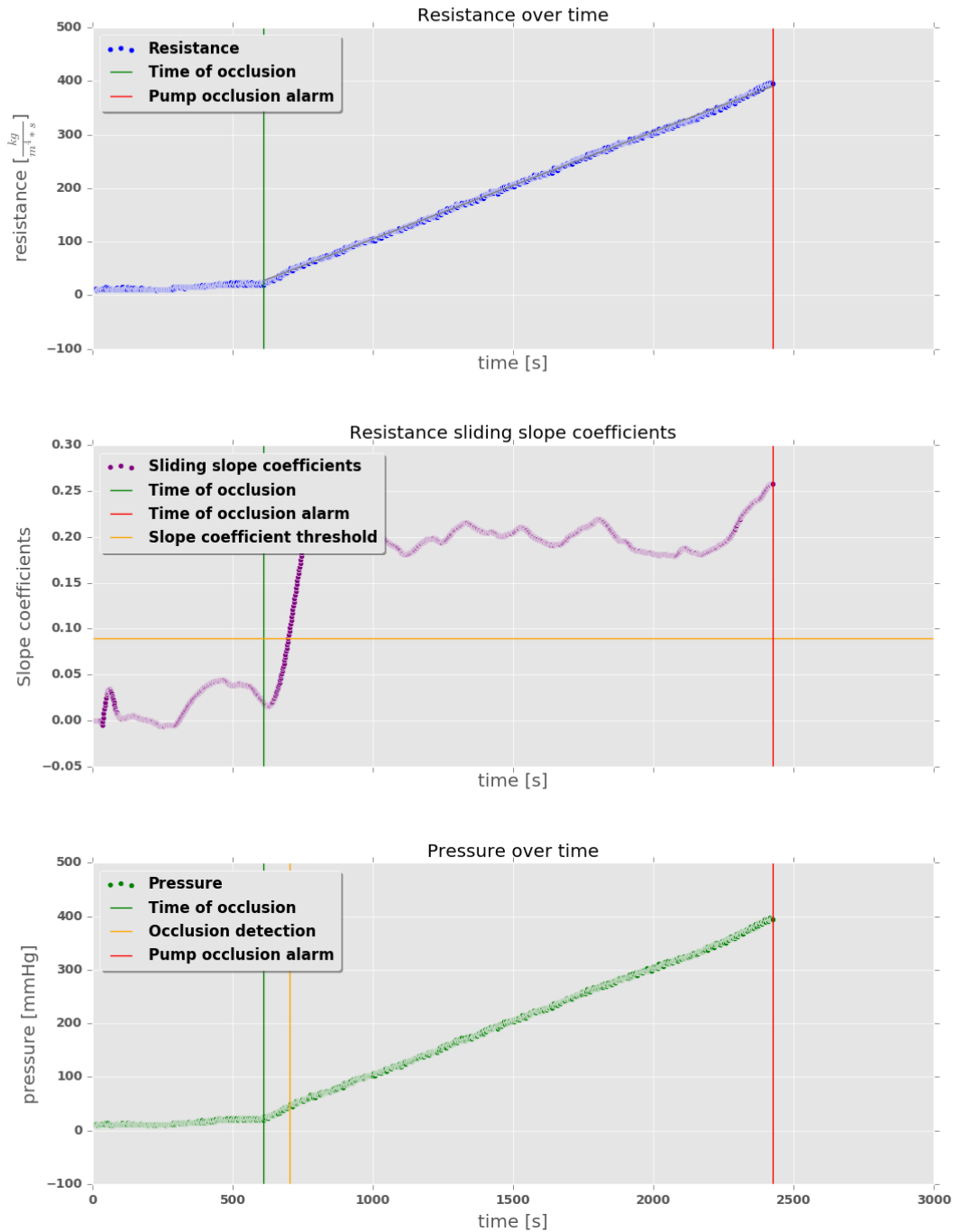


Figure 46: Resistance, sliding slope coefficient and pressure over time for pump 3 in configuration 3 (Figure 28) with an infusion rate of 1 mL/h. For all three plots the time of occlusion (vertical green line) and the time of pump occlusion alarm (vertical red line) have been marked. From the resistance time series (top plot) sliding slope coefficients have been calculated (middle plot). In the middle plot, the horizontal yellow line indicates the occlusion threshold of 0.09. In the bottom plot, the yellow vertical line indicates the time of occlusion detection by the sliding slope coefficient algorithm, when the coefficient first reaches the threshold.

Resistance, sliding slope coefficients and pressure over time for pump 1, while connected to three pumps, with a shared infusion rate of 5.0

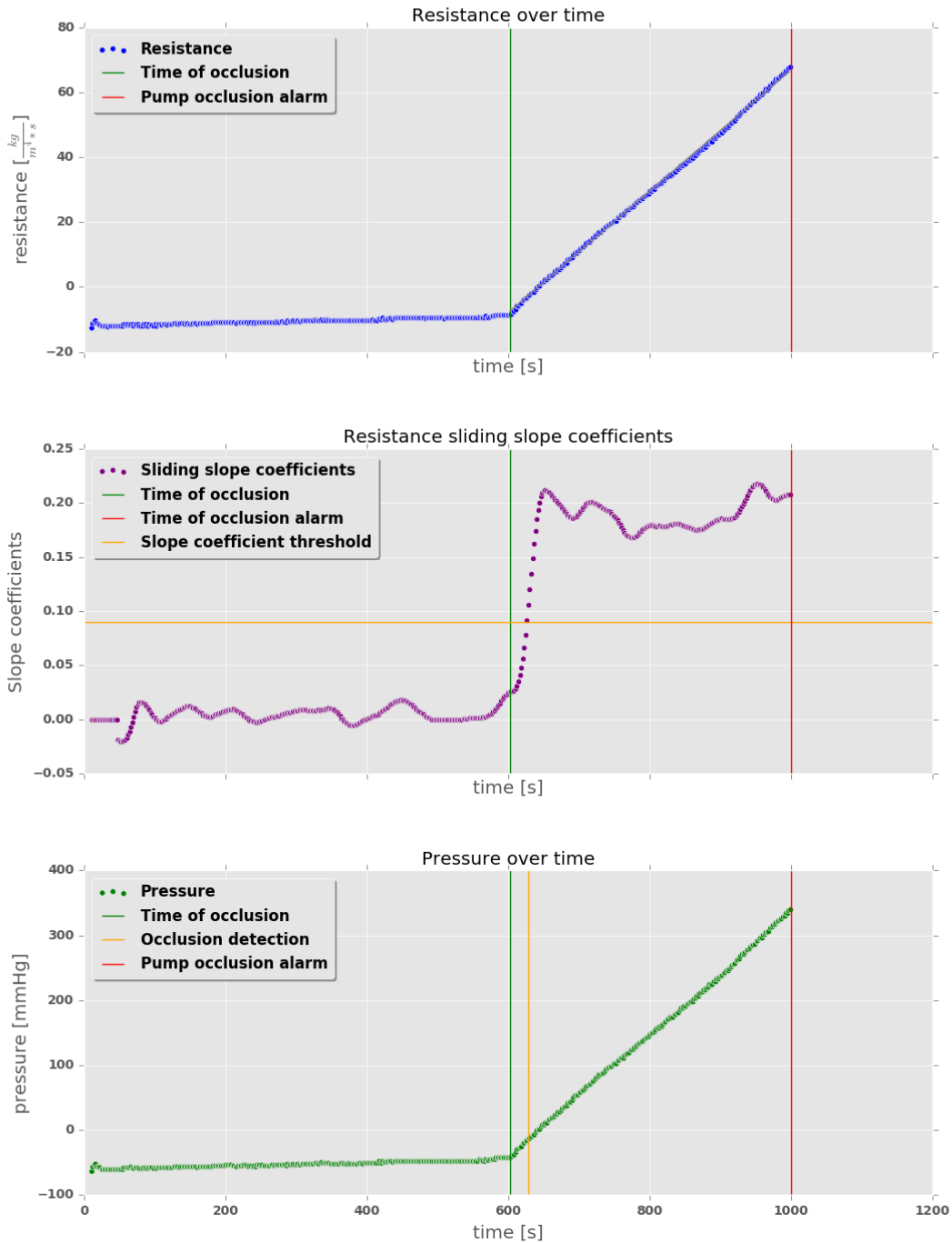


Figure 47: Resistance, sliding slope coefficient and pressure over time for pump 1 in configuration 3 (Figure 28) with an infusion rate of 5 mL/h. For all three plots the time of occlusion (vertical green line) and the time of pump occlusion alarm (vertical red line) have been marked. From the resistance time series (top plot) sliding slope coefficients have been calculated (middle plot). In the middle plot, the horizontal yellow line indicates the occlusion threshold of 0.09. In the bottom plot, the yellow vertical line indicates the time of occlusion detection by the sliding slope coefficient algorithm, when the coefficient first reaches the threshold.

Resistance, sliding slope coefficients and pressure over time for pump 2, while connected to three pumps, with a shared infusion rate of 5.0

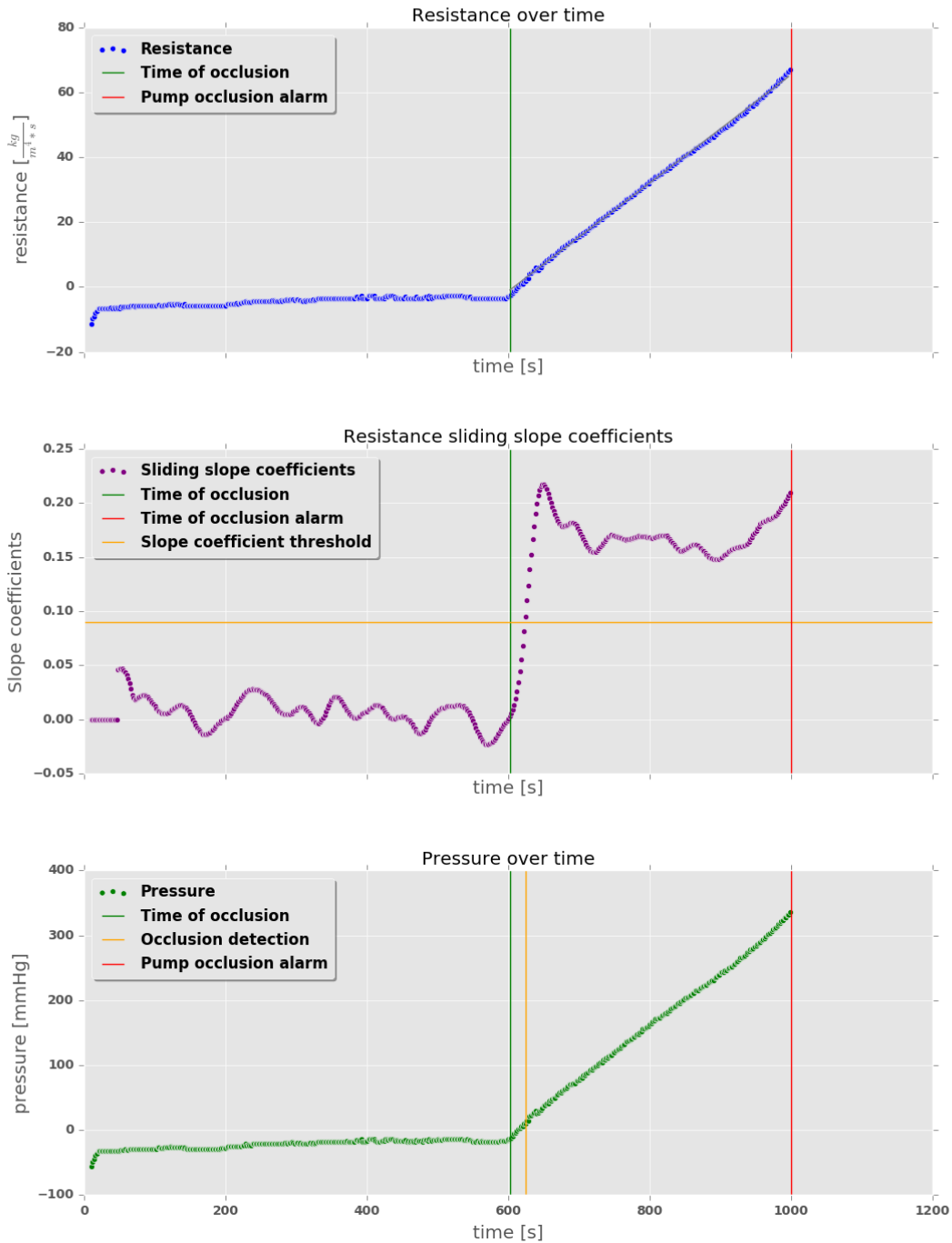


Figure 48: Resistance, sliding slope coefficient and pressure over time for pump 2 in configuration 3 (Figure 28) with an infusion rate of 5 mL/h. For all three plots the time of occlusion (vertical green line) and the time of pump occlusion alarm (vertical red line) have been marked. From the resistance time series (top plot) sliding slope coefficients have been calculated (middle plot). In the middle plot, the horizontal yellow line indicates the occlusion threshold of 0.09. In the bottom plot, the yellow vertical line indicates the time of occlusion detection by the sliding slope coefficient algorithm, when the coefficient first reaches the threshold.

Resistance, sliding slope coefficients and pressure over time for pump 3, while connected to three pumps, with a shared infusion rate of 5.0

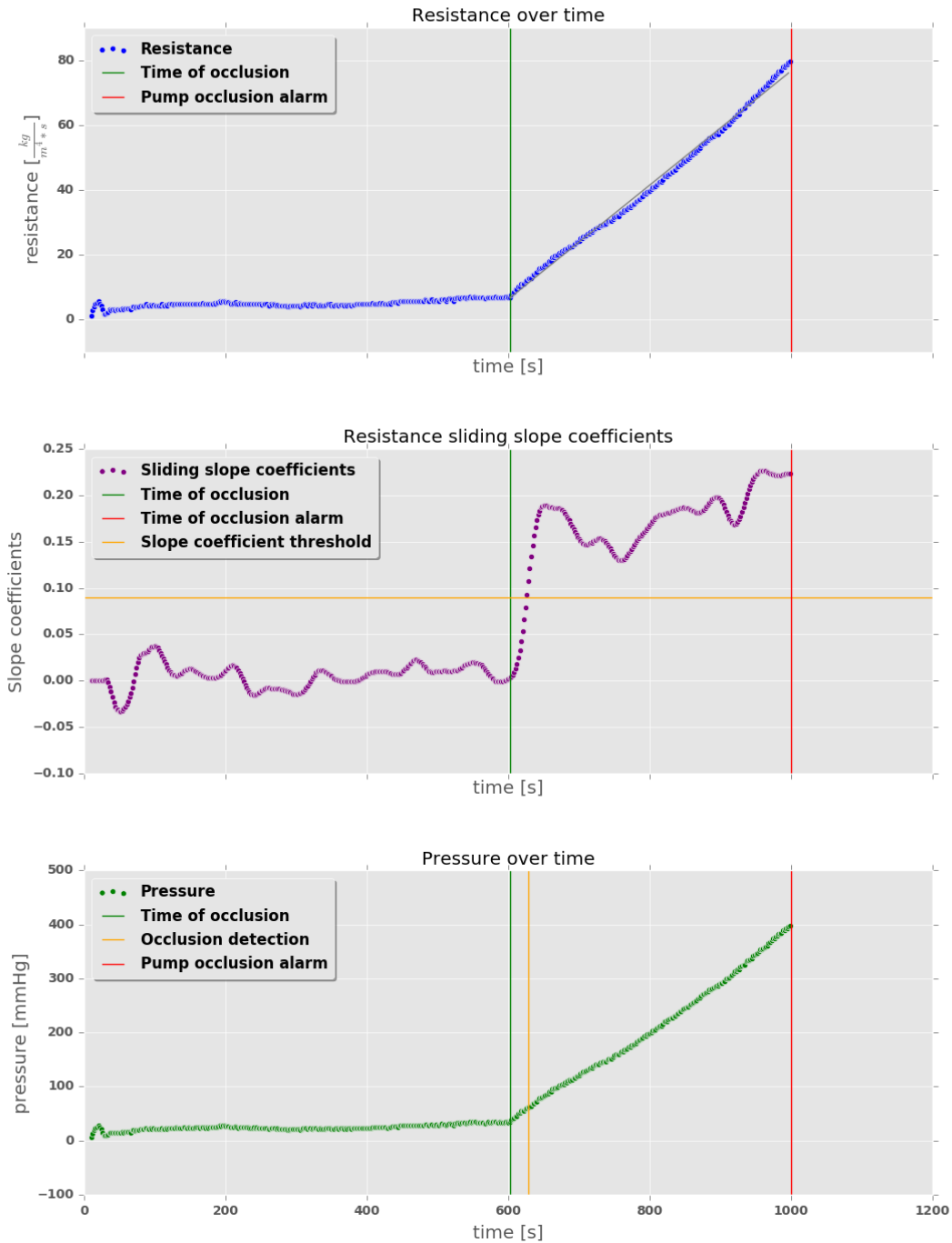


Figure 49: Resistance, sliding slope coefficient and pressure over time for pump 3 in configuration 3 (Figure 28) with an infusion rate of 5 mL/h. For all three plots the time of occlusion (vertical green line) and the time of pump occlusion alarm (vertical red line) have been marked. From the resistance time series (top plot) sliding slope coefficients have been calculated (middle plot). In the middle plot, the horizontal yellow line indicates the occlusion threshold of 0.09. In the bottom plot, the yellow vertical line indicates the time of occlusion detection by the sliding slope coefficient algorithm, when the coefficient first reaches the threshold.

Resistance, sliding slope coefficients and pressure over time for pump 1, while connected to three pumps, with a shared infusion rate of 10.0

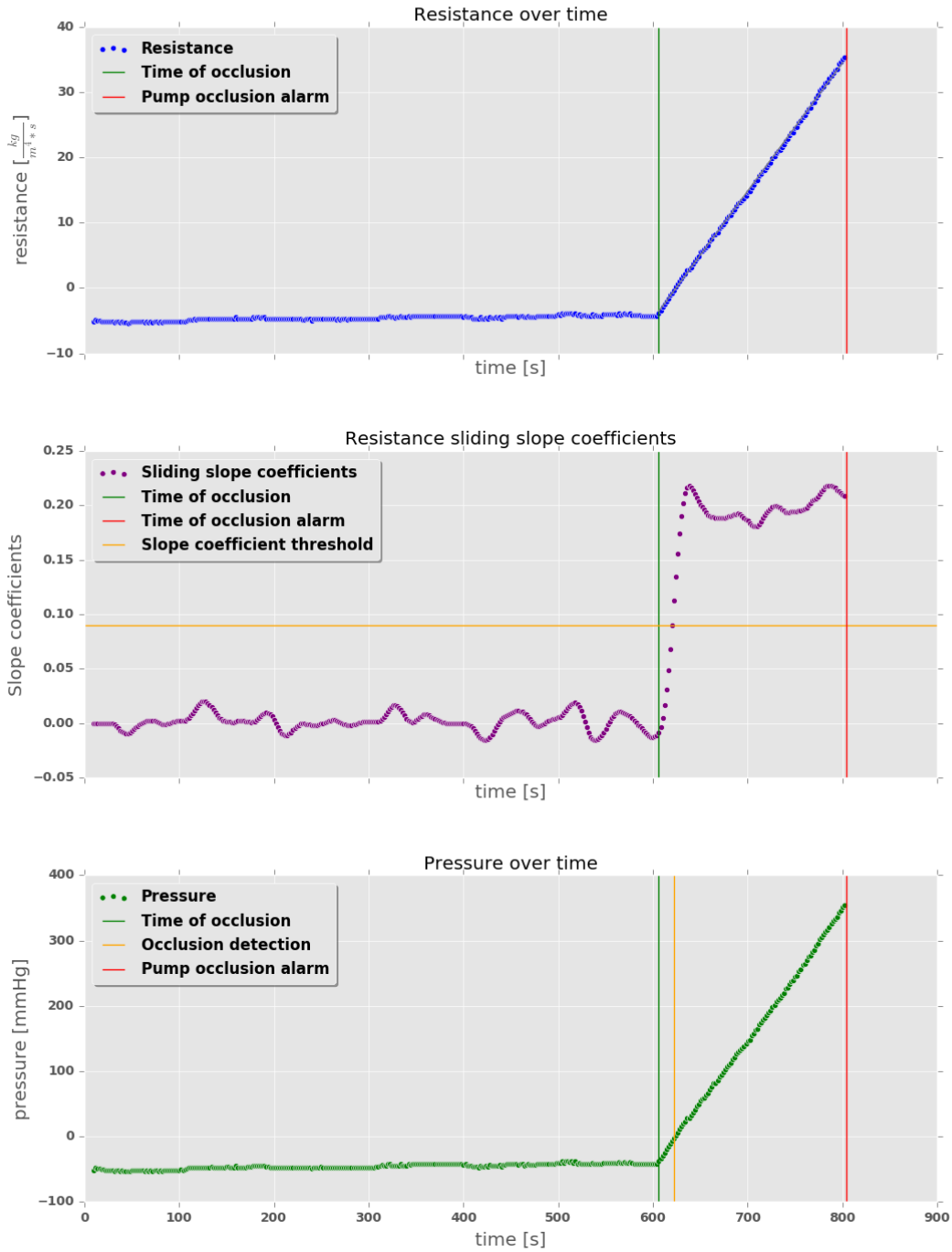


Figure 50: Resistance, sliding slope coefficient and pressure over time for pump 1 in configuration 3 (Figure 28) with an infusion rate of 10 mL/h. For all three plots the time of occlusion (vertical green line) and the time of pump occlusion alarm (vertical red line) have been marked. From the resistance time series (top plot) sliding slope coefficients have been calculated (middle plot). In the middle plot, the horizontal yellow line indicates the occlusion threshold of 0.09. In the bottom plot, the yellow vertical line indicates the time of occlusion detection by the sliding slope coefficient algorithm, when the coefficient first reaches the threshold.

Resistance, sliding slope coefficients and pressure over time for pump 2, while connected to three pumps, with a shared infusion rate of 10.0

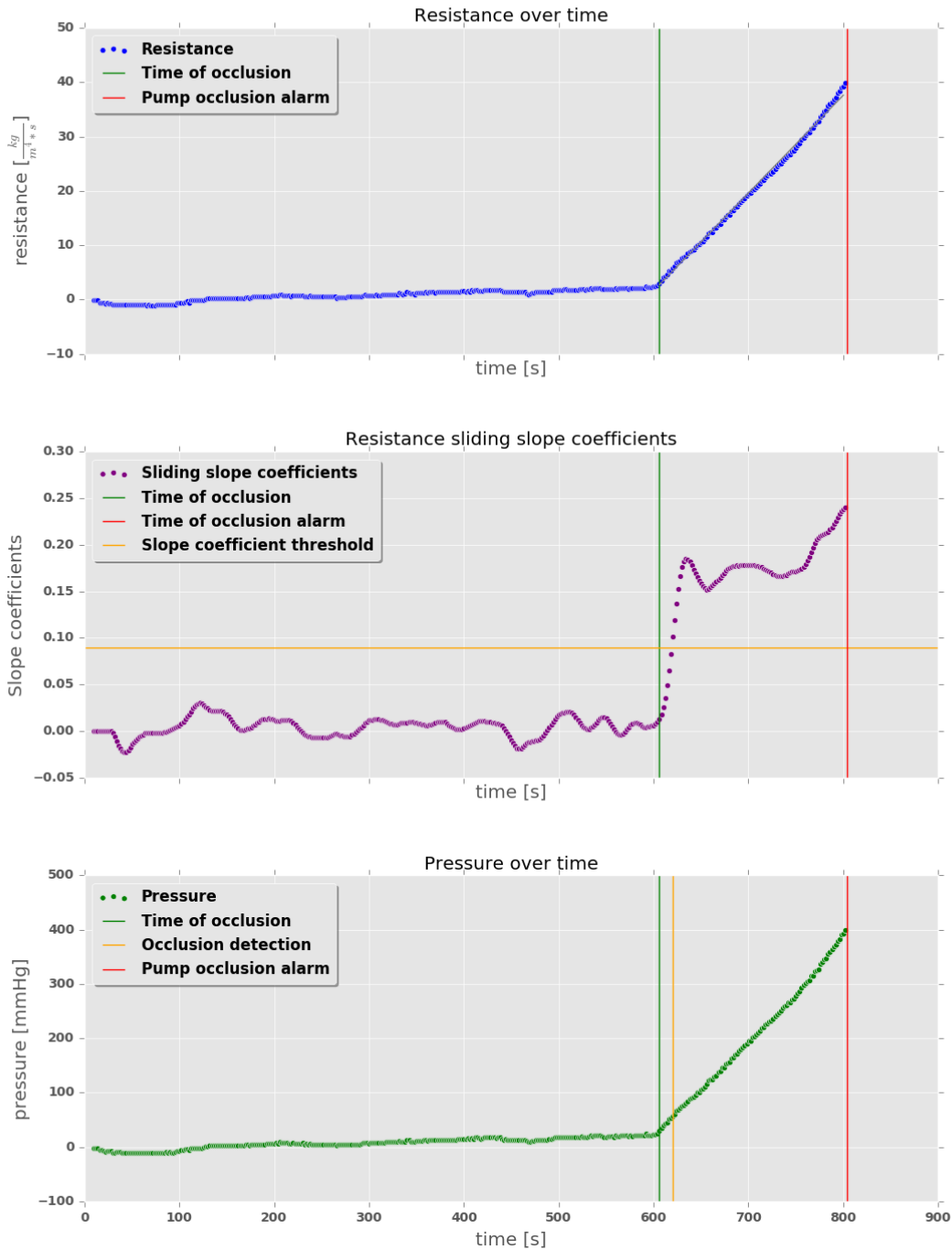


Figure 51: Resistance, sliding slope coefficient and pressure over time for pump 2 in configuration 3 (Figure 28) with an infusion rate of 10 mL/h. For all three plots the time of occlusion (vertical green line) and the time of pump occlusion alarm (vertical red line) have been marked. From the resistance time series (top plot) sliding slope coefficients have been calculated (middle plot). In the middle plot, the horizontal yellow line indicates the occlusion threshold of 0.09. In the bottom plot, the yellow vertical line indicates the time of occlusion detection by the sliding slope coefficient algorithm, when the coefficient first reaches the threshold.

Resistance, sliding slope coefficients and pressure over time for pump 3, while connected to three pumps, with a shared infusion rate of 10.0

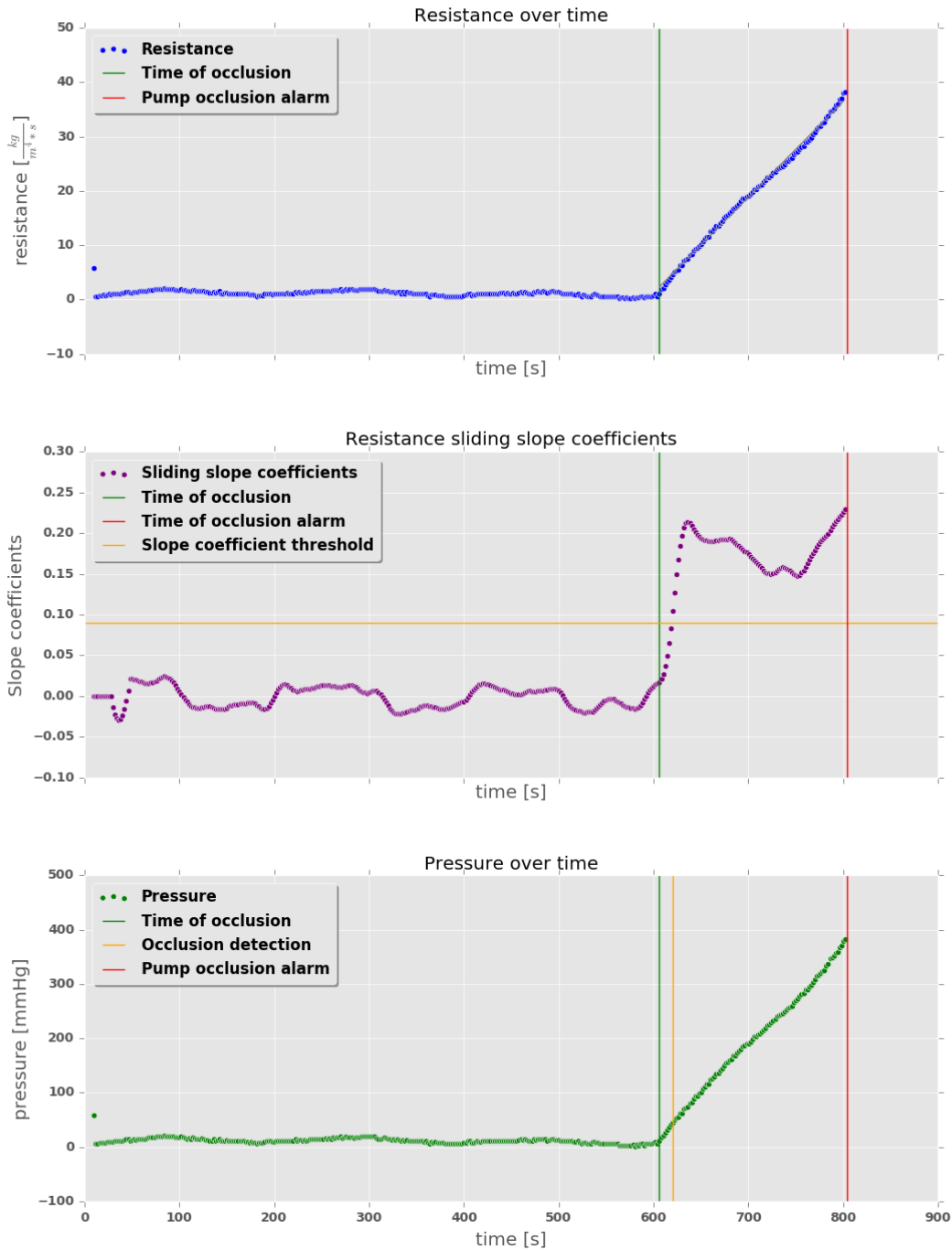


Figure 52: Resistance, sliding slope coefficient and pressure over time for pump 3 in configuration 3 (Figure 28) with an infusion rate of 10 mL/h. For all three plots the time of occlusion (vertical green line) and the time of pump occlusion alarm (vertical red line) have been marked. From the resistance time series (top plot) sliding slope coefficients have been calculated (middle plot). In the middle plot, the horizontal yellow line indicates the occlusion threshold of 0.09. In the bottom plot, the yellow vertical line indicates the time of occlusion detection by the sliding slope coefficient algorithm, when the coefficient first reaches the threshold.

Resistance, sliding slope coefficients and pressure over time for pump 1, while connected to three pumps, with a shared infusion rate of 50.0

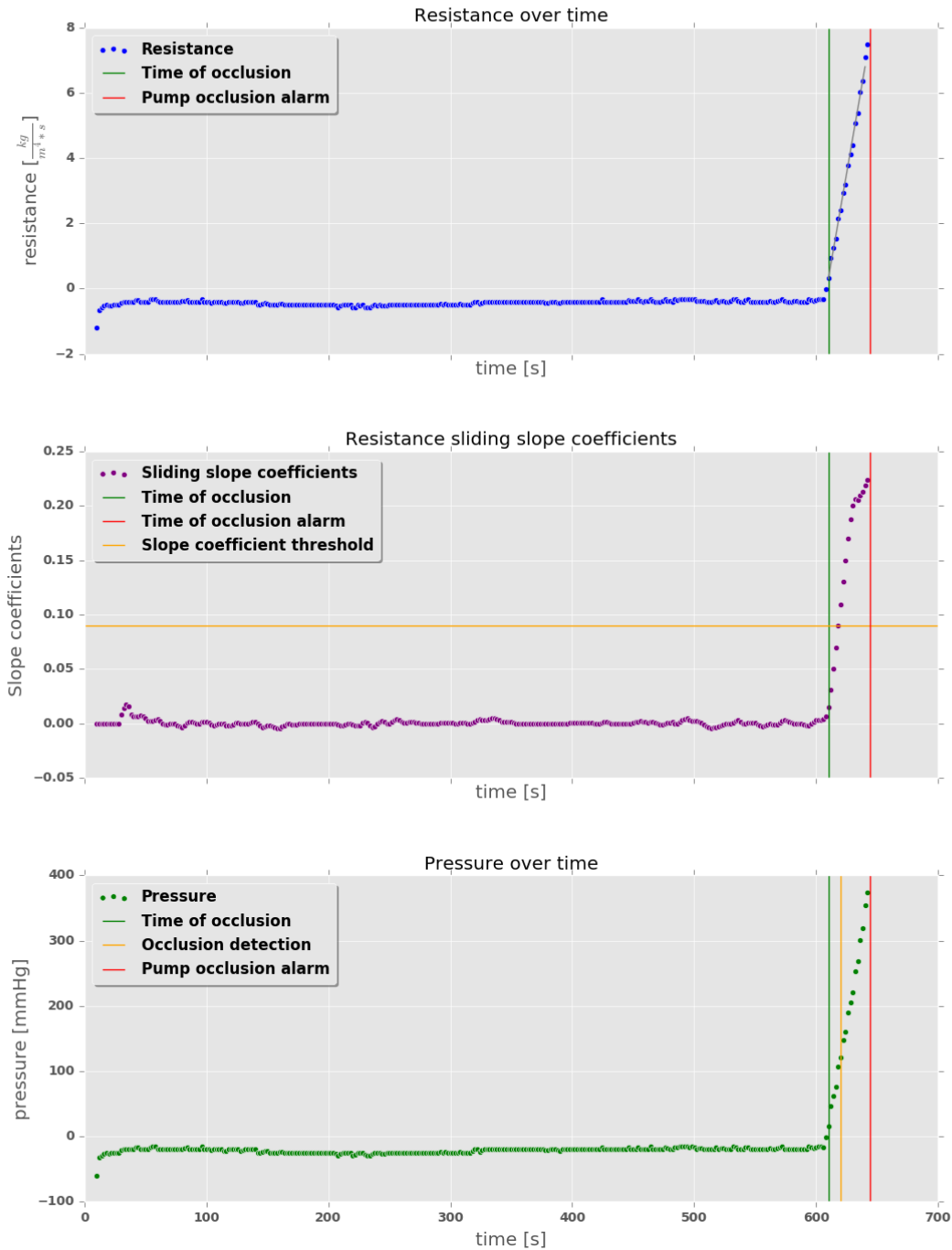


Figure 53: Resistance, sliding slope coefficient and pressure over time for pump 1 in configuration 3 (Figure 28) with an infusion rate of 50 mL/h. For all three plots the time of occlusion (vertical green line) and the time of pump occlusion alarm (vertical red line) have been marked. From the resistance time series (top plot) sliding slope coefficients have been calculated (middle plot). In the middle plot, the horizontal yellow line indicates the occlusion threshold of 0.09. In the bottom plot, the yellow vertical line indicates the time of occlusion detection by the sliding slope coefficient algorithm, when the coefficient first reaches the threshold.

Resistance, sliding slope coefficients and pressure over time for pump 2, while connected to three pumps, with a shared infusion rate of 50.0

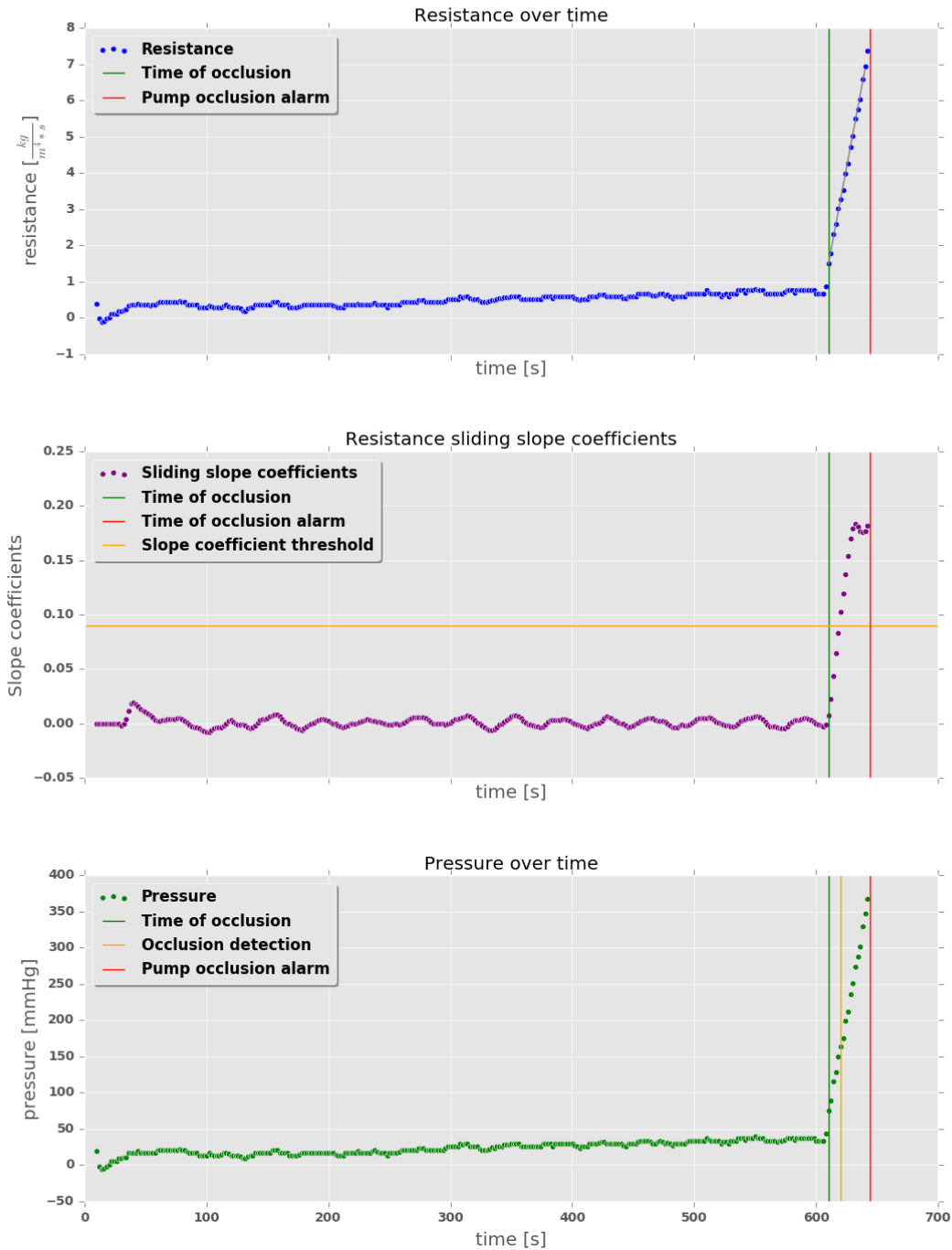


Figure 54: Resistance, sliding slope coefficient and pressure over time for pump 2 in configuration 3 (Figure 28) with an infusion rate of 50 mL/h. For all three plots the time of occlusion (vertical green line) and the time of pump occlusion alarm (vertical red line) have been marked. From the resistance time series (top plot) sliding slope coefficients have been calculated (middle plot). In the middle plot, the horizontal yellow line indicates the occlusion threshold of 0.09. In the bottom plot, the yellow vertical line indicates the time of occlusion detection by the sliding slope coefficient algorithm, when the coefficient first reaches the threshold.

Resistance, sliding slope coefficients and pressure over time for pump 3, while connected to three pumps, with a shared infusion rate of 50.0

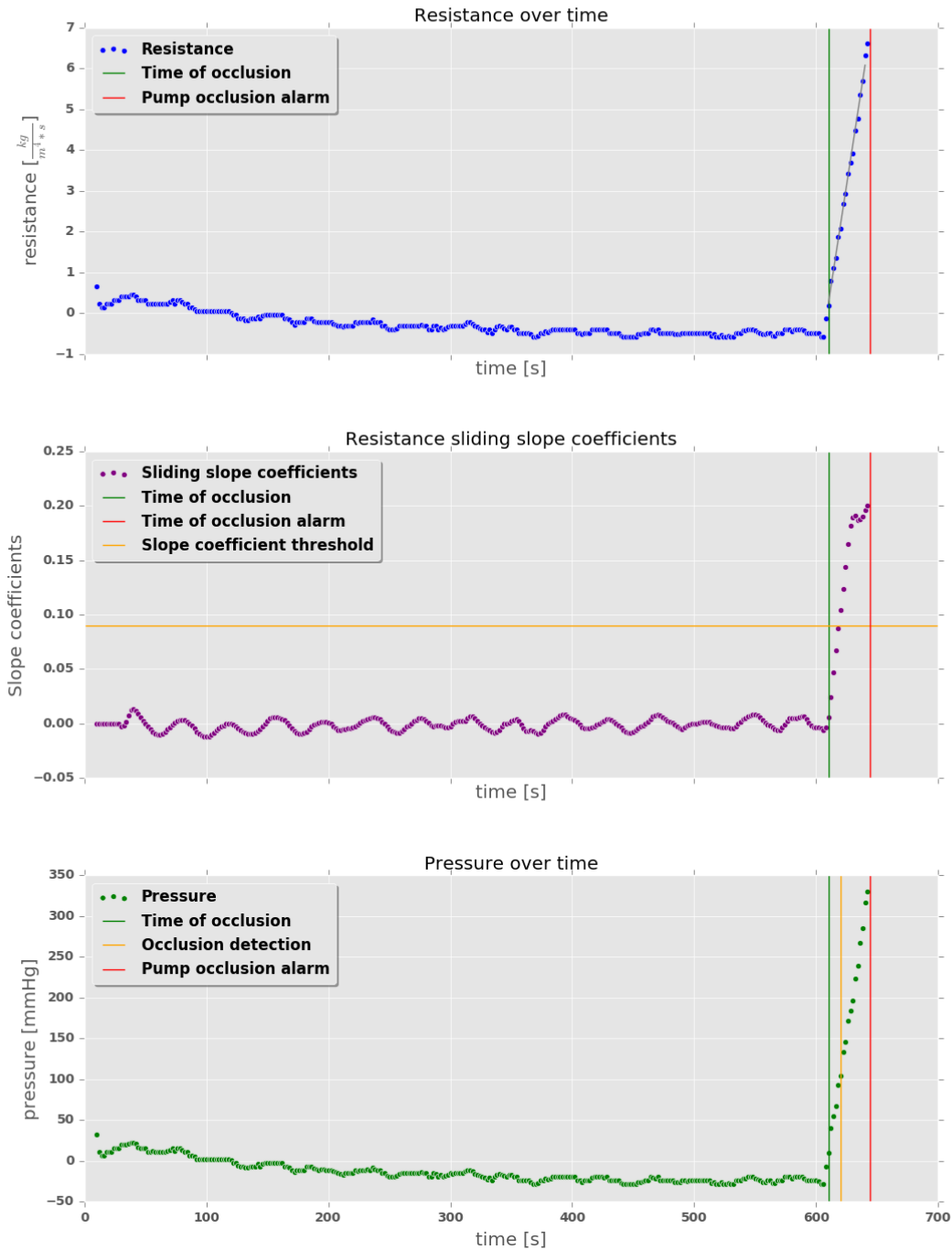


Figure 55: Resistance, sliding slope coefficient and pressure over time for pump 3 in configuration 3 (Figure 28) with an infusion rate of 50 mL/h. For all three plots the time of occlusion (vertical green line) and the time of pump occlusion alarm (vertical red line) have been marked. From the resistance time series (top plot) sliding slope coefficients have been calculated (middle plot). In the middle plot, the horizontal yellow line indicates the occlusion threshold of 0.09. In the bottom plot, the yellow vertical line indicates the time of occlusion detection by the sliding slope coefficient algorithm, when the coefficient first reaches the threshold.

Resistance, sliding slope coefficients and pressure over time for pump 1, while connected to three pumps with infusion rates 1, 10 and 50 mL/h. For this pump the infusion rate is: 1.0 mL/h

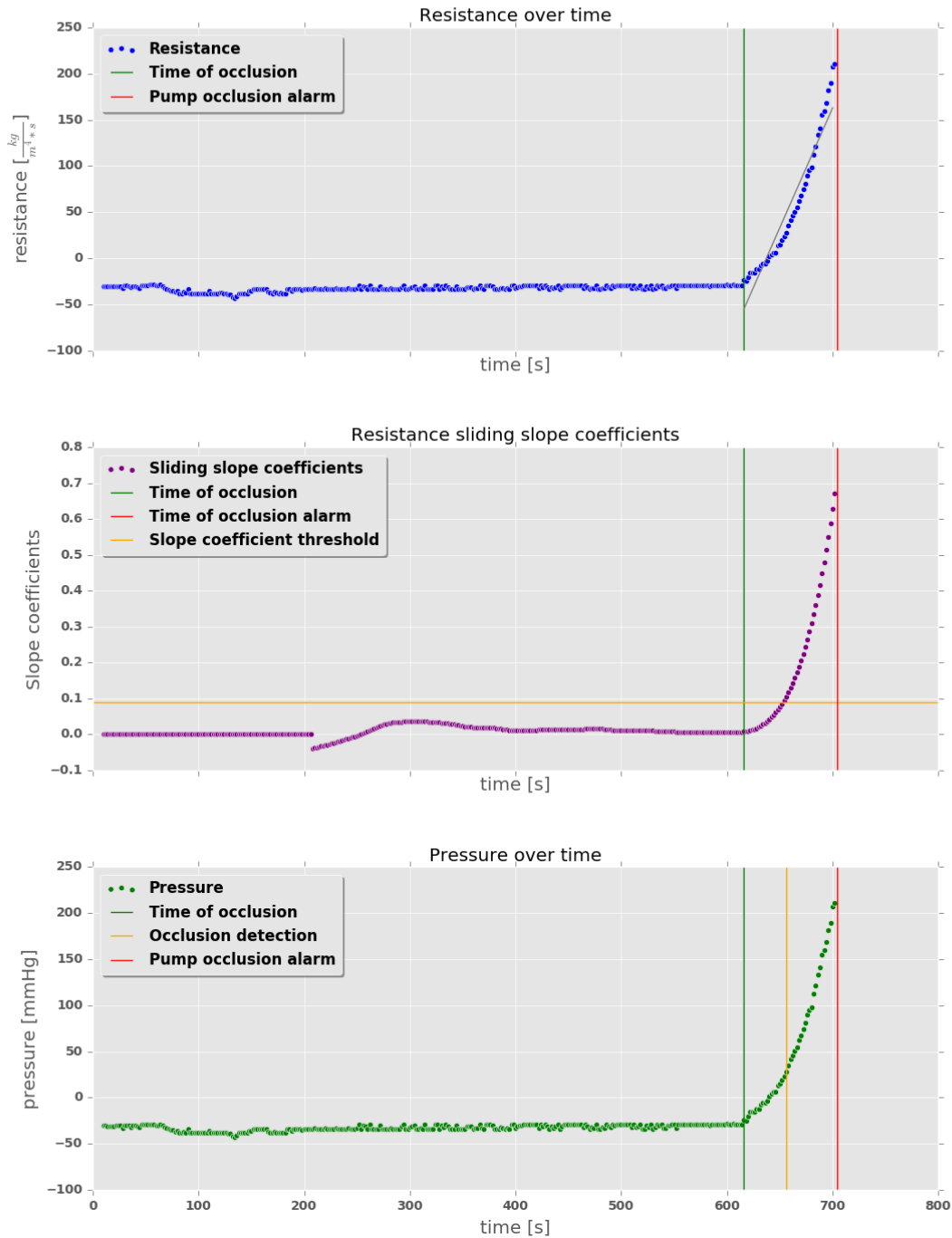


Figure 56: Resistance, sliding slope coefficient and pressure over time for pump 1 in configuration 3 (Figure 28) with an infusion rate of 1 mL/h. In this situation, the three connected pumps were set to the different infusion rates of 1, 10 and 50 mL/h. For all three plots the time of occlusion (vertical green line) and the time of pump occlusion alarm (vertical red line) have been marked. From the resistance time series (top plot) sliding slope coefficients have been calculated (middle plot). The sliding slope coefficient is initially high as the algorithm switches from an incrementing to a sliding window. For the incrementing window, only non-negative values are allowed. In the middle plot, the horizontal yellow line indicates the occlusion threshold of 0.09. In the bottom plot, the yellow vertical line indicates the time of occlusion detection by the sliding slope coefficient algorithm, when the coefficient first reaches the threshold.

Resistance, sliding slope coefficients and pressure over time for pump 2, while connected to three pumps with infusion rates 1, 10 and 50 mL/h. For this pump the infusion rate is: 10.0 mL/h

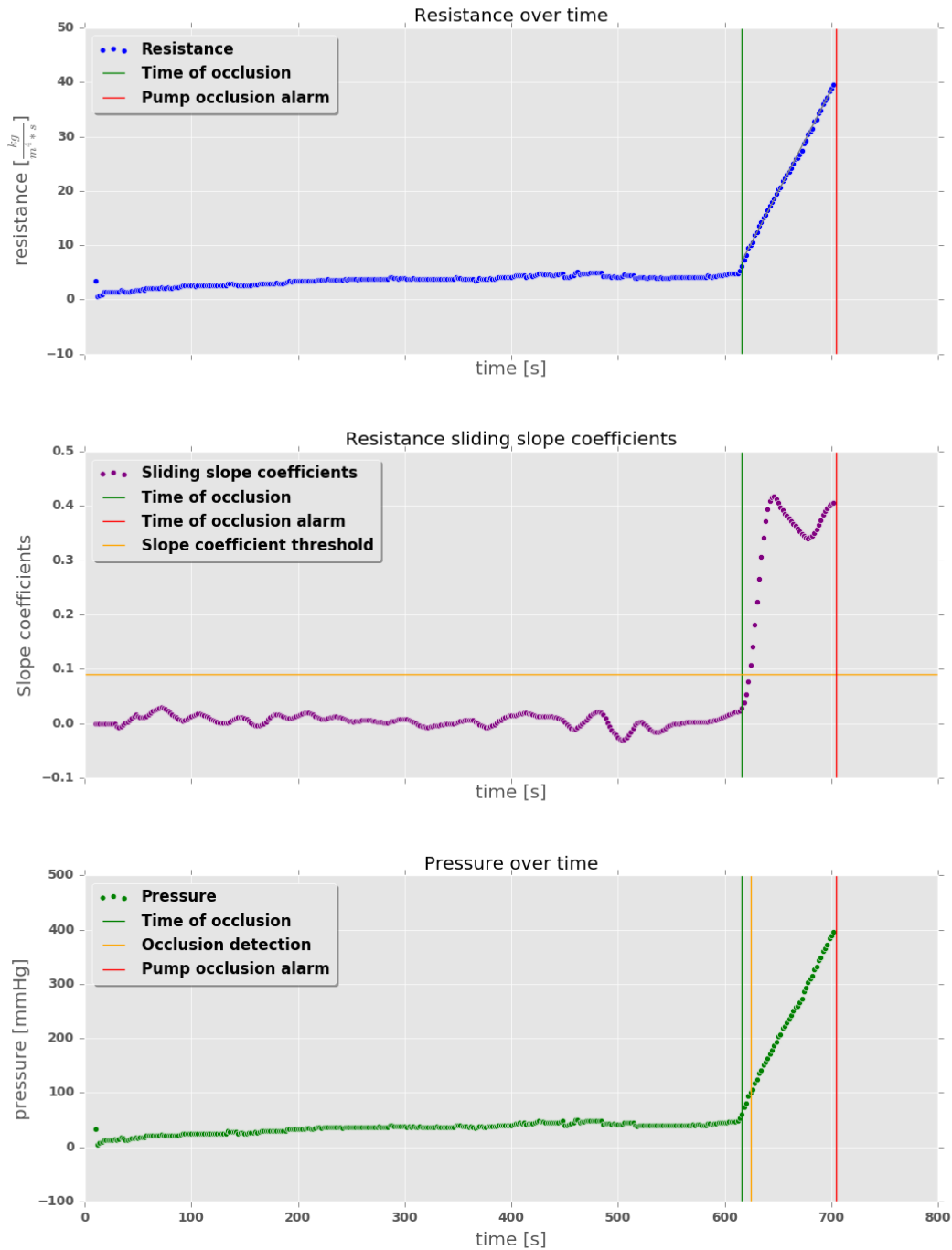


Figure 57: Resistance, sliding slope coefficient and pressure over time for pump 2 in configuration 3 (Figure 28) with an infusion rate of 10 mL/h. In this situation, the three connected pumps were set to the different infusion rates of 1, 10 and 50 mL/h. For all three plots the time of occlusion (vertical green line) and the time of pump occlusion alarm (vertical red line) have been marked. From the resistance time series (top plot) sliding slope coefficients have been calculated (middle plot). In the middle plot, the horizontal yellow line indicates the occlusion threshold of 0.09. In the bottom plot, the yellow vertical line indicates the time of occlusion detection by the sliding slope coefficient algorithm, when the coefficient first reaches the threshold.

Resistance, sliding slope coefficients and pressure over time for pump 3, while connected to three pumps with infusion rates 1, 10 and 50 mL/h. For this pump the infusion rate is: 50.0 mL/h

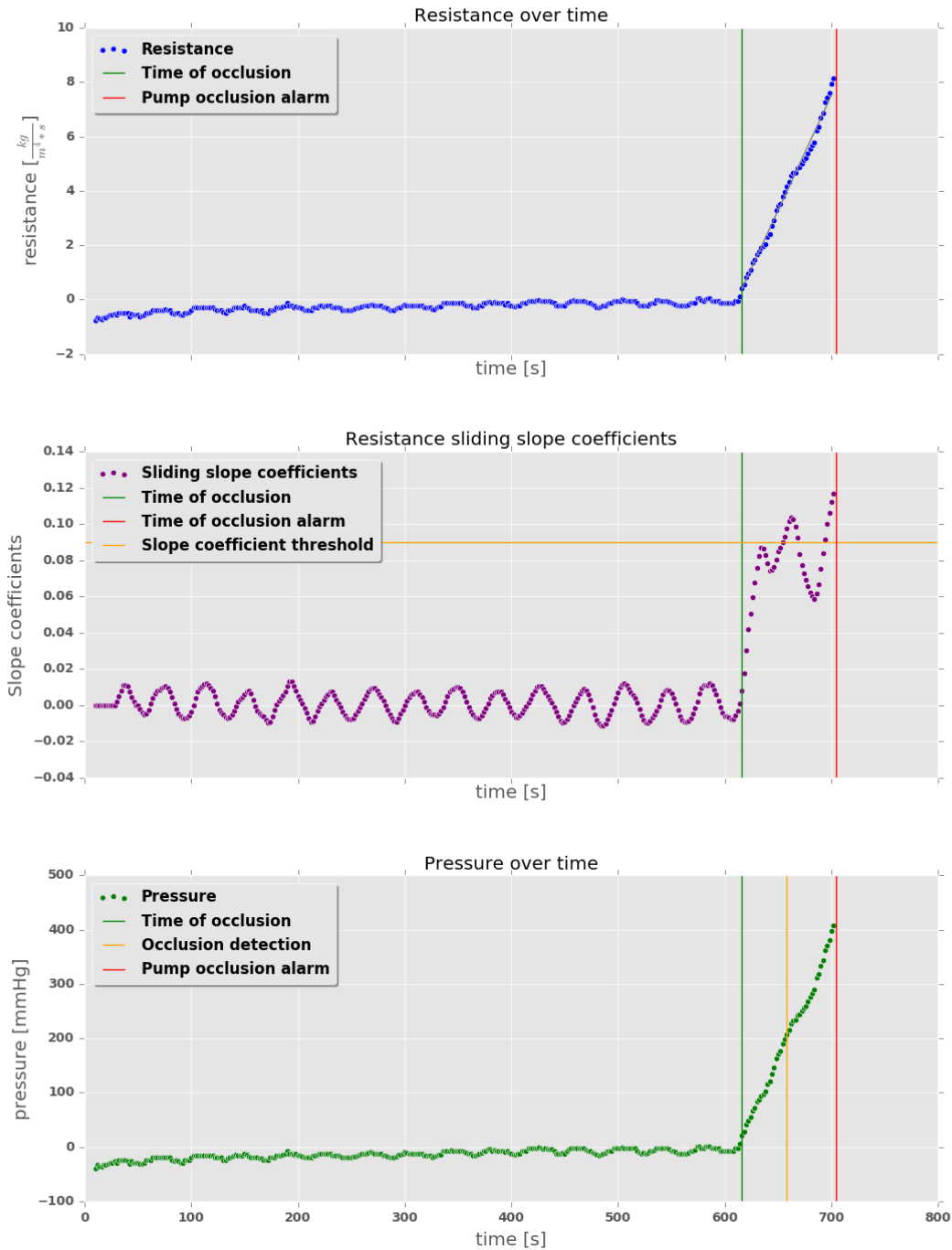


Figure 58: Resistance, sliding slope coefficient and pressure over time for pump 3 in configuration 3 (Figure 28) with an infusion rate of 50 mL/h. In this situation, the three connected pumps were set to the different infusion rates of 1, 10 and 50 mL/h. For all three plots the time of occlusion (vertical green line) and the time of pump occlusion alarm (vertical red line) have been marked. From the resistance time series (top plot) sliding slope coefficients have been calculated (middle plot). In the middle plot, the horizontal yellow line indicates the occlusion threshold of 0.09. In the bottom plot, the yellow vertical line indicates the time of occlusion detection by the sliding slope coefficient algorithm, when the coefficient first reaches the threshold.

Resistance, sliding slope coefficients and pressure over time for pump 1, while connected to three pumps with infusion rates 5, 5 and 10 mL/h. For this pump the infusion rate is: 5.0 mL/h

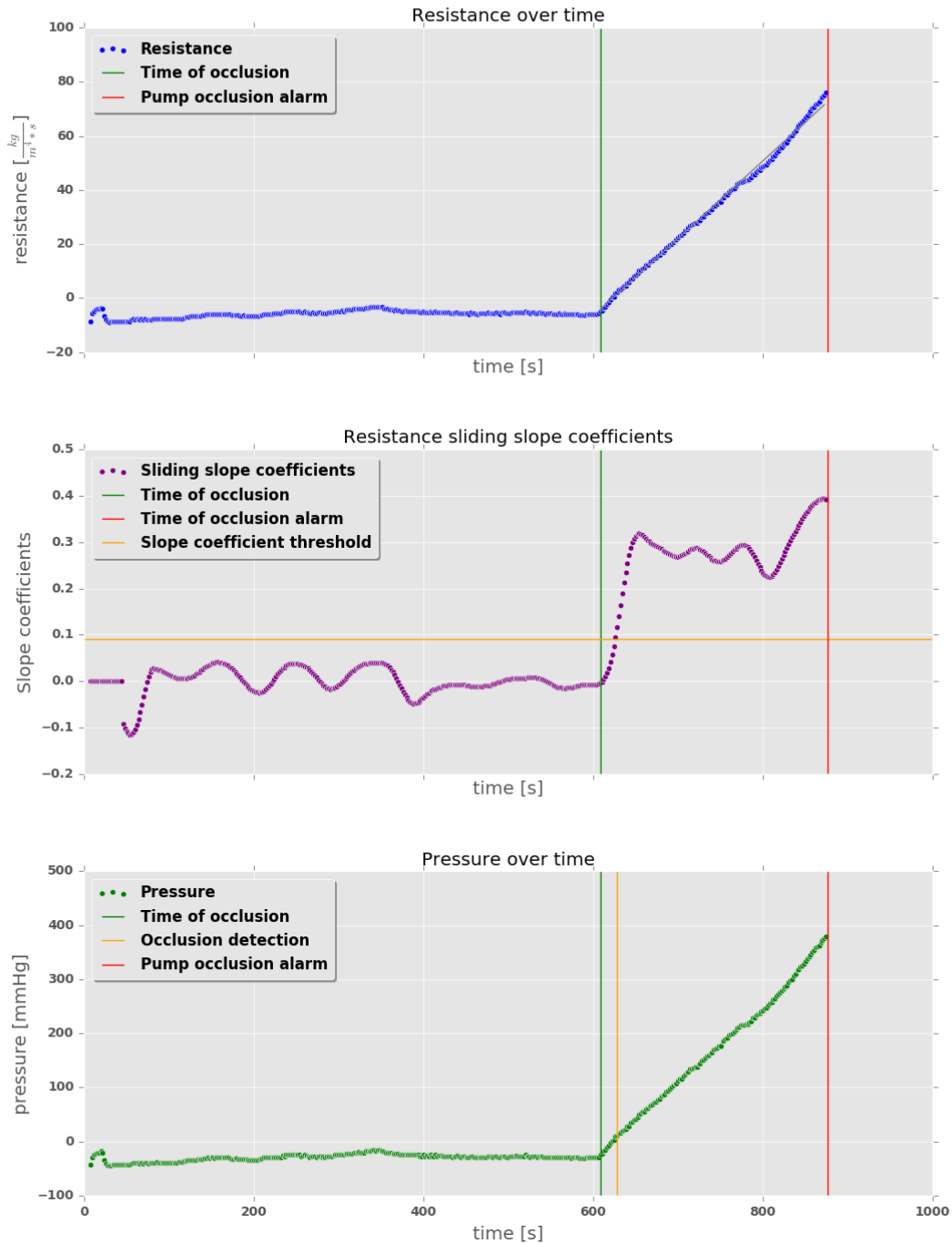


Figure 59: Resistance, sliding slope coefficient and pressure over time for pump 1 in configuration 3 (Figure 28) with an infusion rate of 5 mL/h. In this situation, the three connected pumps were set to the infusion rates of 5, 5 and 10 mL/h. For all three plots the time of occlusion (vertical green line) and the time of pump occlusion alarm (vertical red line) have been marked. From the resistance time series (top plot) sliding slope coefficients have been calculated (middle plot). In the middle plot, the horizontal yellow line indicates the occlusion threshold of 0.09. In the bottom plot, the yellow vertical line indicates the time of occlusion detection by the sliding slope coefficient algorithm, when the coefficient first reaches the threshold.

Resistance, sliding slope coefficients and pressure over time for pump 2, while connected to three pumps with infusion rates 5, 5 and 10 mL/h. For this pump the infusion rate is: 5.0 mL/h

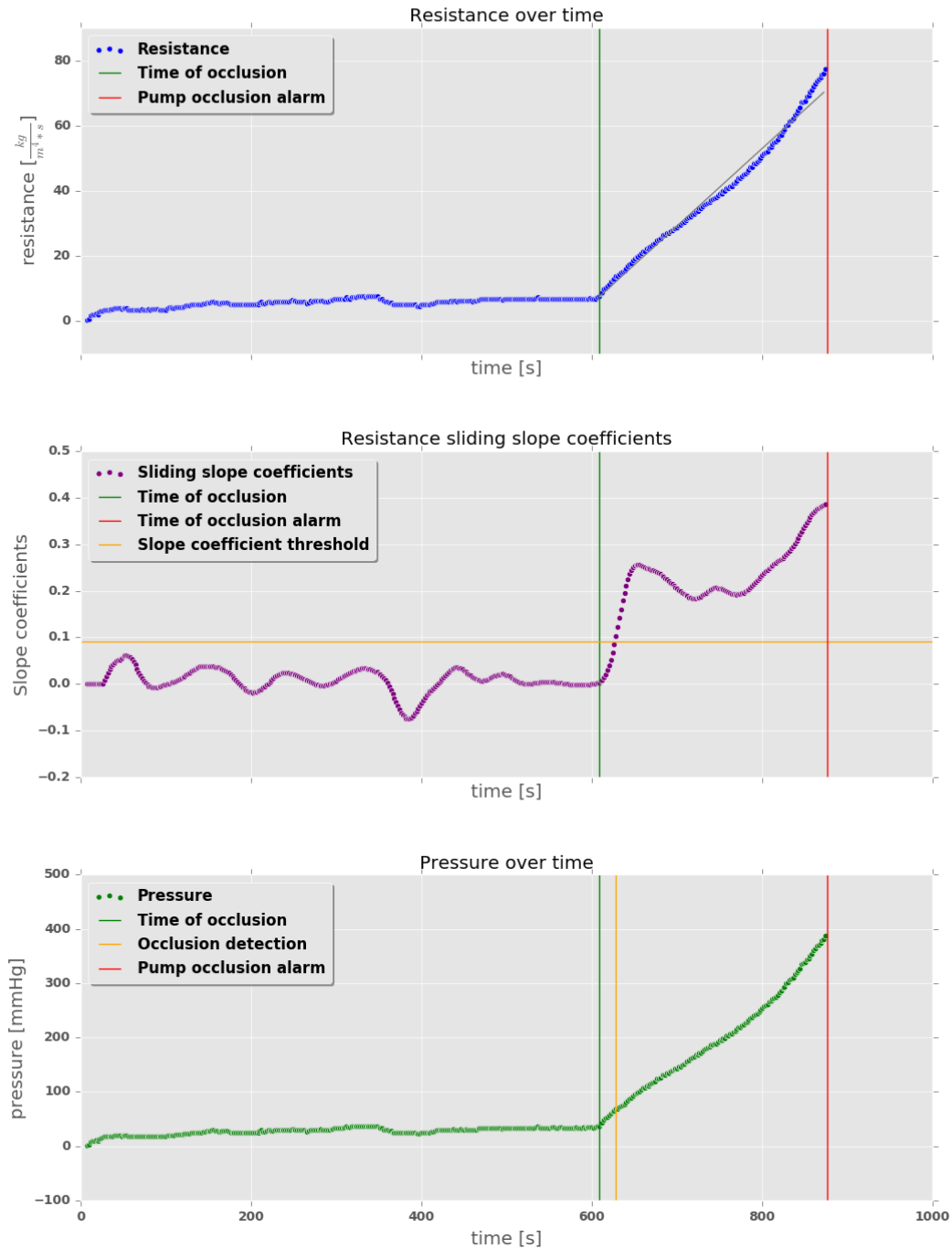


Figure 60: Resistance, sliding slope coefficient and pressure over time for pump 2 in configuration 3 (Figure 28) with an infusion rate of 5 mL/h. In this situation, the three connected pumps were set to the infusion rates of 5, 5 and 10 mL/h. For all three plots the time of occlusion (vertical green line) and the time of pump occlusion alarm (vertical red line) have been marked. From the resistance time series (top plot) sliding slope coefficients have been calculated (middle plot). In the middle plot, the horizontal yellow line indicates the occlusion threshold of 0.09. In the bottom plot, the yellow vertical line indicates the time of occlusion detection by the sliding slope coefficient algorithm, when the coefficient first reaches the threshold.

Resistance, sliding slope coefficients and pressure over time for pump 3, while connected to three pumps with infusion rates 5, 5 and 10 mL/h. For this pump the infusion rate is: 10.0 mL/h

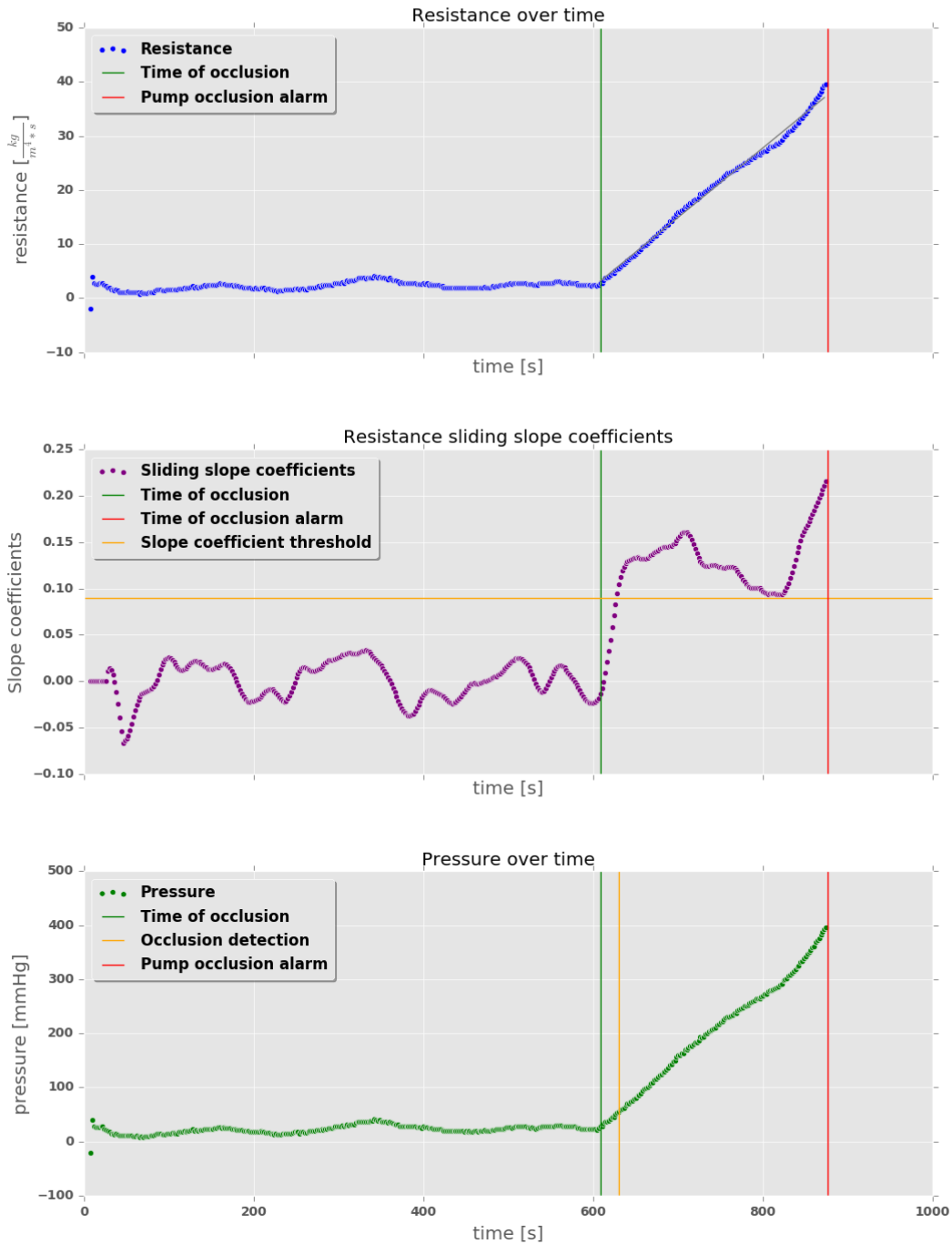


Figure 61: Resistance, sliding slope coefficient and pressure over time for pump 3 in configuration 3 (Figure 28) with an infusion rate of 10 mL/h. In this situation, the three connected pumps were set to the infusion rates of 5, 5 and 10 mL/h. For all three plots the time of occlusion (vertical green line) and the time of pump occlusion alarm (vertical red line) have been marked. From the resistance time series (top plot) sliding slope coefficients have been calculated (middle plot). In the middle plot, the horizontal yellow line indicates the occlusion threshold of 0.09. In the bottom plot, the yellow vertical line indicates the time of occlusion detection by the sliding slope coefficient algorithm, when the coefficient first reaches the threshold.